SELECTIVIVITY OF CONNEXIN43 AND CONNEXIN40 COMPRISED GAP JUNCTIONS

by

Nathanael Heyman

A Dissertation Submitted to the Faculty of the

PHYSIOLOGICAL SCIENCES GRADUATE INTERDISCIPLINARY PROGRAM

In Partial Fulfillment of the Requirements
For the Degree of

DOCTOR OF PHILOSOPHY

In the Graduate College

THE UNIVERSITY OF ARIZONA

2007

THE UNIVERSITY OF ARIZONA
GRADUATE COLLEGE

As members of the Dissertation Committee, we certify that we have read the dissertation prepared by *Nathanael Heyman*

entitled *Selectivity of Connexin43 and Connexin40 Comprised Gap Junctions*

and recommend that it be accepted as fulfilling the dissertation requirement for the *Degree of Doctor of Philosophy*.

_____ Date: (10/18/07)
(Dr. Jan Burt)

_____ Date: (10/18/07)
(Dr. Alex Simon)

_____ Date: (10/18/07)
(Dr. Scott Boitano)

_____ Date: (10/18/07)
(Dr. Tim Secomb)

Final approval and acceptance of this dissertation is contingent upon the candidate's submission of the final copies of the dissertation to the Graduate College.

I hereby certify that I have read this dissertation prepared under my direction and recommend that it be accepted as fulfilling the dissertation requirement.

_____ Date: (10/18/07)
Dissertation Director: (Dr. Jan Burt)

STATEMENT BY AUTHOR

This dissertation has been submitted in partial fulfillment of requirements for an advanced degree at the University of Arizona and is deposited in the University Library to be made available to borrowers under rules of the Library.

Brief quotations from this dissertation are allowable without special permission, provided that accurate acknowledgment of source is made. Requests for permission for extended quotation from or reproduction of this manuscript in whole or in part may be granted by the head of the major department or the Dean of the Graduate College when in his or her judgment the proposed use of the material is in the interests of scholarship. In all other instances, however, permission must be obtained from the author.

SIGNED: Nathanael Heyman

ACKNOWLEDGMENTS

First I would like to thank my advisor, Dr. Jan Burt, for affording me the opportunity to pursue my PhD dissertation in her laboratory. She has been an excellent mentor and friend over the last 5 years and has allowed me to investigate a number of research avenues resulting in a fulfilling educational experience. I would also like to thank all of the members of my committee for their help and guidance, Drs. Dave Kurjiaka and Jose Ek-Vitorin for many useful discussions, and Tasha Nelson for excellent technical support. Finally, I would like to thank these and all other members of the Burt lab for their friendship. All of them have helped to make the past 5 years an enjoyable as well as productive time.

TABLE OF CONTENTS

TABLE OF CONTENTS - *Continued*

ABSTRACT

Gap junctions are aggregates of intercellular channels each formed of protein subunits termed connexins (Cx). Recently published data show that junctional dye permeability relative to conductance (permselectivity) varies across several orders of magnitude for Cx43 junctions, suggesting variable selectivity of the comprising Cx43 channels. Logical candidates for this variable selectivity are variability in charge or size selectivity. Consequently, junctional charge and size selectivities were determined in the current study by simultaneous measurement of junctional permeance to dyes of differing size or charge.

The results show that for a number of dyes differing in size, charge, chemical composition, and structure the primary determinant for selectivity through Cx43 gap junctions was the size of the dye permeant with this selectivity showing essentially no variability beyond that seen between incompletely divided cells, presumably representing the variability inherent to the measurement. As such, selectivity of dye-permeable Cx43 channels is well described by the physical dimensions of the channel pore acting essentially as a simple molecular sieve. The seemingly disparate dye selectivity and permselectivity results can be reconciled by the variable presence of a dye-impermeable but electrically conductive channel conformation for Cx43 channels, affording a possible mechanism for independent regulation of diffusion of larger molecules versus electrical conductance to smaller ions.

Cx40 junctions, known to be cation selective, also showed minimal variability in charge selectivity indicating that Cx40 charge selectivity is also an essentially fixed

parameter. Co-expression of Cx40 and Cx43 lead to charge selectivities ranging from Cx43 to Cx40 with an average intermediate between the two. Activation of PKC leads to an increase in cationic selectivity of Cx40/Cx43 composed junctions by specifically reducing permeability through non-selective Cx43 channels favoring permeation through cation-selective Cx40 channels, allowing for junctional charge selectivity regulation.

The combined data suggest that selectivity properties for dye permeable channels composed of Cx43 or Cx40 are essentially fixed parameters of the channel pore. Only upon co-expression of these connexins is significant variability in selectivity seen. The differential effects of PKC-mediated phosphorylation on permeability of Cx43 and Cx40 channels then allows for regulation of junctional charge selectivity but only in cells expressing both connexins.

CHAPTER 1

INTRODUCTION AND BACKGROUND

Gap junctions are clusters of channels that connect the cytoplasm of adjacent cells and are present in essentially all organ systems of the human body. They serve as intercellular conduits for transfer of ions and molecules less than approximately 1,000 Daltons in size. This intercellular communication plays critical roles in the growth, development, and proper functioning of multicellular organisms, where cell and thus organism survival is dependent upon proper communication between and coordination of a large number of cells and cell types. Gap junctions and the direct intercellular communication they afford help to facilitate this intercellular coordination.

Gap junction channels are composed of protein subunits termed connexins. There are twenty-one and twenty genes in human and mouse genomes respectively that encode connexin (Cx) proteins. The increasing number of hereditary diseases linked to connexin mutations as well as the results of targeted deletion and replacement studies are yielding increasing evidence for the importance of gap junctions in normal development and function in a diverse array of tissues, organs and organ systems. Expression of the different connexins, including Cx43 and Cx40 which are the focus of the current study, within the body varies with time, location, and physiological state. The presence of a large number of connexin isoforms and their controlled expression suggests properties that are unique and specific to each connexin. Indeed, the various connexins form channels with different conductance, permeability, and selectivity properties. These

properties appear to be regulated in a connexin and tissue specific manner such that some physiological roles appear to be better served by specific connexins.

The properties of each connexin that make them suited for specific functional roles are not yet clear. Since the signature function of connexin proteins is the formation of channels that mediate direct intercellular communication, understanding 1) the biophysical parameters that dictate channel permeation and selectivity and 2) how those parameters could be regulated are clearly important in defining the contribution of connexin channels to coordinated function. The goals of the current study are to define these biophysical parameters and regulation thereof by PKC-mediated phosphorylation for gap junctions composed of Cx43, Cx40, and both Cx43 and Cx40.

Gap junction structure and nomenclature:

As mentioned, gap junctions are ubiquitous protein channels that are located at places of apposed cell membranes affording direct access between the cytosols of neighboring cells for transfer of electrical current and small molecules. Each cell contributes a half or hemichannel to a full gap junction channel. Each hemichannel is composed of six protein subunits termed connexins, which are named according to their molecular weight in kilodaltons. Connexin proteins contain four transmembrane domains; both amino and carboxy termini are located intracellularly resulting in two extracellular loops and one intracellular loop. Comparison of sequences of the different connexin isoforms reveals high levels of homology for the transmembrane domains, whereas the N and C termini and extracellular loop show divergence. Some connexins are capable of interacting to form channels of mixed connexin composition.

Hemichannels consisting of only one connexin isoform are termed homomeric, while hemichannels consisting of more than one connexin isoform are termed heteromeric. Junctional channels comprised of two hemichannels of similar composition are termed homotypic, while junctional channels composed of hemichannels with differing compositions are termed heterotypic.

Role of gap junctions in organ development and function:

The importance of gap junctions in development and function is increasingly evident from the number of hereditary diseases in humans attributed to connexin mutations and the results of targeted deletion studies in mice. Mutations in Cx32 lead to a demyelinating peripheral neuropathy (Charcot Marie Tooth Syndrome)(1); mutations in Cx26 lead to sensorineural deafness; and mutations in Cx50 lead to congenital cataracts (2-4). Targeted deletion studies have shown that: Cx43 and Cx45 are necessary for normal cardiac development (5,6); Cx37 is necessary for normal female fertility (7); Cx40 is required for normal conducted responses in blood vessels and for maintenance of normal blood pressure (8); Cx43 is necessary for normal excitation of the mature heart (9,10); and Cx45 is necessary for normal vascular development (6). Additionally, targeted gene replacement studies have shown that functional roles cannot necessarily be fulfilled by any of the connexins but rather require specific connexins with presumably unique, critical properties. For example, replacement of Cx43 with Cx26 results in dysfunctional reproductive organs and slowed ventricular conduction in the heart (11); and replacement of Cx43 with Cx31 leads to malformation in the subpulmonary outlet of the right ventricle and postnatal death similar to the Cx43 knockout animal (12). These

combined data suggest that gap junction channels and particularly channels formed of specific connexins are vital to proper development and function of cells, tissues, organs, and organ systems.

Role of gap junctions in the cardiovascular system:

One organ system where gap junctions have proven to play vital roles is that of the cardiovascular system. Gap junctions of the cardiovascular system include connexins 43, 40, 37, and 45. These connexins are often co-expressed in the same tissues and even the same cells. Connexin expression changes during development, in response to injury, and in various disease processes (13-16). Cx43 is expressed without Cx40 in the adult ventricle, but Cx40 expression precedes Cx43 in the developing ventricle before being gradually replaced by Cx43 over a period of several days (17). Hypertension leads to changes in expression level of Cx43 in resistance vessels and large arteries (18,19) and can also alter expression of Cx43 and Cx40 in the heart (20). Targeted ablation studies have demonstrated that Cx43 is necessary for normal cardiac development (5) and normal excitation of the mature heart (21,22). Cx43 deletion slows conduction in the atria (21) and ventricles (22) and predisposes the heart to atrial (21) and ventricular (23) arrhythmias. In vascular injury models Cx43 is upregulated and Cx37 downregulated in the endothelium such that Cx40 and Cx43 are co-expressed in injured regions (24,25), and wound healing is impaired if these changes in connexin expression are prevented (25). Cx43 is also involved in endothelial-induced mesenchymal cell differentiation into smooth muscle (26). All of these studies and many others suggest that gap junctions are

integrally involved in the development of the cardiovascular system and its function under both physiological and pathophysiological conditions and show that multiple connexins, including Cx43 and Cx40, can be variably expressed and co-expressed in a number of tissues.

Role of Gap junctions in growth control:

Another important process in which gap junctions appear to play a vital role is that of regulation and control of cell growth. Lowenstein (27) was the first to propose that gap junctions are important in intercellular transmission of molecules necessary for growth control, based on observations that the absence or disruption of intercellular communication resulted in disturbance of cellular growth control. Since that time, much more evidence has supported the idea that gap junctions do play a vital role in proper growth control, although the specific mechanism for this control has not been clearly defined. What is known is that disruption of gap junctional communication and development of cancer are correlated. Gap junction communication has repeatedly been shown to be decreased or absent in cancerous cell types (28). This decrease in junctional communication is often accompanied by a decrease in connexin expression in these cells (28). A study by Mesnil et al (29) showed that eight different carcinoma lines derived from tumors from a number of human and murine organs all showed a lack of gap junctional communication and connexin protein.

Further support for the role of gap junctional communication in proper control of cell growth comes from studies showing that when gap junctional communication is

disrupted, tumorigenesis is increased. For example, the Cx32 knockout mouse demonstrated an increased susceptibility to both spontaneous and chemically induced tumor formation (30). Conversely, the induction of expression of connexins in cancer cell lines has been shown to decrease growth rate *in vivo* (31). These combined data clearly suggest yet to be defined roles for gap junctions in control of cell growth.

Permeability of gap junctions to cytoplasmic molecules:

In some electrically excitable tissues, such as the heart, the important role of gap junctions in propagation of action potentials to allow for coordinated activity is well described (32,33). Gap junctions are also widely expressed in non-excitable cells, where their primary role for communication is not the electrical propagation of action potentials. In these cell types, as well as in electrically excitable cell types, diffusion of signaling molecules and metabolites may be key to the functional role of gap junction channels. Indeed, gap junctions of different types have been shown to be permeated by virtually all soluble second messengers, amino acids, nucleotides, calcium ions, glucose and its metabolites (34) and more recently by siRNA (35). The primary determinant for whether a substance demonstrates any permeability through gap junctions of a particular type appears to be the size of the permeant, whereas the ease with which each molecule transits certain connexin channels is determined by more complex factors, which include the charge and possibly the structure of the permeant molecule (34). The specific role that each connexin isoform plays in the communication of such signals and the potential ability to modulate communication of these signals are far from being fully understood.

Selectivity of gap junctions:

Given the large number of possible cytoplasmic permeants, it is reasonable to assume that one reason for the ≈20 connexin isoforms might be the ability of different connexin isosforms to differentially discriminate amongst these permeants for channel permeation. Mounting evidence suggests that different connexins do in fact show different abilities for permeation by endogenous cytoplasmic molecules (34) as well as exogenous molecules such as fluorescent dyes (36,37). The charge selectivities of connexin channels range from moderately anion selective for Cx32 (38) to approximately ≈10:1 cation selective for Cx40 (39), Cx45 (40), and Cx37 (40)(unpublished observations). Additionally, a number of studies have shown significant levels of selectivity amongst endogenous cytoplasmic permeants for individual connexin isoforms as well as differences in selecitivity between different connexin isoforms for the same permeants (34,41). When taken together with the fact that unitary channel conductance can vary from ≈10-300pS for different connexin isoforms, the combined conductance and selectivity data suggest a large amount of heterogeneity in geometry and electrostatic environment of channels formed from the various connexins.

While many advances have been made and continue to be made, our knowledge of the selectivities of channels formed of each of the connexin isoforms as well as the physical basis for such selectivities is far from complete. Even the relatively simple principles of charge and size selectivity have not been fully elucidated for gap junction channels of each of the connexin isoforms and certainly not for channels and junctions of more than one connexin isoform. Additionally, the extent to which selectivities for given

connexin isoforms might vary from one junction to the next and show the potential to be regulated has not been investigated. This variable selectivity may seem a probable result given that many connexins are known to form channels with several different levels of conductance and most connexins are phosphoproteins. The alteration in channel geometry which results in subconductance states as well as the added negative charge and potential change in geometry resulting from connexin phosphorylation could certainly give rise to altered charge or size selectivity for gap junction channels. One reason for the lack of further insight into these selectivities is the lack of a sufficiently quantitative approach for measurement of junctional charge and size selectivity, particularly for molecules in the size range of many of the cytoplasmic permeants being discussed.

To date, most selectivity measurements have involved either semi-quantitative comparison of dye movements across separate junctions, measurements of conductance using different salt solutions, the measurement of junctional reversal potentials under asymmetric transjunctional salt concentrations, or measurement of permselectivity (dye permeability/conductance) for different dyes across different junctions. While each of these approaches can provide some information with regard to selectivity properties of channels and junctions formed of each connexin isoform, all but the reversal potential strategy involve comparison of measurements across different junctions and thus different populations of channels between different cells. This then requires the assumption that each junction compared for a given connexin isoform must have the same selectivity properties, which may not be correct. Reversal potential experiments can yield quantitative charge selectivity measurements from a single channel or set of

channels, but is a technique that can be best applied only to isolated hemichannels or very poorly coupled cell pairs, situations that might not reflect the selectivity of transfer across typical gap junctions. Thus a quantitative measure of junctional charge or size selectivity that can be made across a single gap junction is needed for determination of the extent to which charge or size selectivity might vary from one junction to the next. Development of such a technique is one of the goals of the current study.

Independence of permeability and conductance:

It is well established that unitary conductance of gap junction channels is a poor predictor of permeability to fluorescent tracers or to the maximum size of a molecule that can permeate a channel formed of a given connexin type (36,42,43). This has been tested by measurement of permselectivity, where it has been found that channels with smaller unitary conductances can have higher permselectivities for a given dye than channels with larger unitary conductances (36,37). For example, by permselectivity measurement, Cx43 channels were shown to have a ≈10 fold higher permeability to Lucifer Yellow than Cx40 channels despite having only ≈60% the unitary conductance (≈100pS vs 180pS for Cx43 and Cx40 respectively) (37). Recently published data also shows that the permselectivity value for a given dye can vary by as much as several orders of magnitude for channels formed of the same connexin (Cx43) in the same cell types, presumably due to channels formed of the same connexin isoform showing significantly different levels of selectivity (44,45).

These permselectivity measurements can represent the sole impact of the physical cross section of the channel pore impeding diffusion through the channel but can also be complicated by electrostatic interactions of the dye permeant with any resident charges lining the channel pore, which can impede or enhance diffusion through the channel depending upon polarity. This turns out to be the case in the Cx43 vs Cx40 Lucifer Yellow permselectivity mentioned above, as Cx43 is generally non-selective with regards to charge whereas Cx40 shows an ≈10:1 preference for permeation by cations over anions (39). It is thus difficult to determine the extent to which the physical dimensions of the pore or resident charges lining the pore are contributing to the observed channel dye permeabilities.

In order to overcome such complications of charge selectivity, studies have been done using neutral polyethylene glycol probes (PEGs) of different sizes to investigate the size cutoff for permeation through different connexin channels. In these studies, conductance was measured before and after addition of PEGs and channel permeation by PEGs was evidenced by reduction in conductance through interference of the PEGs with ions attempting to traverse the channel carrying electrical current. The results of one such study (43) showed that for connexins 32, 26, and 37 the size cutoff was actually inversely related to unitary conductance. Cx37, which has the highest unitary conductance (≈300pS), showed the lowest size cutoff; and Cx32, which has the lowest unitary conductance (≈55pS), showed the highest size cutoff. Unitary conductance is thus not a reliable predictor of size selectivity for gap junction channels.

The above data suggest that at least some connexins form channels with heterogeneous geometries along their length. Both the high conductance/low size limit and low conductance/high size limit scenarios described above can be explained by simple variations in channel geometry. In channels as large as gap junction channels, conductance to small ions is dominated by average channel cross-section, while permeability to larger molecules can be dominated by the narrowest portion or limiting diameter of the channel pore. If an otherwise wider channel has a short section of its length with a much narrower diameter, this could significantly inhibit the diffusion of larger molecules while having a negligible impact on conductance of smaller ions, resulting in the high conductance/low size limit scenario. By contrast, if a channel is relatively narrow along its length but is devoid of any significant constrictions, this could result in a lower unitary conductance with a relatively higher permeability to larger molecules giving rise to the low conductance/high size limit scenario. Clearly, permeation through gap junction channels can be quite complex and cannot necessarily be predicted from the general measure of electrical conductance.

Significance:

Based on the rate at which Lucifer Yellow traverses some Cx43 gap junctions (37), it was suggested that rates of intercellular diffusion were insufficient to allow for significant communication of such short-lived signaling molecules as cyclic nucleotides, calcium and inositol tris phosphate (IP3). Recent data, however, indicate that the flux rates for larger solutes across junctions can vary by several orders of magnitude and

approach rates much higher than those initially proposed, which would make transmission of even short-lived signals through gap junctions a viable possibility (36,44,45). Thus the large number of cytoplasmic molecules that have been shown to permeate gap junction channels could effectively do so, even at physiological concentrations. Furthermore, the specific permeability of different connexins to each permeant could allow for connexin-specific roles in communication of particular signals and help explain the necessity for the large number of connexin isoforms and their controlled expression.

The potential ability to regulate the effective permeability of a gap junction in a selective manner (such that it discriminates between metabolites and chemical signals) over a broad range of permeabilities and selectivities, possibly without significantly altering its ability to transmit electrical signals (44,45), could be of physiological benefit in a number of situations. One such situation is myocardial ischemia and reperfusion, where the ability to control intercellular transit of metabolites and signaling molecules without significantly impacting electrical conductance could prove quite valuable. Interestingly, activation of PKC, which has been shown to phosphorylate Cx43, cause it to gate to a subconductance state (46) and to alter channel permselectivity (44), has been shown to occur early in ischemia and has cardioprotective effects (47-49). Specific predictions for the possible physiological impact of junctional selectivity and regulation of junctional selectivity in a broad range of scenarios await further understanding of the selectivity and permeability properties of junctions and channels formed of each

connexin and the extent and manner to which these selectivity and permeability properties can be regulated.

Summary

Gap junctions are clusters of membrane channels that directly connect the cytoplasm of adjacent cells allowing for electrical and chemical communication and intercellular coordination. The large number of gap junction protein isoforms, their controlled expression, and the results of targeted deletion and replacement studies suggest a variety of important and sometimes connexin-specific roles. A key role for connexin proteins is their ability to form gap junctions and to communicate a large number of cytoplasmic molecules between neighboring cells. The ability to communicate such molecules in a selective manner as a result of connexin-specific selectivities as well as the potential for regulation of these selectivities could prove to be vital in the role of gap junction channels in a broad range of situations. Understanding the biophysical principles governing these junctional selectivities and the extent to which these parameters can be altered by variable connexin expression or phosphorylation for gap junctions composed of Cx43, Cx40, or both connexins is the goal of the current study.

DESCRIPTION OF DISSERTATION FORMAT

The remainder of the dissertation contains four major chapters: a brief summary and conclusions chapter labeled 'Present Study', two research studies that have been published (Appendices A and C with supplemental data in Appendices B and D respectively), and one study that is not yet published (APPENDIX E). In addition, there is a brief chapter describing possible future directions for research (APPENDIX F). Each of the research chapters and supplemental materials is included as a separate appendix. Directly following this introduction is a brief chapter labeled "present study" that outlines the results and conclusions from the research chapters attached as appendices. I performed some of the control experiments and aided in data interpretation but was not the primary author for the study in APPENDIX A with supplemental data in APPENDIX B. For this study, my specific contribution was basically in two areas: First, I performed and analyzed the experiments demonstrating that the observed variability in permselectivity for the dye NBD-M-TMA was not due to the variable transport of NBD-M-TMA across the cell membrane via an organic cation transporter. Second, my preliminary dye selectivity results eventually published in APPENDIX C helped in interpretation of the permselectivity experiments by suggesting that variable permselectivity was not due to variable charge selectivity, which was being considered as a possible explanation. I performed all of the experiments and analysis and was the primary author for the study in APPENDIX C with data supplement in APPENDIX D. I performed a large majority of the experiments, all of the analysis, and was the primary author of the study in APPENDIX E.

PRESENT STUDY

The methods, results, and conclusions of this study are presented in several papers that are appended to this dissertation. The following is a summary of the most important findings in this document.

The aims of the present study were to:

1. *Determine the selectivity of Cx43 and Cx40 gap junctions and the extent to which these selectivities show interjunctional heterogeneity*.

2. *Determine the selectivity of gap junctions formed in Cx40/Cx43 co-expressing cells and the extent to which this selectivity shows interjunctional heterogeneity*.

3. *Determine the extent to which the selectivity of gap junctions formed in Cx43, Cx40, and Cx40/Cx43 co-expressing cells can be regulated by PKC-mediated phosphorylation*.

Each of these aims has been significantly investigated and following is a brief summary of the results and the conclusions drawn from these results.

Aim #1. *Determine the selectivity of Cx43 and Cx40 gap junctions and the extent to which these selectivities show interjunctional heterogeneity*.

This aim was investigated in two studies (Appendices A and C). In the first study (APPENDIX A) the permselectivity (dye permeability/electrical conductance) was investigated for the small cationic dye NBD-M-TMA across Cx43 gap junctions. There are two important findings from this study with regard to Cx43 junctional selectivity: 1. Permselectivity of junctions formed of a single connexin (Cx43) can vary across several orders of magnitude. 2. Phosphorylation of Cx43 by Protein Kinase C (PKC) at serine368 modulates junctional permselectivity to NBD-M-TMA. These data suggest that Cx43 can exist in at least two different states with considerably different permselectivity properties.

The variable permselectivity of Cx43 junctions could be explained by variability in charge or size selectivity of Cx43 channels and thus junctions. The extent to which Cx43 charge and size selectivity is variable was investigated in the study in APPENDIX C by simultaneous comparison of junctional permeance to dyes differing by either size or charge. There are two key findings from this study:

1. Cx43 charge and size dye selectivity are not significantly variable parameters.

2. Cx43 dye selectivity is well described by simple hindered diffusion through an aqueous pore approximately 20Å in diameter.

These data suggest that all dye-permeable Cx43 channels share similar selectivity characteristics that are based primarily on permeant size.

The seemingly disparate permselectivity and dye selectivity results can be reconciled by the variable presence of a dye-impermeable but electrically conductive

channel substate for Cx43 channels, which could afford a mechanism for independent regulation of diffusion of larger molecules versus electrical conductance to smaller ions.

Aim #2. *Determine the selectivity of gap junctions formed in Cx40/Cx43 co-expressing cells and the extent to which this selectivity shows interjunctional heterogeneity*.

This aim is investigated in the study attached as APPENDIX E. Using the same dual dye approach described in APPENDIX C, the selectivity of cells expressing Cx40, Cx43, or both Cx40 and Cx43 was investigated. There are three important results from this study with regard to aim #2:

1. Cx43 and Cx40 junctional dye selectivities are essentially fixed parameters with Cx43 being non-selective and Cx40 showing ≈11:1 cationic selectivity.

2. Average charge selectivity of cells expressing both Cx40 and Cx43 increases as the relative contribution of Cx40 (the more selective connexin) increases.

3. Cells that co-express Cx43 and Cx40 display individual junctional dye selectivities ranging from that of pure Cx43 to that of pure Cx40.

These data suggest that, while selectivity of Cx43 and Cx40 junctions appear fixed, co-expression of Cx43 and Cx40 allows for selectivities ranging from that of Cx40 to that of Cx43.

Aim #3. *Determine the extent to which the selectivity of gap junctions formed in Cx43, Cx40, and Cx40/Cx43 co-expressing cells can be regulated by PKC-mediated phosphorylation*.

This aim was investigated in the study attached as APPENDIX E. To test this, the charge selectivity of cells expressing Cx43, Cx40, and both Cx40 and Cx43 was investigated using the approach described in APPENDIX B under variable PKC-mediated phosphorylation conditions. There are three important findings from this study related to aim #3:

1. Variable phosphorylation of the Cx43 C-terminus does not result in significant changes in dye selectivity of Cx43 junctions, but PKC activation appears to eliminate dye permeability.

2. PKC activation has no effect on coupling or selectivity of Cx40 junctions.

3. PKC activation results in increased cationic junctional selectivity between cells expressing both Cx40 and Cx43.

These data suggest that, while dye selectivity of Cx43 and Cx40 junctions are not regulated by PKC, the charge selectivity of junctions expressing both Cx40 and Cx43 can be increased by PKC activation, likely by specifically decreasing dye permeability through less selective Cx43 channels without affecting permeability through Cx40 channels.

SUMMARY

The combined results of this work show several findings. First, the permeability to molecules the size of some fluorescent dyes (≈4-7 Å radii) can be independently regulated from conductance to smaller ions across Cx43 junctions and thus channels and that this could be the result of the variable presence of a dye-impermeable but electrically

conductive channel substate for Cx43 channels. Second, the dye selectivities of both Cx40 and Cx43 channels appear to be fixed properties of the channel pore. Finally, co-expression of Cx40 and Cx43 allows for regulation of junctional charge selectivity through PKC-mediated phosphorylation that is not available to cells expressing only Cx40 or Cx43.

REFERENCE LIST

1. Bergoffen,J., S.S.Scherer, S.Wang, M.Oronzi Scott, L.J.Bone, D.L.Paul, K.Chen, M.W.Lensch, P.F.Chance, and K.H.Fischbeck. 1993. Connexin mutations in X-linked Charcot-Marie-Tooth disease. *Science* 262:2039-2042.

2. Kerscher,S., R.L.Church, Y.Boyd, and M.F.Lyon. 1995. Mapping of four mouse genes encoding eye lens-specific structural, gap junction, and integral membrane proteins: *Cryba1 (Crystallin A3/A1), crybb2 (CrystallinB2), Gja8 (MP70),* and *lim2* (MP19). *Genomics* 29:445-450.

3. Pal,J.D., V.M.Berthoud, E.C.Beyer, D.Mackay, A.Shiels, and L.Ebihara. 1999. Molecular mechanism underlying a Cx50-linked congenital cataract. *Am. J. Physiol.* 276:C1443-6.

4. Berry,V., D.Mackay, S.Khaliq, P.J.Francis, A.Hameed, K.Anwar, S.Q.Mehdi, R.J.Newbold, A.Ionides, A.Shiels, T.Moore, and S.S.Bhattacharya. 1999. Connexin 50 mutation in a family with congenital "zonular nuclear" pulverulent cataract of Pakistani origin. *Hum. Genet.* 105:168-170.

5. Reaume,A.G., P.A.De Sousa, S.Kulkarni, B.L.Langille, D.Zhu, T.C.Davies, S.C.Juneja, G.M.Kidder, and J.Rossant. 1995. Cardiac Malformation in neonatal mice lacking connexin43. *Science* 267:1831-1834.

6. Kruger,O., A.Plum, J.S.Kim, E.Winterhager, S.Maxeiner, G.Hallas, S.Kirchhoff, O.Traub, W.H.Lamers, and K.Willecke. 2000. Defective vascular development in connexin 45-deficient mice. *Development* 127:4179-4193.

7. Simon,A.M., D.A.Goodenough, E.Li, and D.L.Paul. 1997. Female infertility in mice lacking connexin 37. *Nat.* 385:525-529.

8. de Wit,C., F.Roos, S.S.Bolz, S.Kirchhoff, O.Kruger, K.Willecke, and U.Pohl. 2000. Impaired conduction of vasodilation along arterioles in connexin40- deficient mice. *Circ. Res.* 86:649-655.

9. Simon,A.M., D.A.Goodenough, and D.L.Paul. 1998. Mice lacking connexin40 have cardiac conduction abnormalities characteristic of atroventricular block and bundle branch block. *Curr. Biol.* 8:295-298.

10. Kirchhoff,S., E.Nelles, A.Hagendorff, O.Kruger, O.Traub, and K.Willecke. 1998. Reduced cardiac conduction velocity and predisposition to arrhythmias in connexin40-deficient mice. *Curr. Biol.* 8:299-302.

11. Winterhager,E., N.Pielensticker, J.Freyer, A.Ghanem, J.W.Schrickel, J.S.Kim, R.Behr, R.Grummer, K.Maass, S.Urschel, T.Lewalter, K.Tiemann, M.Simoni, and K.Willecke. 2007. Replacement of connexin43 by connexin26 in transgenic mice leads to dysfunctional reproductive organs and slowed ventricular conduction in the heart. *BMC. Dev. Biol.* 7:26.:26.

12. Zheng-Fischhofer,Q., A.Ghanem, J.S.Kim, M.Kibschull, G.Schwarz, J.O.Schwab, J.Nagy, E.Winterhager, K.Tiemann, and K.Willecke. 2006. Connexin31 cannot functionally replace connexin43 during cardiac morphogenesis in mice. *J. Cell Sci.* 119:693-701.

13. Saffitz,J.E. 2000. Regulation of intercellular coupling in acute and chronic heart disease. *Braz. J. Med. Biol. Res.* 33:407-413.

14. Severs,N.J., S.Rothery, E.Dupont, S.R.Coppen, H.I.Yeh, Y.S.Ko, T.Matsushita, R.Kaba, and D.Halliday. 2001. Immunocytochemical analysis of connexin expression in the healthy and diseased cardiovascular system. *Microsc. Res. Tech.* 52:301-322.

15. Coppen,S.R., R.A.Kaba, D.Halliday, E.Dupont, J.N.Skepper, S.Elneil, and N.J.Severs. 2003. Comparison of connexin expression patterns in the developing mouse heart and human foetal heart. *Mol. Cell Biochem.* 242:121-127.

16. Levin,M. 2002. Isolation and community: a review of the role of gap-junctional communication in embryonic patterning. *J. Membr. Biol.* 185:177-192.

17. Delorme,B., E.Dahl, T.Jarry-Guichard, J.P.Briand, K.Willecke, D.Gros, and M.Theveniau-Ruissy. 1997. Expression pattern of connexin gene products at the early developmental stages of the mouse cardiovascular system. *Circ. Res.* 81:423-437.

18. Haefliger,J.A., P.Meda, A.Formenton, P.Wiesel, A.Zanchi, H.R.Brunner, P.Nicod, and D.Hayoz. 1999. Aortic connexin43 is decreased during hypertension induced by inhibition of nitric oxide synthase. *Arterioscler. Thromb. Vasc. Biol.* 19:1615-1622.

19. Haefliger,J.A., E.Castillo, G.Waeber, G.E.Bergonzelli, J.F.Aubert, E.Sutter, P.Nicod, B.Waeber, and P.Meda. 1997. Hypertension increases connexin43 in a tissue-specific manner. *Circ.* 95:1007-1014.

20. Bastide,B., L.Neyses, D.Ganten, M.Paul, K.Willecke, and O.Traub. 1993. Gap junction protein Connexin40 is preferentially expressed in vascular endothelium and conductive bundles of rat myocardium and is increased under hypertensive conditions. *Circ. Res.* 73:1138-1149.

21. Kanagaratnam,P., S.Rothery, P.Patel, N.J.Severs, and N.S.Peters. 2002. Relative expression of immunolocalized connexins 40 and 43 correlates with human atrial conduction properties. *J. Am. Coll. Cardiol.* 39:116-123.

22. Vaidya,D., H.S.Tamaddon, C.W.Lo, S.M.Taffet, M.Delmar, G.E.Morley, and J.Jalife. 2001. Null mutation of connexin43 causes slow propagation of ventricular activation in the late stages of mouse embryonic development. *Circ. Res.* 88:1196-1202.

23. Betsuyaku,T., A.Kovacs, J.E.Saffitz, and K.A.Yamada. 2002. Cardiac structure and function in young and senescent mice heterozygous for a connexin43 null mutation. *J. Mol. Cell Cardiol.* 34:175-184.

24. Gabriels,J.E. and D.L.Paul. 1998. Connexin43 is highly localized to sites of disturbed flow in rat aortic endothelium but connexin37 and connexin40 are more uniformly distributed [see comments]. *Circ. Res.* 83:636-643.

25. Kwak,B.R., M.S.Pepper, D.B.Gros, and P.Meda. 2001. Inhibition of endothelial wound repair by dominant negative connexin inhibitors. *Mol. Biol. Cell* 12:831-845.

26. Hirschi,K.K., J.M.Burt, K.D.Hirschi, and C.Dai. 2003. Gap junction communication mediates transforming growth factor-beta activation and endothelial-induced mural cell differentiation. *Circ. Res.* 93:429-437.

27. Loewenstein,W.R. 1979. Junctional intercellular communication and the control of growth. *Biochim. Biophys. Acta* 560:1-65.

28. Leithe,E., S.Sirnes, Y.Omori, and E.Rivedal. 2006. Downregulation of gap junctions in cancer cells. *Crit Rev. Oncog.* 12:225-256.

29. Mesnil,M., D.Rideout, N.M.Kumar, and N.B.Gilula. 1994. Non-communicating human and murine carcinoma cells produce $\square_1$ gap junction mRNA. *Carcinogenesis* 15:1541-1547.

30. Temme,A., A.Buchmann, H.D.Gabriel, E.Nelles, M.Schwarz, and K.Willecke. 1997. High incidence of spontaneous and chemically induced liver tumors in mice deficient for connexin32. *Curr. Biol.* 7:713-716.

31. Eghbali,B., J.A.Kessler, L.M.Reid, C.Roy, and D.C.Spray. 1991. Involvement of gap junctions in tumorigenesis: Transfection of tumor cells with connexin 32 cDNA retards growth in vivo. *Proc. Natl. Acad. Sci.* 88:10701-10705.

32. Cole,W.C., J.B.Picone, and N.Sperelakis. 1988. Gap junction uncoupling and discontinuous propagation in the heart. *Biophys. J.* 53:809-818.

33. Brink,P.R., K.Cronin, and S.V.Ramanan. 1996. Gap junctions in excitable cells. [Review] [46 refs]. *J. Bioenerg. Biomembr.* 28:351-358.

34. Harris,A.L. 2007. Connexin channel permeability to cytoplasmic molecules. *Prog. Biophys. Mol. Biol.* 94:120-143.

35. Valiunas,V., Y.Y.Polosina, H.Miller, I.A.Potapova, L.Valiuniene, S.Doronin, R.T.Mathias, R.B.Robinson, M.R.Rosen, I.S.Cohen, and P.R.Brink. 2005. Connexin-specific cell-to-cell transfer of short interfering RNA by gap junctions. *J. Physiol.* 568:459-468.

36. Weber,P.A., H.C.Chang, K.E.Spaeth, J.M.Nitsche, and B.J.Nicholson. 2004. The permeability of gap junction channels to probes of different size is dependent on connexin composition and permeant-pore affinities. *Biophys. J.* 87:958-973.

37. Valiunas,V., E.C.Beyer, and P.R.Brink. 2002. Cardiac gap junction channels show quantitative differences in selectivity. *Circ. Res.* 91:104-111.

38. Suchyna,T.M., J.M.Nitsche, M.Chilton, A.L.Harris, R.D.Veenstra, and B.J.Nicholson. 1999. Different ionic selectivities for connexins 26 and 32 produce rectifying gap junction channels. *Biophys. J.* 77:2968-2987.

39. Heyman,N.S. and J.M.Burt. 2007 *in press*. Hindered diffusion through an aqueous pore describes invariant dye selectivity of Cx43 junctions. *Biophys. J.*

40. Veenstra,R.D., H.-Z.Wang, E.C.Beyer, and P.R.Brink. 1994. Selective dye and ionic permeability of gap junction channels formed by connexin45. *Circ. Res.* 75:483-490.

41. Goldberg,G.S., V.Valiunas, and P.R.Brink. 2004. Selective permeability of gap junction channels. *Biochim. Biophys. Acta* 1662:96-101.

42. Veenstra,R.D., H.Z.Wang, D.A.Beblo, M.G.Chilton, A.L.Harris, E.C.Beyer, and P.R.Brink. 1995. Selectivity of connexin-specific gap junctions does not correlate with channel conductance. *Circ. Res.* 77:1156-1165.

43. Gong,X.Q. and B.J.Nicholson. 2001. Size selectivity between gap junction channels composed of different connexins. *Cell Commun. Adhes.* 8:187-192.

44. Ek-Vitorin,J.F., T.J.King, N.S.Heyman, P.D.Lampe, and J.M.Burt. 2006. Selectivity of connexin 43 channels is regulated through protein kinase C-dependent phosphorylation. *Circ. Res.* 98:1498-1505.

45. Eckert,R. 2006. Gap-junctional single-channel permeability for fluorescent tracers in Mammalian cell cultures. *Biophys. J.* 91:565-579.

46. Lampe,P.D., E.M.Tenbroek, J.M.Burt, W.E.Kurata, R.G.Johnson, and A.F.Lau. 2000. Phosphorylation of connexin43 on serine368 by protein kinase C regulates gap junctional communication. *J. Cell Biol.* 149:1503-1512.

47. Garcia-Dorado,D., M.Ruiz-Meana, F.Padilla, A.Rodriguez-Sinovas, and M.Mirabet. 2002. Gap junction-mediated intercellular communication in ischemic preconditioning. *Cardiovasc. Res.* 55:456-465.

48. Armstrong,S.C. 2004. Protein kinase activation and myocardial ischemia/reperfusion injury. *Cardiovasc. Res.* 61:427-436.

49. Cross,H.R., E.Murphy, R.Bolli, P.Ping, and C.Steenbergen. 2002. Expression of activated PKC epsilon (PKC epsilon) protects the ischemic heart, without attenuating ischemic H(+) production. *J. Mol. Cell Cardiol.* 34:361-367.

APPENDIX A

SELECTIVITY OF CONNEXIN43 CHANNELS IS REGULATED THROUGH PROTEIN KINASE C-DEPENDENT PHOSPHORYLATION

Jose F. Ek-Vitorin, Timothy J. King, Nathanael S. Heyman, Paul D. Lampe, Janis M. Burt

LIPPINCOTT
WILLIAMS & WILKINS
A Wolters Kluwer Company

October 22, 2007

Nathanael Heyman
PhD Graduate Student
University of Arizona
Department of Physiology
PO Box 245051
Tucson, AZ 85724

VIA EMAIL TO: nheyman@email.arizona.edu October 10, 2007

FEE: None

RE: Selectivity of connexin 43 channels is regulated through protein kinase C-dependent phosphorylation. Circ Res. 2006 Jun 23;98(12):1498-505. Epub 2006 May 18.

USE: Thesis

CONDITION OF AGREEMENT

Permission is granted upon the return of this signed agreement to Lippincott Williams & Wilkins (LWW). Please sign and date this form and return to:

Lippincott Williams & Wilkins
David O'Brien, Worldwide Copyright Management
351 W Camden Street, 4 North
Baltimore, MD 21201
USA

Permission is granted and is subject to the following conditions:

1) A credit line will be prominently placed and include the journal article author and article title, journal title, volume number, issue number, and the inclusive pages.
2) The requestor warrants that the material shall not be used in any manner, which may be derogatory to the title, content, or authors of the material or to LWW.
3) Permission is granted for one time use only as specified in your correspondence. Rights herein do not apply to future reproductions, editions, revisions, or other derivative works.
4) Permission granted is non-exclusive, and is valid throughout the world in the English language.
5) LWW cannot supply the requestor with the original artwork or a "clean copy".
6) Permission is valid if the borrowed material is original to a LWW imprint (Lippincott-Raven Publishers, Williams & Wilkins, Lea & Febiger, Harwal, Igaku-Shoin, Rapid Science, Little Brown & Company, Harper & Row Medical, American Journal of Nursing Co., and Urban & Schwarzenberg-English language.)

Requestor accepts: Nathanael Heyman Date: 10/22/07

Cellular Biology

Selectivity of Connexin 43 Channels Is Regulated Through Protein Kinase C–Dependent Phosphorylation

Jose F. Ek-Vitorin, Timothy J. King, Nathanael S. Heyman, Paul D. Lampe, Janis M. Burt

Abstract—Coordinated contractile activation of the heart and resistance to ischemic injury depend, in part, on the intercellular communication mediated by Cx43-composed gap junctions. The function of these junctions is regulated at multiple levels (assembly to degradation) through phosphorylation at specific sites in the carboxyl terminus (CT) of the Cx43 protein. We show here that the selective permeability of Cx43 junctions is regulated through protein kinase C (PKC)-dependent phosphorylation at serine 368 (S368). Selective permeability was measured in several Cx43-expressing cell lines as the rate constant for intercellular dye diffusion relative to junctional conductance. The selective permeability of Cx43 junctions under control conditions was quite variable, as was the open-state behavior of the comprising channels. Coexpression of the CT of Cx43 as a distinct protein, treatment with a PKC inhibitor, or mutation of S368 to alanine, all reduced (or eliminated) phosphorylation at S368, reduced the incidence of 55- to 70-pS channels, and reduced by 10-fold the selective permeability of the junctions for a small cationic dye. Because PKC activation during preischemic conditioning is cardioprotective during subsequent ischemic episodes, we examined no-flow, ischemic hearts for Cx43 phosphorylated at S368 (pS368). Consistent with early activation of PKC, pS368-Cx43 was increased in ischemic hearts; despite extensive lateralization of total Cx43, pS368-Cx43 remained predominantly at intercalated disks. Our data suggest that the selectivity of gap junction channels at intercalated disks is increased early in ischemia. (*Circ Res*. 2006;98:1498-1505.)

Key Words: gap junction ■ connexin 43 ■ phosphorylation ■ selectivity ■ ischemia

Gap junctions are clusters of intercellular channels that mediate electrical and chemical signaling throughout the cardiovascular system.[1,2] Gap junction channels are formed when hemichannels (connexons) in the membranes of neighboring cells dock. Each hemichannel is a hexamer of connexin subunits; in cells of the cardiovascular system, 4 members of the connexin gene family are commonly expressed: Cx45, Cx43, Cx40, and Cx37. The predominant connexin expressed in ventricular cells is Cx43, the focus of the current study. In the normally functioning ventricle, Cx43 is localized to intercalated disks where it supports the longitudinal and transverse (zigzag) spread of the action potential, such that coordinated contractile activation of the heart occurs. The contractile failure and arrhythmias occurring during ischemia reflect, in addition to compromised metabolism, altered excitability, and reduced electrical coupling.[3]

Exposure of the heart to a brief period of ischemia and reperfusion (termed ischemic preconditioning) before a prolonged ischemic period protects the heart against necrosis and fatal arrhythmias.[4] During the ischemic preconditioning period, receptor-mediated activation of protein kinase C (PKC) occurs and appears to be necessary for protection against injury during the subsequent prolonged ischemic period. Thus, PKC activation (and translocation to the particulate fraction) is the initial step in a complex cascade of intracellular events that constitute an intrinsic defense strategy.[5] The immediate consequences of PKC activation are unclear but ultimately, during the subsequent prolonged ischemic period, apoptosis is reduced, the cytoskeleton stabilized, and mitochondrial function preserved. Some of these effects may well be mediated by kinases such as mitogen-activated protein kinase (MAPK) and Src, which are activated in parallel with or downstream from PKC activation.

PKC, MAPK, and Src directly phosphorylate Cx43, effecting an acute (within minutes) reduction of channel conductance and/or open probability.[6–10] Over a somewhat longer time frame (tens of minutes to multiple hours), activation of these kinases leads to compromised Cx43 targeting/retention at intercalated disks and ultimately altered Cx43 gene expression.[11,12] In the heart, these phosphorylation-dependent changes in gap junction function likely contribute to an overall reduction in conduction velocity and increased dispersion of action potential duration and refractory properties, which combine to form the substrate for potentially lethal arrhythmias.[13] Consequently, these phosphorylation events appear to be counterproductive to continued coordinated activation of the heart and yet are ultimately protective to the

heart and to other tissues in injury settings.[14–16] These apparently contradictory observations suggest that phosphorylation modulates an as yet unidentified parameter of channel function (eg, selectivity) in a manner that is ultimately beneficial to tissue survival. We demonstrated previously that serine 368 (S368) is required for a PKC-mediated reduction in channel conductance.[8] We show here that this site is involved in regulating the selective permeability of the junction. We further show, using a whole heart model, that following 30 minutes of flow-deprivation at 37°C, Cx43 phosphorylated at this site was increased but remained predominantly localized at the intercalated disks despite ongoing gap junction remodeling.

Materials and Methods

Cells

Normal rat kidney epithelial (NRK) cells, transfected (or not) with the carboxyl terminus (CT) of Cx43 (NRK-CT)[17]; Rin43 cells, a rat insulinoma cell line stably transfected with rCx43 (CMV promoter)[18]; Re43 and Re43-S368A cells, derived from $Cx43^{-/-}$ cells and stably transfected with rCx43 (22C-3 or MC:Re43)[19,20] or rCx43-S368A (pI8),[8] and Chinese Hamster Ovary (CHO) cells transfected with hOCT2, were all grown and maintained as appropriate (see the expanded Materials and Methods section in the online data supplement available at http://circres.ahajournals.org).

Junctional Permeability, Junctional Conductance, Single-Channel Conductance

Cells were visualized on an upright microscope equipped for epifluorescence and differential interference contrast (DIC) observation. The donor cell was accessed with a patch-type microelectrode containing our standard solution,[21,22] 0.1 mg/mL of rhodamine-labeled dextran (≈3000 Da), and either 0.25 mmol/L NBD-M-TMA (*N,N,N*-trimethyl-2-[methyl(7-nitro-2,1,3-benzoxadiazol-4-yl)amino]ethanaminium, charge 1+; molecular mass, 280 Da[23]) or 1 mmol/L LY (Lucifer Yellow CH, charge 2−, molecular mass 443 Da). Multiple images of NBD-M-TMA or LY fluorescence were acquired[21]; after 10 to 20 minutes, the recipient cell was accessed and both cells voltage clamped (0 mV holding potential) to assess macroscopic (V_j=10 mV) and single-channel (V_j=40 mV, following application of halothane) conductances using standard techniques but with discontinuous single-electrode voltage clamp amplifiers.[21] Rhodamine–dextran fluorescence was typically imaged after measurements of junctional conductance. (See the expanded Materials and Methods section in the online data supplement for more details).

Data Analysis

Junctional permeability to a specific dye was quantified as the rate constant for intercellular diffusion of that dye (k_2) according to the procedures described by Ek-Vitorin and Burt.[21] The selective permeability for a specific dye was calculated as $k_{2\text{-}dye}/g_j$. Junctional conductance (g_j) and channel conductances were calculated from Ohm's law (see the expanded Materials and Methods section in the online data supplement). Single channel conductances were binned in 5-pS bins.

Whole Heart Studies

All mouse studies were conducted under Institutional Animal Care and Use Committee approval (FHCRC). Inbred mice (11 months of age in a FVB/N:C57BL6 background) were anesthetized (avertin, 0.3 mg/g body weight), hearts excised and placed either in cold PBS (with or without 1.8 mmol/L calcium, glucose free) for 30 to 60 seconds (control group), or incubated without coronary perfusion in warm (37°C), nonoxygenated PBS for 30 minutes ("ischemic group"). Although not thoroughly characterized,[24] this treatment reproduces the effects of ischemia on Cx43 electrophoretic mobility and gap junction remodeling (see Results) revealed in better characterized models of ischemia.[25,26] Hearts in both groups were next longitudinally bisected and either immediately sonicated in Laemmli sample buffer (for Western analysis) or fixed overnight at 4°C in 10% formalin (for immunohistochemistry).

Western Blots

After blotting, protein was detected with rabbit primary antibodies against Cx43 phosphorylated at S368 (pS368; 1:1000, Cell Signaling Inc), GAPDH (Ambion), or vinculin (Sigma) and mouse anti-Cx43NT.[27] Primary antibodies were visualized with either AlexaFluor 680 goat anti-rabbit (Molecular Probes) or IRDye800-conjugated donkey anti-mouse IgG (Rockland Immunochemicals) and directly quantified using the LI-COR Biosciences Odyssey infrared imaging system and associated software (inverted images are shown). See the expanded Materials and Methods section in the online data supplement.

Immunohistochemistry

Formalin-fixed tissue was paraffin embedded, sectioned (4 μm), immuno- and counterstained (hematoxylin/eosin [H&E]), and microscopically analyzed as previously described.[28] See the expanded Materials and Methods section in the online data supplement.

Results

Gap Junction Selective Permeability: Control Setting

The rate constant (k_2) for intercellular diffusion of either LY ($k_{2\text{-}LY}$) or NBD-M-TMA ($k_{2\text{-}NBD}$) was determined and related to the junction's conductance (g_j)[21] in NRK (endogenous expression of rCx43),[29,30] Rin43,[31,32] and Re43[20] cells. Figure 1 illustrates our strategy for determining k_2. A and B show DIC, LY, or NBD fluorescence, and rhodamine–dextran fluorescence images of pairs of NRK cells. Fluorescence intensity as a function of time is plotted for both donor and recipient cells in Figure 1C (LY) and 1D (NBD-M-TMA), and the fluorescence of the recipient cell was fit to determine k_2 for each junction.[21] Although g_j was nearly 2-fold larger in the LY cell pair, the rate constant for intercellular diffusion of LY versus NBD-M-TMA was nearly 10-fold less. $k_{2\text{-}NBD}$ versus g_j data from 25 NRK pairs, 26 Rin43 pairs, 7 Re43 pairs, and $k_{2\text{-}LY}$ versus g_j data for 10 NRK pairs (g_j>1nS for all pairs) are plotted in Figure 1E. Neither $k_{2\text{-}NBD}$ nor $k_{2\text{-}LY}$ was linearly related to g_j (R^2_{NBD}=0.07; R^2_{LY}=0.133). On average, $k_{2\text{-}LY}$ was nearly 10-fold lower than $k_{2\text{-}NBD}$ (NBD-M-TMA: 1.07±0.20 sec^{-1}, n=25; LY: 0.13±0.04 sec^{-1}, n=10; P<0.0001).

NBD-M-TMA was designed as a fluorescent substrate for organic cationic transporters (eg, OCT-1 and OCT-2)[23] and was later recognized as a superb junctional permeant.[21] To rule out a possible contribution of OCTs to our k_2 and g_j data (absence of a linear relationship), we cocultured Rin43 or NRK cells with hOCT2-transfected CHO cells, exposed the cocultures to 250 μmol/L NBD-M-TMA for 10 minutes under conditions that support OCT-mediated facilitated diffusion, and examined the cells for dye uptake. Neither the NRK or Rin43 cells expressed functional OCT-mediated uptake (Figure 2); however, when these cells formed contacts with the hOCT2-CHO cells, they were sometimes observed to contain dye. These results indicate that OCT-mediated transport played no role in the variable relationship between k_2 and g_j and further indicate that heterocellular junctions capable of

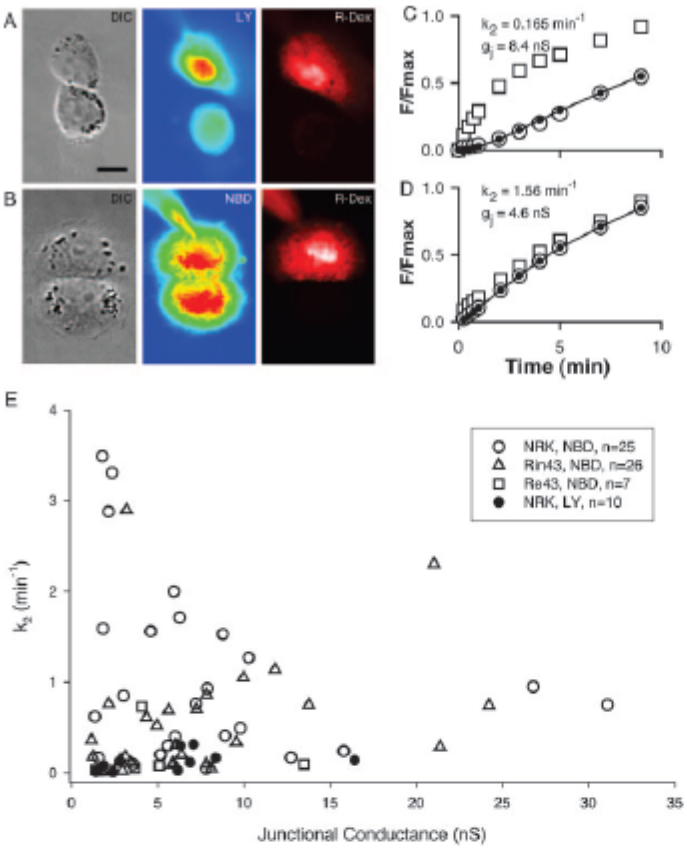

Figure 1. Intercellular diffusion rate for LY and NBD-M-TMA in Cx43-expressing cells is not predicted by junctional conductance. A and B, DIC and false-colored fluorescence images of NRK cell-pairs showing LY (A) or NBD-M-TMA (B) in donor and recipient cells 5 minutes after access to the donor cell was achieved. For both cell pairs, rhodamine–dextran (R-Dex) was observed only in the donor cell, which indicates that a gap junction rather than a cytoplasmic bridge connected the cells (calibration, 10 μm). C and D show, for the cells in A and B, respectively, the time course of fluorescence increase (F/Fmax, where F is the fluorescence at the indicated time and Fmax the maximum observed fluorescence) in the donor (squares) versus recipient cells (open circles). Closed circles and line represent the best fit[21] of the recipient fluorescence data; k_2 and g_j values for each pair are noted in the figure. E shows the k_2 vs g_j values for multiple cell pairs. Note the absence of correlation between the two parameters. The range of values for $k_{2\text{-NBD}}/g_j$ was considerably larger in NRK vs Rin43 cells, 0.006 to 1.93 min^{-1}nS^{-1} vs 0.006 to 0.906 min^{-1}nS^{-1}, respectively.

supporting intercellular dye diffusion can form between OCT2-CHO and other Cx43 expressing cells.

Nonlinearity of Intercellular Dye Permeability Versus Junctional Conductance

If the selectivity of all channels comprising Cx43 junctions were identical (ie, if they behave as simple pores), then k_2 and g_j would be expected to increase in a related fashion as the number of junctional channels increased. A linear relationship between ostensibly comparable parameters was previously reported[33] for LY permeation of Cx43 junctions as formed by HeLa cells; thus, the result shown in Figure 1E was somewhat unexpected.[33,34] We hypothesized that the lack of linear correlation between k_2 and g_j observed in our experiments reflected differential phosphorylation of Cx43, an indicator of which is variable channel open-state behavior.[6,8] To evaluate this possibility, we studied channel behavior; Figure 3 shows multiple segments of single channel records and associated all-points histograms derived from Rin43 (A through C) and NRK (D through F) cell pairs. Successive traces from the same cell pair as well as from different pairs demonstrated that not all channels in the junctions formed by these cells opened to the same conductance level. Figure 4 shows amplitude histograms compiled from multiple Rin43 (A) or NRK (B) cell pairs; for both cell types, multiple open states were evident, but their relative frequencies differed. Shown in Figure 4C (Rin43) and 4D (NRK) are amplitude histograms derived from cell pairs with high versus low selective permeability for NBD-M-TMA ($k_{2\text{-NBD}}/g_j$). The data show that high selective permeability for NBD-M-TMA occurred in pairs with a high incidence of 55- to 70-pS channels, whereas low selective permeability for NBD-M-TMA was observed in pairs where such events were rare.

pS368 and Junctional Selective Permeability

We hypothesized that phosphorylation of Cx43 at S368 (pS368) was necessary for high junctional NBD-M-TMA selective permeability, because this site is also necessary for PKC-induced formation of the 50- to 60-pS conductance state. We used 3 strategies to reduce the contribution of pS368 to total Cx43 protein: the Rin43 cells were treated with the PKC inhibitor BIM (bisindolylmaleimide); the parental fibroblast line used to create the Re43 cells[8] was stably transfected with Cx43-S368A; and the NRK cells were transfected such that expression of the CT of Cx43 as a separate entity could be induced.[17] To demonstrate that overexpression of the CT was effective at reducing pS368, we immunoblotted total protein from NRK and NRK-CT cells for total and pS368-Cx43 content. The NRK cells endoge-

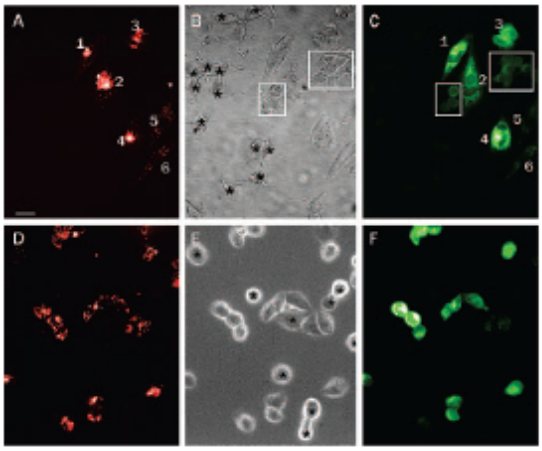

Figure 2. Rin43 and NRK cells do not express functional organic cation transport. hOCT2- CHO cells prelabeled with DiI (red cells) were cocultured with unlabeled Rin43 (A through C) or NRK (D through F) cells and exposed to 250 μmol/L NBD-M-TMA in Waymouth's buffer for 10 minutes. Robust uptake (C) of NBD-M-TMA was evident in DiI-labeled, hOCT2-CHO cells but not in isolated Rin43 cells (labeled with asterisks in the phase image, B). Rin43 cells contacting a hOCT-CHO cell either directly or via another Rin43 cell (boxed cells) received dye in a contact-dependent manner. Similar results are shown in D through F for NRK cells, which also do not express functional organic cation transport. (Images presented in false color. Calibration bar=20 μm, applies to all panels.)

nously express Cx43 in P and P_0 forms (Figure 5). Induced expression of the CT did not significantly change total Cx43 expression; however, pS368-Cx43 content was decreased by 30% ($P<0.015$).

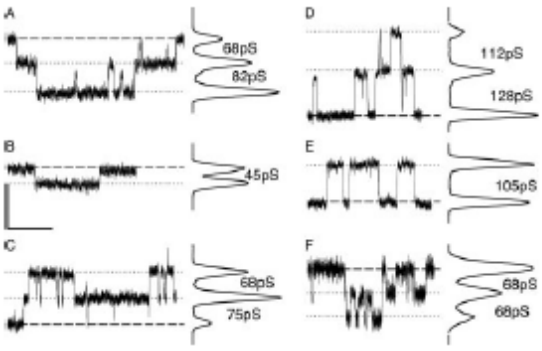

Figure 3. Cx43 opens to multiple conductance levels in both Rin43 (A through C) and NRK (D through F) cells. Shown are single-channel events and corresponding all-points histograms obtained from the same pair of Rin43 cells (A and B) following two different halothane treatments and from a second pair of Rin43 cells (C). Similar data are shown for a pair of NRK cells (D and E) and a second NRK pair (F). Events of different amplitudes are evident both within and between pairs; conductances of corresponding channel events are indicated as interpeak values on the all-points histograms. Dashed lines indicate the position of zero current; dotted lines mark open-state current levels. (V_j in all records: 40 mV; calibrations: y=5 pA, x=2 seconds, except for C, where it is 4 seconds; all records were sampled at 2 kHz and subsequently filtered at 100 Hz.)

Figure 6 shows single channel records with all-points histograms for BIM-treated Rin43 (A and B) and NRK-CT (C and D) cells. In both groups, 55- to 70-pS events like those in C were rarely observed. Figure 7 shows amplitude histograms compiled from multiple pairs of BIM-treated Rin43 (B) and NRK-CT (C) cells. The contribution of 55- to 70-pS events to the total population of events was drastically reduced in both groups, consistent with reduced phosphorylation at S368.

The $k_{2\text{-NBD}}$ versus g_j plots for the three pS368-reduction strategies revealed that $k_{2\text{-NBD}}$ was significantly reduced (control: 0.75 ± 0.12 min^{-1} (n=58); pS368-reduced: 0.23 ± 0.05 min^{-1} (n=27), $P<0.0001$), particularly at lower g_j values (compare k_2 versus g_j plot in Figure 7A to that in Figure 1E). These data strongly suggest that phosphorylation at S368 is necessary for high selective permeability for NBD-M-TMA as well as the 55- to 70-pS open state. The overall effect of phosphorylation at this site on selective permeability was evident in the significant reduction in $k_{2\text{-NBD}}/g_j$ resulting from BIM treatment of Rin43 cells ($k_{2\text{-NBD}}/g_j$ in Rin43: 0.12 ± 0.04 min^{-1}nS^{-1}, n=26 versus Rin43+BIM: 0.02 ± 0.007 min^{-1}nS^{-1}, n=6; $P<0.02$) or CT expression in NRK cells ($k_{2\text{-NBD}}/g_j$ in NRK: 0.33 ± 0.10 min^{-1}nS^{-1}, n=25 versus NRK-CT: 0.05 ± 0.02 min^{-1}nS^{-1}, n=13; $P<0.014$). Low $k_{2\text{-NBD}}/g_j$ values were also obtained for cells expressing the Cx43-S368A mutant (0.02 ± 0.009 min^{-1}nS^{-1}, n=8).

Phosphorylation of Cx43 in Ischemic Heart

The data presented above suggest that permeability and conductance are parameters of Cx43 channel function regulated by PKC-dependent phosphorylation of Cx43 at S368. PKC activation during ischemic preconditioning treatments is cardioprotective during subsequent ischemic events; consequently, we asked whether phosphorylation at this residue increased early during no-flow ischemia. Previous studies showed that the electrophoretic mobility of Cx43 isolated from ischemic heart is increased, such that most of the protein travels in a band that comigrates with dephosphorylated Cx43, the P_0 band.[25] The P_0 band can, however, contain Cx43 phosphorylated at S368.[29] Consequently, we evaluated total protein isolated from three control and three ischemic hearts for total Cx43 and pS368-Cx43. Consistent with previous observations, the electrophoretic mobility of Cx43 isolated from no-flow ischemic hearts was increased compared with normal (Figure 8A, each lane represents a separate heart). In addition, a decrease of total Cx43, possibly attributable to some loss of the protein during ischemia or, alternatively, to lower avidity of the antibody for less-phosphorylated forms of Cx43, was observed. Figure 8A further shows that pS368-Cx43 content increased ~5-fold ($P<0.02$) relative to total Cx43 in the ischemic hearts and that nearly all of this pS368-Cx43 comigrated with the "dephosphorylated" Cx43 (P_0 band). Identical results were obtained whether the PBS contained 1.8 mmol/L $CaCl_2$ or was calcium free; moreover, the described changes in electrophoretic mobility of Cx43 were evident, although less prominently, after only 5 minutes of no-flow ischemia (not shown).

The distribution of pS368-Cx43 versus total Cx43 in ischemic versus control tissue was quite distinct. Figure 8B shows that in control hearts virtually all Cx43 was localized

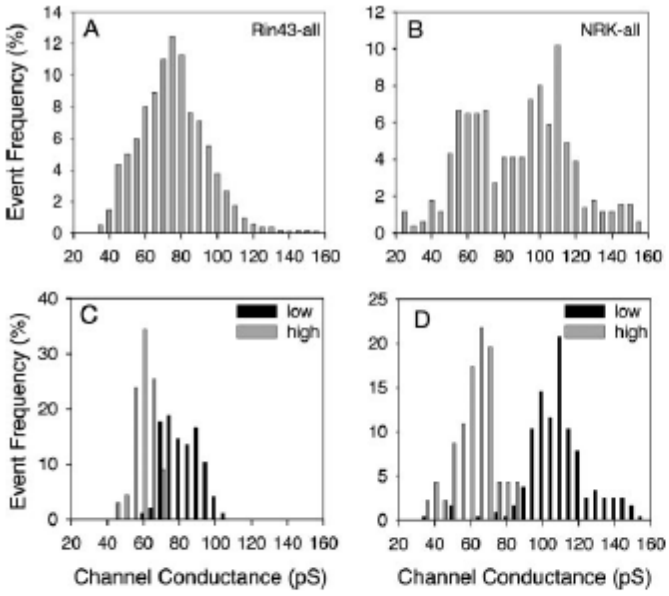

Figure 4. Amplitude histograms reveal variable open-state behavior of Cx43 channels in both Rin43 and NRK cells; high selective permeability for NBD-M-TMA occurred in pairs with a high incidence of 55- to 70-pS events. A and B, Amplitude histograms compiled from multiple Rin43 (N=10, n=1384) and NRK pairs (N=5, n=511). C and D, Amplitude histograms derived from Rin43 or NRK cell pairs with high vs low NBD-M-TMA selective permeability. Selective permeability (in $min^{-1}nS^{-1}$): Rin43-low 0.013; Rin43-high 0.91; NRK-low 0.006; NRK-high 0.34. Total events: Rin43-low 96, Rin43-high 67, NRK-low 241, NRK-high 46. Note that 55- to 70-pS events were rare in pairs with low junctional NBD-M-TMA selective permeability.

to intercalated disks. As shown previously for the ischemic heart,[25] a considerable increase in Cx43 localized at the lateral borders of myocytes was observed in the ischemic group hearts. Cx43 phosphorylated at S368 was largely absent in control hearts but significantly increased in the ischemic group hearts; despite obvious gap junction remodeling, most of the pS368-Cx43 remained localized at intercalated disks in these hearts.

Discussion

Selective Permeability, Phosphorylation, and Ion Flux

Receptor-mediated PKC activation occurs in most tissues in response to growth and injury stimuli, settings where functional gap junctions are crucial to normal tissue response.[1,4] In Cx43 expressing cells, including ventricular myocytes, PKC activation results in reduced dye coupling (LY, 6-carboxyfluorescein), which could reflect the combined effects of reduced channel number, open probability or permeability.[6,11,35,36] Using quantitative methods we show here that permeation of Cx43 gap junctions by NBD-M-TMA varies widely and without a linear correlation with their own g_j values under control conditions. This variability was reduced nearly 10-fold (to a level comparable to LY) when phosphorylation at S368 was reduced, blocked, or eliminated. The data indicate that the selectivity of Cx43 gap junction channels is regulated via phosphorylation-dependent mechanisms and suggest that phosphorylation at S368 leads to reduced or unchanged permeation by current carrying ions (predominantly K and Cl) but enhanced permeation by some larger molecules (eg, NBD-M-TMA).

Successful permeation of gap junction channels depends on the size, charge, shape, and molecular constituents of candidate permeants.[37] Connexin-specific selectivity differences can be as large as 300-fold,[27,38] and discrimination between extremely similar solutes by a specific homotypic channel can be profound.[39] Nevertheless, Valiunas et al[33]

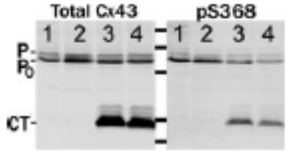

Figure 5. Phosphorylation of Cx43 at S368 is reduced in NRK cells that express the CT of Cx43 as a separate protein. Total protein isolated from NRK (lanes 1 and 2) and NRK-CT cells (lanes 3 and 4) was probed for total Cx43 or pS368-Cx43. Note the 30% decrease in pS368-Cx43 relative to total Cx43 in the CT-expressing NRK cells.

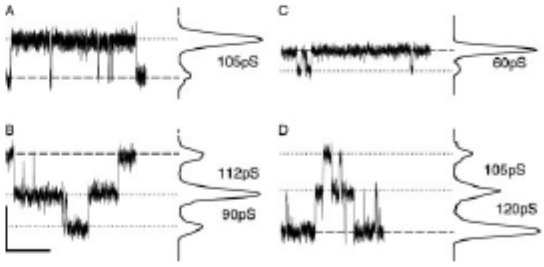

Figure 6. Multiple open states are observed in Rin43 and NRK cells following treatments that reduced the contribution of pS368 to the total Cx43 protein pool. Shown are single-channel events and corresponding all-points histograms derived from BIM-treated Rin43 cells (A and B) and NRK-CT cells (C and D). Events of different amplitudes are evident in both, although conductance states (indicated as interpeak values on the all-points histograms) smaller than the fully open (100 to 120 pS) channel were rare in BIM-treated Rin43 cells. Dashed line indicates the position of 0 current; dotted lines mark open state current levels. (V_j in all records: 40 mV; calibrations: y=5 pA, x=2 seconds; all records were sampled at 2 kHz and subsequently filtered at 100 Hz.)

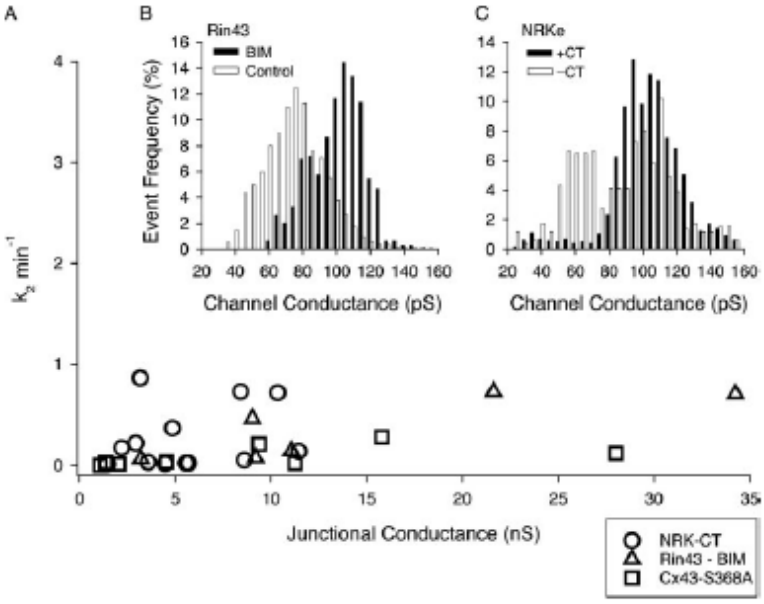

Figure 7. Reduced pS368 levels lead to a decreased frequency of the 55- to 70-pS open state and lowered junctional NBD-M-TMA selective permeability. In A, $k_{2\text{-NBD}}$ as a function of g_j is plotted for NRK-CT (n=13), BIM-treated Rin43 cells (n=6), and Re43-S368A (n=8). Junctions with high $k_{2\text{-NBD}}$ values were absent irrespective of junctional conductance (compare with Figure 1E, which is plotted with the same x/y axis scaling). B and C, Single-channel conductance histograms obtained from the cell pairs illustrated in A for which single channel data were obtained (control data from Figure 3 is shown for comparison). B, Rin43-BIM (N=5, n=643); C, NRK-CT (N=6, n=1786). Note the significant reduction in frequency of the 55- to 70-pS events.

concluded from Cx43-expressing HeLa cells studied with LY that junctional permeability and conductance were linearly related, a result strikingly different from that reported here and elsewhere.[21,40,41] The differing results could reflect differences in sample size, methodology, cell-specific regulation of Cx43, and/or dye selection. The fully open state of Cx43 is heavily favored in HeLa cells (long-lived substate behavior is infrequent), suggesting that the impact of phosphorylation on channel permeability and substate behavior is low. Further, the PKC-induced channel conformation(s) may not be as readily permeated by LY as NBD-M-TMA (as the data herein suggest), in which case the presence of PKC-induced conformations would be poorly detected with LY. Thus, the conditions of the Valiunas study[33] may not have been favorable for observation of variable permeability.

Previously reported estimates of per channel flux rates (at 1 mmol/L) for negatively charged dyes through Cx43 channels differ by 400-fold: ~750 molecules/second for LY[33] versus ~300 000 molecules/second for Alexa488,[37] a range comparable to that recently reported by Eckert.[41] Although the methodology used in these studies differed, two method-independent explanations were advanced to explain the differing per channel flux rates. First, permeant-pore interactions were suggested to limit the diffusion of LY through the pore to a far greater extent than Alexa 488 (despite their similar size and charge); second, the permeation state of the Cx43 channels formed in oocytes[37] versus HeLa[33] cells differed, possibly attributable to cell-specific differential phosphorylation. The range of per channel flux rates for NBD-M-TMA (calculated from k_2 and junctional conductance, assuming a cell volume of 1pL, dye concentration of 1 mmol/L, and channel conductance of 105 pS) observed under control conditions in our study was 6600 to 2 000 000 molecules/sec, an ~300-fold difference for the same permeant. Treatments aimed at decreasing or eliminating pS368 reduced the range (as much as 80-fold) and mean (as much as 7-fold) of observed $k_{2\text{-NBD}}$ values (see online data supplement), but notably, none of the pS368 reduction strategies resulted in a uniform population of fully open (100 to 120 pS) channels and none resulted in a linear $k_{2\text{-NBD}}$ versus g_j relationship. Thus, our results indicate that, indeed, selective permeability is a regulated parameter of junctional function that involves changes in the relative contribution to the junction of channels with high versus intermediate or low selectivity and is, in part, determined by phosphorylation of the channel proteins at S368.

Despite the wide variability and sometimes very high $k_{2\text{-NBD}}$ and $k_{2\text{-NBD}}/g_j$ values, the per channel flux rate for dye was always less than that for K^+, basically because the mobility of K^+ in solution is greater than that of the dye. For a sensible estimation of NBD-M-TMA to K flux ratio, a comparison of flux caused by a concentration gradient (according to Fick's law) versus an electrical gradient (according to Ohms Law) was done (see the online data supplement). The results show that NBD-M-TMA to K flux was 1:4.5 (0.22) for channels in junctions with the highest selective NBD-M-TMA permeability; however, for most channels, the NBD-M-TMA to K flux ratio of 0.011 was comparable to that reported for LY:K (0.025).[33]

Our data suggest that phosphorylation of Cx43 at S368 increases the permeability of the channel by as much as 300-fold, yet either has no effect on or reduces the conductance of the channel by only 2-fold. One model of channel function that accommodates a stable or decreased conductance but increased large molecule permeation involves phosphorylation-induced stabilization of the fluid movements of the CT such that random interference with pore entry by large molecules is reduced (permeation increased). If the CT

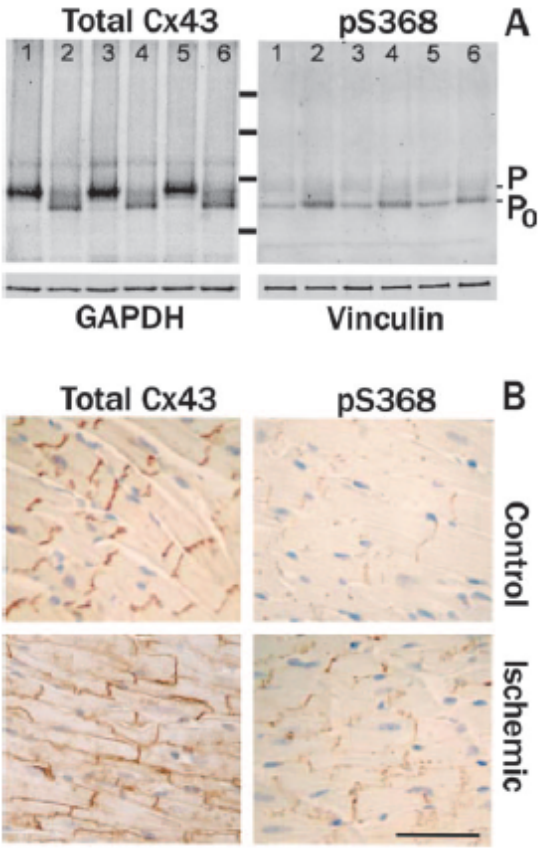

Figure 8. Cx43 phosphorylated at S368 increases in ischemic hearts but remains localized to the intercalated disk despite lateralization of Cx43. A, Western blots of total protein isolated from 3 control (lanes 1, 3, and 5) and 3 no-flow ischemic (30 minutes at 37°C; lanes 2, 4, and 6) hearts (each lane a distinct heart) probed for total Cx43 (N-terminal antibody) or pS368-Cx43. The total protein load per lane was approximately equal, as shown by blotting an equally loaded gel with GAPDH and Vinculin antibodies (lower panels as marked). Note Cx43 phosphorylated at S368 increased ≈5-fold in ischemic vs control hearts. B, In control tissue, Cx43 was localized to intercalated disks, whereas in ischemic tissue, Cx43 was fairly uniformly distributed around each myocyte. Cx43 phosphorylated at S368 was detected at low levels in control tissue but at high levels in ischemic tissue. Most of the pS368-Cx43 was localized to the intercalated disks, even in ischemic tissue. (Calibration 100 μm.)

were stabilized in a way that increased pore length, channel conductance would decrease despite increased permeation by large molecules. Testing this model (and others) will clearly require additional work, but it represents a plausible starting point for such investigations.

Physiological Relevance of Junctional Selectivity

The possible significance of regulated selectivity is suggested by our data showing a significant increase in pS368-Cx43 early during no-flow ischemia as well as by its timely appearance in wound healing.[42] The latter study showed that pS368-Cx43 was uniformly distributed in unwounded human epidermal layers; however, at 24, but not 6, hours postwounding, pS368-Cx43 levels were substantially increased in basal keratinocytes and virtually eliminated from the suprabasal layers in the region of the wound. These alterations in Cx43 phosphorylation and localization were suggested to result in the formation of communication compartments in the region of the wound that might facilitate repair and delay differentiation in suprabasal cells until appropriate; the current data support this possibility.

Relative to the heart, the data presented herein indicate that early in no-flow ischemia phosphorylation of Cx43 at S368 increases significantly, despite dephosphorylation and relocation of substantial amounts of Cx43 to lateral borders. Given the enhanced permselectivity of Cx43 channels and junctions containing pS368-Cx43, the localization of pS368-Cx43 to intercalated disks suggests that intercellular signaling along the longitudinal versus transverse axes might differ in the ischemic versus normal heart. Reduced longitudinal conduction velocity is expected (and observed) consequent to the reduction at intercalated disks of channel number and conductance (attributable to pS368). Transverse conduction is not, however, expected to increase in parallel with the redistribution of Cx43 to the lateral borders, as dephosphorylated Cx43 does not assemble channels efficiently.[30,43] Because of the complexity of impulse propagation in the heart, it is not entirely clear that these (combined) effects of Cx43 phosphorylation/dephosphorylation and relocation are antiarrhythmic; however, PKC activation occurs during ischemic preconditioning, is required for the protection (against arrhythmias and cell injury) conferred by preconditioning, and is sufficient to protect the ischemic heart against ischemic injury.[44–46] We therefore suggest that in addition to any electrical benefits that phosphorylation at S368 might confer on the ischemic heart, the metabolic and signaling consequences of altered selective permeability on tissue survival and repair might be more profound.[42] For instance, by facilitating or preventing the intercellular movement (between nonischemic and ischemic cells) of metabolites and signaling molecules, altered junctional selective permeability might be crucial for cell survival and tissue function during and following ischemic insults.

Acknowledgments

The NBD-M-TMA and hOCT2-CHO cells were a generous gift from Dr Stephen Wright, whose consultation in designing the transport experiments presented herein is gratefully acknowledged.

Sources of Funding

Supported by NIH grants HL058732, HL076260 (to J.M.B.); GM055632 (to P.D.L.); and training grant support to N.S.H. (HL07249); and the American Heart Association, Pacific Mountain Affiliate (0550258z to J.M.B.).

Disclosures

None.

References

1. Saez JC, Berthoud VM, Branes MC, Martinez AD, Beyer EC. Plasma membrane channels formed by connexins: their regulation and functions. *Physiol Rev.* 2003;83:1359–1400.

2. Severs NJ, Coppen SR, Dupont E, Yeh HI, Ko YS, Matsushita T. Gap junction alterations in human cardiac disease. *Cardiovasc Res*. 2004;62: 368–377.
3. Severs NJ, Dupont E, Coppen SR, Halliday D, Inett E, Baylis D, Rothery S. Remodelling of gap junctions and connexin expression in heart disease. *Biochim Biophys Acta*. 2004;1662:138–148.
4. Cohen MV, Baines CP, Downey JM. Ischemic preconditioning: from adenosine receptor to KATP channel. *Annu Rev Physiol*. 2000;62: 79–109.
5. Dawn B, Bolli R. Role of nitric oxide in myocardial preconditioning. *Ann N Y Acad Sci*. 2002;962:18–41.
6. Moreno AP, Saez JC, Fishman GI, Spray DC. Human connexin43 gap junction channels: regulation of unitary conductances by phosphorylation. *Circ Res*. 1994;74:1050–1057.
7. Cottrell GT, Lin R, Warn-Cramer BJ, Lau AF, Burt JM. Mechanism of v-Src- and mitogen-activated protein kinase-induced reduction of gap junction communication. *Am J Physiol Cell Physiol*. 2003;284: C511–C520.
8. Lampe PD, Tenbroek EM, Burt JM, Kurata WE, Johnson RG, Lau AF. Phosphorylation of connexin43 on serine368 by protein kinase C regulates gap junctional communication. *J Cell Biol*. 2000;149:1503–1512.
9. Warn-Cramer BJ, Cottrell GT, Burt JM, Lau AF. Regulation of connexin43 gap junctional intercellular communication by mitogen-activated protein kinase. *J Biol Chem*. 1998;273:9188–9196.
10. Cameron SJ, Malik S, Akaike M, Lee JD, Lerner-Marmarosh N, Yan C, Abe JI, Yang J. Regulation of EGF-induced connexin 43 gap junction communication by BMK1/ERK5 but not ERK1/2 kinase activation. *J Biol Chem*. 2003;278:18682–18688.
11. Laird DW. Connexin phosphorylation as a regulatory event linked to gap junction internalization and degradation. *Biochim Biophys Acta*. 2005; 1711:172–182.
12. Solan JL, Lampe PD. Connexin phosphorylation as a regulatory event linked to gap junction channel assembly. *Biochim Biophys Acta*. 2005; 1711:154–163.
13. Poelzing S, Rosenbaum DS. Nature, significance, and mechanisms of electrical heterogeneities in ventricle. *Anat Rec A Discov Mol Cell Evol Biol*. 2004;280:1010–1017.
14. Daleau P, Boudriau S, Michaud M, Jolicoeur C, Kingma JG Jr. Preconditioning in the absence or presence of sustained ischemia modulates myocardial Cx43 protein levels and gap junction distribution. *Can J Physiol Pharmacol*. 2001;79:371–378.
15. Qiu C, Coutinho P, Frank S, Franke S, Law LY, Martin P, Green CR, Becker DL. Targeting connexin43 expression accelerates the rate of wound repair. *Curr Biol*. 2003;13:1697–1703.
16. Coutinho P, Qiu C, Frank S, Wang CM, Brown T, Green CR, Becker DL. Limiting burn extension by transient inhibition of Connexin43 expression at the site of injury. *Br J Plast Surg*. 2005;58:658–667.
17. Shin JL, Solan JL, Lampe PD. The regulatory role of the C-terminal domain of connexin43. *Cell Commun Adhes*. 2001;8:271–275.
18. Vozzi C, Ullrich S, Charollais A, Philippe J, Orci L, Meda P. Adequate connexin-mediated coupling is required for proper insulin production. *J Cell Biol*. 1995;131:1561–1572.
19. Martyn KD, Kurata WE, Warn-Cramer BJ, Burt JM, Tenbroek E, Lau AF. Immortalized connexin43 knockout cell lines display a subset of biological properties associated with the transformed phenotype. *Cell Growth Differ*. 1997;8:1015–1027.
20. Hirschi KK, Burt JM, Hirschi KD, Dai C. Gap junction communication mediates transforming growth factor-β activation and endothelial-induced mural cell differentiation. *Circ Res*. 2003;93:429–437.
21. El-Vitorin JF, Burt JM. Quantification of gap junction selectivity. *Am J Physiol Cell Physiol*. 2005;289:C1535–C1546.
22. Cottrell GT, Wu Y, Burt JM. Functional characteristics of heteromeric Cx40-Cx43 gap junction channel formation. *Cell Commun Adhes*. 2001; 8:193–197.
23. Bednarczyk D, Mash EA, Aavula BR, Wright SH. NBD-TMA: a novel fluorescent substrate of the peritubular organic cation transporter of renal proximal tubules. *Pflugers Arch*. 2000;440:184–192.
24. Sutherland FJ, Hearse DJ. The isolated blood and perfusion fluid perfused heart. *Pharmacol Res*. 2000;41:613–627.
25. Beardslee MA, Lerner DL, Tadros PN, Laing JG, Beyer EC, Yamada KA, Kleber AG, Schuessler RB, Saffitz JE. Dephosphorylation and intracellular redistribution of ventricular connexin43 during electrical uncoupling induced by ischemia. *Circ Res*. 2000;87:656–662.
26. Wit AL. Remodeling of cardiac gap junctions: the relationship to the genesis of ventricular tachycardia. *J Electrocardiol*. 2001;34(suppl): 77–83.
27. Goldberg GS, Moreno AP, Lampe PD. Gap junctions between cells expressing connexin 43 or 32 show inverse permselectivity to adenosine and ATP. *J Biol Chem*. 2002;277:36725–36730.
28. King TJ, Lampe PD. The gap junction protein connexin32 is a mouse lung tumor suppressor. *Cancer Res*. 2004;64:7191–7196.
29. Solan JL, Fry MD, Tenbroek EM, Lampe PD. Connexin43 phosphorylation at S368 is acute during S and G2/M and in response to protein kinase C activation. *J Cell Sci*. 2003;116:2203–2211.
30. Cooper CD, Lampe PD. Casein kinase 1 regulates connexin-43 gap junction assembly. *J Biol Chem*. 2002;277:44962–44968.
31. Banach K, Weingart R. Connexin43 gap junctions exhibit asymmetrical gating properties. *Pflugers Arch*. 1996;431:775–785.
32. Cottrell GT, Burt JM. Heterotypic gap junction channel formation between heteromeric and homomeric Cx40 and Cx43 connexons. *Am J Physiol Cell Physiol*. 2001;281:C1559–C1567.
33. Valiunas V, Beyer EC, Brink PR. Cardiac gap junction channels show quantitative differences in selectivity. *Circ Res*. 2002;91:104–111.
34. Bukauskas FF, Bukauskiene A, Verselis VK. Conductance and permeability of the residual state of connexin43 gap junction channels. *J Gen Physiol*. 2002;119:171–186.
35. Kwak BR, Jongsma HJ. Regulation of cardiac gap junction channel permeability and conductance by several phosphorylating conditions. *Mol Cell Biochem*. 1996;157:93–99.
36. Doble BW, Chen Y, Bosc DG, Litchfield DW, Kardami E. Fibroblast growth factor-2 decreases metabolic coupling and stimulates phosphorylation as well as masking of connexin43 epitopes in cardiac myocytes. *Circ Res*. 1996;79:647–658.
37. Weber PA, Chang HC, Spaeth KE, Nitsche JM, Nicholson BJ. The permeability of gap junction channels to probes of different size is dependent on connexin composition and permeant-pore affinities. *Biophys J*. 2004;87:958–973.
38. Goldberg GS, Lampe PD, Nicholson BJ. Selective transfer of endogenous metabolites through gap junctions composed of different connexins. *Nat Cell Biol*. 1999;1:457–459.
39. Bevans CG, Kordel M, Rhee SK, Harris AL. Isoform composition of connexin channels determines selectivity among second messengers and uncharged molecules. *J Biol Chem*. 1998;273:2808–2816.
40. Biegon RP, Atkinson MM, Liu TF, Kam EY, Sheridan JD. Permeance of novikoff hepatoma gap junctions: quantitative video analysis of dye transfer. *J Membr Biol*. 1987;96:225–233.
41. Eckert R. Gap-junctional single channel permeability for fluorescent tracers in mammalian cell cultures. *Biophys J*. In press.
42. Richards TS, Dunn CA, Carter WG, Usui ML, Olerud JE, Lampe PD. Protein kinase C spatially and temporally regulates gap junctional communication during human wound repair via phosphorylation of connexin43 on serine368. *J Cell Biol*. 2004;167:555–562.
43. Musil LS, Goodenough DA. Biochemical analysis of connexin43 intracellular transport, phosphorylation, and assembly into gap junctional plaques. *J Cell Biol*. 1991;115:1357–1374.
44. Garcia-Dorado D, Ruiz-Meana M, Padilla F, Rodriguez-Sinovas A, Mirabet M. Gap junction-mediated intercellular communication in ischemic preconditioning. *Cardiovasc Res*. 2002;55:456–465.
45. Armstrong SC. Protein kinase activation and myocardial ischemia/reperfusion injury. *Cardiovasc Res*. 2004;61:427–436.
46. Cross HR, Murphy E, Bolli R, Ping P, Steenbergen C. Expression of activated PKC e (PKC e) protects the ischemic heart, without attenuating ischemic H(+) production. *J Mol Cell Cardiol*. 2002;34:361–367.

APPENDIX B

DATA SUPPLEMENT TO APPENDIX A

Expanded Materials and Methods

Cells: NRK and NRK-CT[1] were grown in DMEM (Sigma D-1152 with 4.5 mg/mL glucose). The NRK-CT medium was supplemented with 500 µg/mL G418 and hygromycin; CT expression was induced in the NRK-CT cells with 1 µg/mL doxycycline for 24-48h. Rin43[2] cells were grown in RPMI 1640 (Sigma R1383) supplemented with 300 µg/mL G418. Re43 (22C-3 or MC:Re43)[3] and Re43-S368A cells (pI8)[4] were grown in DMEM (Sigma D-1152 with 4.5 mg/mL glucose) supplemented with 350 µg/mL zeocin, 6 µg/mL puromycin, 300 µg/mL hygromycin, respectively. hOCT2 transfected CHO cells [5;6] were grown in Ham's F12-Kaighn's modification (F12K, Sigma-Aldrich) supplemented with 1mg/ml Geneticin (Invitrogen). All media were additionally supplemented with 10% FBS (Gemini BioProducts), 300 µg/mL Penicillin G, and 500 µg/mL Streptomycin. Cells were maintained at 37°C in a 5% CO_2, humidified incubator.

Co-cultures: To facilitate formation and identification of heterocellular junctions with hOCT2 expressing CHO cells, NRK or Rin43 cells were co-cultured overnight with DiI (DS - Molecular Probes) labeled hOCT2-CHO cells. **DiI labeling**: Cells in a 100mm plate were incubated for 60-75 minutes at 37°C in medium containing 1µg/mL DiI (DS). Cells were rinsed with fresh medium before lifting (0.05% trypsin, 0.2g/L EDTA in Ca-, Mg-free balanced salts solution) and replating cells in co-culture with either NRK or Rin43 cells.

OCT dye uptake assay: hOCT2-CHO cells co-cultured with Rin43 or NRK cells were exposed at 37°C for 30-60 minutes to 200 µmol/L of NBD-M-TMA in Waymouth's buffer (WB; in mmol/L: 135 NaCl, 13 HEPES, 28 D-glucose, 5 KCl, 1.2 $MgCl_2$, 2.5 $CaCl_2$, 0.8 $MgSO_4$, pH adjusted to 7.4 with NaOH) and washed with and viewed in ice-cold WB containing 250 µmol/L of the OCT blocker tetrapentylammonium (TPeA). Uptake relative to cell type was documented with fluorescence and phase contrast images of the co-cultures (see figure 2 main manuscript).

hOCT2-CHO cells were exposed at room temperature for 10 minutes to 250 μmol/L of NBD-M-TMA in Waymouth's buffer or external solution (see below). Cells were washed with ice-cold Waymouth's or external solution supplemented with 250 μmol/L TPeA. Relative uptake under the two uptake conditions was documented with fluorescence images of the cells (see Online Figure 1).

Junctional Permeability and Conductance, Single Channel Conductance:[7] Cells were plated onto glass coverslips and allowed to adhere for several hours; coverslips were then mounted in a custom-made chamber and superfused with our standard external solution (in mmol/L:142.5 NaCl , 4 KCl, 15 CsCl, 5 Glucose, 1 $MgCl_2$, 2 Na Pyruvate, 10 HEPES, 10 TEACl, 1 $BaCl_2$, 1 $CaCl_2$, osmolarity adjusted to 310 mOsmol/L with H_2O after pH adjustment to 7.2). The cells were visualized on an upright (Olympus BX50WI) microscope equipped for epifluorescence and differential interference contrast (DIC) observation; cell-pairs in which the cells were of similar size and shape were selected for evaluation of junctional function. The donor cell's interior was accessed (in current clamp mode) with a patch-type microelectrode containing our standard internal solution (in mmol/L: 124 KCl, 14 CsCl, 9 HEPES, 9 EGTA, 0.5 $CaCl_2$, 5 Glucose, 9 TEACl, 3 $MgCl_2$, 5 Na_2 ATP, pH 7.2, 310 mOsmol/L),[7;8] and the selected dyes. Images were acquired with a SenSys CCD camera (Photometrics).[7]

Data Analysis: Junctional permeability to a specific dye was quantified as the rate constant for intercellular diffusion of that dye ($k_{2\text{-dye}}$). To determine this rate constant the fluorescence intensity of donor and recipient cells was quantified from the digital images as the mean intensity of equivalent cell areas/volumes using V++ software (Digital Optics Ltd.) according to the procedures described by Ek-Vitorin & Burt.[7] Briefly, fluorescence at each time point was normalized to the maximum observed donor cell fluorescence, and plotted as a function of time.

k_2 was determined by fitting the data with an implicit finite-difference numerical method that relied on intensity of the donor cell as a function of time. The selective permeability of a junction for a specific dye was calculated as $k_{2\text{-dye}}/g_j$.

Junctional conductance (g_j) was calculated from Ohm's law, $g_j=I_j/V_j$, using the applied V_j and the I_j measured (pClamp8, Axon Instruments) from the current record of the non-stepped cell. Channel conductances, measured as transitions between open and closed states (dwell time >100 msec) in current records where only one or two channels were active, were calculated and the results binned in 5pS bins for event amplitude histograms.

Immunohistochemistry:[9] Briefly, tissue sections were deparaffinized, antigen retrieved, blocked and detected using rabbit primary antibodies against Cx43 (1:250, Sigma) or pS368-Cx43 (1:200, Cell Signaling, Inc). Slides were washed and incubated with a biotinylated anti-rabbit secondary antibody (1:250, Vector Labs) and detected with ABC-avidin/biotin conjugate (Vectastain, Vector Labs).

Statistics: Comparisons between groups were performed with a Student's T test and values are given as mean ± SEM; P values of 0.05 or less were considered significant.

Results: Transjunctional diffusion of NBD-M-TMA.

NBD-M-TMA is a substrate for members of the organic cationic transporter (OCTs) family;[10] OCTs mediate facilitated diffusion – as such their activity depends on the magnitude of the electrochemical gradient. When the electrical gradient is absent concentrative transport is not possible.[5;6] All of the studies presented in the main manuscript were done in the presence of our external solution, which blocks K-channel activity and results in depolarization to near zero levels. This depolarization blocks hOCT2 mediated NBD-M-TMA uptake, as illustrated in

Online Figure 1. In Waymouth's Buffer (WB), which preserves the resting membrane potential, containing 250 μmol/L NBD-M-TMA, uptake of dye by hOCT2-CHO cells is robust (left panel). In contrast uptake of dye by these same cells from external solution containing 250 μmol/L NBD-M-TMA is virtually undetectable (right panel). Clearly, the presence of an inwardly directed concentration gradient is not sufficient for hOCT2 to concentrate dye intracellularly.

Discussion: Transjunctional diffusion (no uptake) of NBD-M-TMA. Although NBD-M-TMA is a substrate for OCTs, the appearance of this dye in the recipient cells is the result of its transjunctional diffusion from the donors. This conclusion is supported by several facts. First, NRK and Rin43 cells do not express functional OCTs even when the conditions (absence of other OCT substrates, no OCT blockers, warm temperature) favor dye uptake by these transporters (as evidenced by the hOCT2-CHO dye uptake – see figure 2 main manuscript). Second, in our studies the cells were depolarized by the presence in our internal and external solutions of Cs and TEA (and Ba in the internal) – see Online Figure 1. Third, there was no detectable dye in the extracellular solution (see figure 1 of the manuscript); indeed, the concentration gradient was outwardly directed. Fourth, TEA is an extremely good substrate, indeed the model substrate, for the OCTs: at 10 mmol/L, the TEA concentration was at least 40x greater than the intracellular NBD-M-TMA concentration, much greater than the extracellular NBD-M-TMA concentration (which was virtually zero), and more than 100x greater than the K_m of the OCT for TEA;[11;12] thus, if OCTs were present they would be saturated by TEA at both faces of the membrane. Thus, under the conditions of our experiments, uptake of dye by the recipient cells from the external solution does not occur.

Discussion: Flux rates per channel. Flux rates per channel (*f*) were calculated as

$$f = (V\ C_1\ N_A\ k_2) / N/t$$

where V is the donor cell volume (L, assumed to be 1 pL), C_1 is the concentration of NBD-M-TMA in the donor cell (mmol/L, assumed to be 1 mmol/L), N_A is Avogadro's number, k_2 is our experimentally determined rate constant (in min^{-1}), N is the number of channels (from the measured junctional conductance and an assumed unitary conductance of 105 pS; i.e. g_j/105 pS) and t is time (to convert minutes to seconds). The range of per channel flux rates observed under control conditions in our studies revealed an ~300 fold difference (f_{max} / f_{min}) in channel permeability for the same permeant (Online Table 1). Reduction of pS368 decreased the absolute range and average *f* of the junctions, although a uniform population of fully open channels and a linear $k_{2\text{-NBD}}$ vs. g_j relationship were not achieved.

Discussion: Comparison of NBD-M-TMA vs. K flux. The very high $k_{2\text{-NBD}}$ values reported herein might create the impression that the dye diffuses faster than potassium ions in some of our pairs; this impression would be incorrect. It is generally assumed that the movement of ions through the pore of a gap junction channel can be described by their movement in bulk solution, which is determined by the ion's molecular diffusivity. Judging from their size alone, potassium should be much more mobile in solution than NBD-M-TMA (ionic radius of K = 1.33 Å; NBD size= 11.7x6x3.85 Å). The rate constant $\boldsymbol{k_{2\text{-NBD}}}$ is a measure of concentration gradient driven flux whereas $\mathbf{g_j}$ is a measure of electrical gradient driven flux. To ascertain the ratio of dye:K flux, one must either determine $k_{2\text{-K}}$ or g_j when only dye is present to carry the current. Unidirectional flux without an electrical driving force for two ions can be related by the differences in their diffusivity.[13] We measured the conductivity of KBr vs. NBD-M-TMA-Br at equivalent concentrations and found that K^+ conductivity was 5x higher than NBD-M-TMA^+. Thus, the equivalent K^+ flux for an NBD-M-TMA flux of $2x10^6$ molecules/sec would be $1x10^7$

molecules/sec for a ratio of 1 to 5 or 0.2. One can also calculate the equivalent g_j if only NBD-M-TMA were available to carry current, which for a 105 pS channel (determined with K^+ and Cl^- contributing equally to the current) would be 11.3 pS. This conductance can then be used with Ohms law to calculate the voltage equivalent of the 1mmol/L concentration difference (28mV) and the corresponding K^+ flux of $9x10^6$ ions/s (NBD-M-TMA flux:K^+ flux = 0.22). For most of the selective permeabilities measured in our studies the NBD-M-TMA:K flux ratio was far less; the average $k_{2\text{-NBD}}$ corresponds to a ratio of 0.011, a value similar to that reported by Valiunas and colleagues for the ratio of LY to K flux of 0.025.[14]

Reference List

1. Shin JL, Solan JL, Lampe PD. The regulatory role of the C-terminal domain of connexin43. *Cell Commun Adhes.* 2001;8:271-275.

2. Vozzi C, Ullrich S, Charollais A, Philippe J, Orci L, Meda P. Adequate connexin-mediated coupling is required for proper insulin production. *J Cell Biol.* 1995;131:1561-1572.

3. Martyn KD, Kurata WE, Warn-Cramer BJ, Burt JM, Tenbroek E, Lau AF. Immortalized connexin43 knockout cell lines display a subset of biological properties associated with the transformed phenotype. *Cell Growth Differ.* 1997;8:1015-1027.

4. Lampe PD, Tenbroek EM, Burt JM, Kurata WE, Johnson RG, Lau AF. Phosphorylation of connexin43 on serine368 by protein kinase C regulates gap junctional communication. *J Cell Biol.* 2000;149:1503-1512.

5. Kaewmokul S, Chatsudthipong V, Evans KK, Dantzler WH, Wright SH. Functional mapping of rbOCT1 and rbOCT2 activity in the S2 segment of rabbit proximal tubule. *Am J Physiol Renal Physiol.* 2003;285:F1149-F1159.

6. Wright SH, Dantzler WH. Molecular and cellular physiology of renal organic cation and anion transport. *Physiol Rev.* 2004;84:987-1049.

7. Ek-Vitorin JF, Burt JM. Quantification of Gap Junction Selectivity. *Am J Physiol Cell Physiol.* 2005;289:C1535-C1546.

8. Cottrell GT, Wu Y, Burt JM. Functional characteristics of heteromeric Cx40-Cx43 gap junction channel formation. *Cell Commun Adhes.* 2001;8:193-197.

9. King TJ, Lampe PD. The gap junction protein connexin32 is a mouse lung tumor suppressor. *Cancer Res.* 2004;64:7191-7196.

10. Bednarczyk D, Mash EA, Aavula BR, Wright SH. NBD-TMA: a novel fluorescent substrate of the peritubular organic cation transporter of renal proximal tubules. *Pflugers Arch.* 2000;440:184-192.

11. Suhre WM, Ekins S, Chang C, Swaan PW, Wright SH. Molecular determinants of substrate/inhibitor binding to the human and rabbit renal organic cation transporters hOCT2 and rbOCT2. *Mol Pharmacol.* 2005;67:1067-1077.

12. Volk C, Gorboulev V, Budiman T, Nagel G, Koepsell H. Different affinities of inhibitors to the outwardly and inwardly directed substrate binding site of organic cation transporter 2. *Mol Pharmacol.* 2003;64:1037-1047.

13. Hille B. Elementary Properties of Pores. In: Ion Channels of Excitable Membranes. Sinauer Associates, Inc, Sunderland. 2001; 347-377.

14. Valiunas V, Beyer EC, Brink PR. Cardiac gap junction channels show quantitative differences in selectivity. *Circ Res*. 2002;91:104-111.

Online Table 1. Blocking phosphorylation of Cx43 at S368 reduces NBD-M-TMA flux/channel/s.

Group (n)	Absolute *f* Range (molecules/sec)	*f*max/*f*min	Mean *f* ± SEM (molecules/sec)
Control (58)	6,600-2,000,000	300	205,214 ± 51,854
NRK-CT (13)	3539-286,052	81	56,909 ± 22,712
S368A mutant (8)	1,600-24,000	15	10,791 ± 2,618
BIM treatment (6)	8,600 to 54,000	6	25,746 ± 7,355

Online Figure 1 – Uptake of NBD-M-TMA by hOCT2-CHO cells is blocked in external solution. Uptake of NBD-M-TMA by hOCT2-CHO cells over a ten minute period is robust from WB solution containing 250μmol/L (left panel). When external solution (containing 15 mmol/L Cs, 1mmol/L Ba and 10mmol/L TEA) replaced WB, uptake was essentially blocked (images displayed with the same fixed range of pixel intensity).

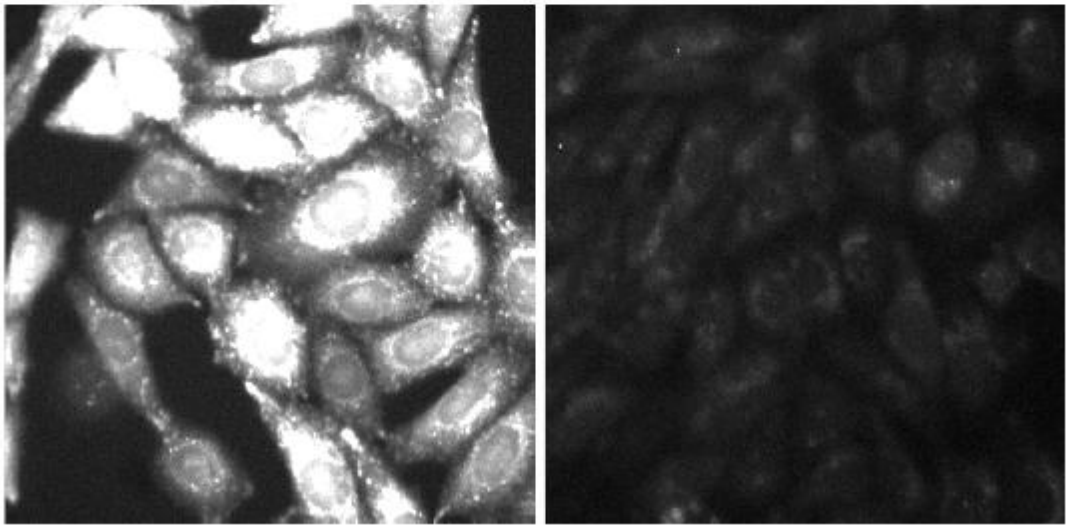

APPENDIX C

HINDERED DIFFUSION THROUGH AN AQUEOUS PORE DESCRIBES INVARIANT DYE SELECTIVITY OF CX43 JUNCTIONS

Nathanael S. Heyman, Janis M. Burt

Biophysical Society

Biophysical Journal
Copyright Permission Form

In order to obtain copyright permission, please answer the questions below. When you have completed the form you may fax it to (301) 634-7267 or email it as an attachment to bj@biophysics.org. Once your request is processed, it will be sent back to you for your records.

Name: Nathanael Heyman

Address: Dept. Physiology
University of Arizona
PO Box 245051
Tucson, AZ 85724

Phone: 520-626-6740

Fax: 520-626-2382

Email: nheyman@email.arizona.edu

*note: I am requesting permission to include this paper, which I wrote, as an appendix to my dissertation.

I am requesting permission to reprint Figure(s) (whole manuscript) (figure numbers) by Heyman (author names) and Burt from the article Hindered diffusion through an aqueous pore describes invariant dye selectivity of Cx43 junctions. (title) in Biophys. J. 2007 (year) E-pub (vol.) (issue) (page numbers). I understand that I am obligated to notify the original author(s) and will provide appropriate attribution to the Biophysical Society and said author(s) for use of these materials.

OFFICE USE ONLY:

Permission granted Rachel Elayan Date 10/11/07

This un-edited manuscript has been accepted for publication in Biophysical Journal and is freely available on BioFast at http://www.biophysj.org . The final copyedited version of the paper may be found at http://www.biophysj.org .

Hindered diffusion through an aqueous pore describes invariant dye selectivity of Cx43 junctions

Nathanael S. Heyman, Janis M. Burt

Abstract

The permselectivity (permeance/conductance) of Cx43 comprised gap junctions is a variable parameter of junctional function. To ascertain whether this variability in junctional permselectivity is explained by heterogeneous charge or size selectivity of the comprising channels, the permeance of individual Cx43 gap junctions to combinations of two dyes differing in either size or charge was determined in four cell types: Rin43, NRKe, HeLa43, and cardiac myocytes. The results show that Cx43 junctions are size but not charge selective and that both selectivities are constant parameters of junctional function. The consistency of dye selectivities indicates that the large continuum of measured junctional permselectivities cannot be ascribed to an equivalent continuum of individual channel selectivities. Further, the relative dye permeance sequence of NBD-M-TMA ≈ Alexa 350 > Lucifer Yellow > Alexa 488 >> Alexa 594 (Stokes radii of 4.3Å, 4.4Å, 4.9Å, 5.8Å and 7.4Å respectively) and the conductance sequence of KCl > TEACl ≈ KGlutamate are well described by hindered diffusion through an aqueous pore with a ≈10Å radius and 160Å length. The permselectivity and dye selectivity data suggest the variable presence in Cx43-comprised junctions of conductive channels that are either dye impermeable or dye permeable.

Introduction

Gap junctions are clusters of channels that connect the cytoplasms of adjacent cells and serve as intercellular conduits for diffusion of inorganic ions (electrical communication) and other small molecules (chemical communication). These channels are composed of two hemichannels, each consisting of six protein subunits called connexins (Cx). There are twenty-one genes in the human genome and twenty in the mouse genome that encode Cx proteins (1). The increasing number of hereditary diseases linked to Cx mutations (2) as well as the results of targeted deletion and replacement studies (2) provide increasing evidence for the importance of gap junctions in normal development and function of a diverse array of tissues, organs, and organ systems. Expression of the different Cxs, including Cx43, which is the focus of the current study, varies with time, location, and physiological state (3,4). The presence of so many Cx types and the control of their expression suggest properties that are unique and specific to each.

The various Cxs form channels with different conductance, permeance, and selectivity properties (5), suggesting Cx-specific roles for gap junction mediated

intercellular communication (6-8). The importance of electrical communication via gap junctions is well documented but does not alone necessitate so many Cx types. Modulation of electrical coupling could be accomplished by changes in channel number or open probability, resulting in a broad range of electrical communication levels independent of changes in channel conductance afforded by different Cx isoforms. Perhaps of equal importance, junctions composed of different Cx isoforms are able to uniquely discriminate amongst chemical signals that could diffuse intercellularly (9) and possibly differentially regulate this selectivity. Indeed, with regards to small inorganic ions gap junctions are relatively non-selective (9-12); however, increasing evidence suggests that some gap junctions can discriminate between very similar permeants of larger size (13-15). Understanding the basic principles leading to such discrimination should provide further insight into specific functional roles of communication via gap junctions formed of different connexins.

Gap junction mediated intercellular communication (GJIC) is typically measured in one of two ways: intercellular diffusion of fluorescent dyes (permeance) or passage of electrical current (conductance). The former is generally regarded as indicative of metabolic or chemical communication and the latter of electrical communication. For a simple, non-selective, cylindrical pore, the properties of permeance and conductance should be linearly related; as the number of open channels increases both permeance and conductance should increase according to a defined and constant proportion. Comparison of electrical conductance and permeance of the same junction to either the small cationic dye NBD-M-TMA (16,17) or the slightly larger anionic dyes Lucifer Yellow or Calcein (18) reveal that these parameters are not well correlated for Cx43 channels. Indeed, the range of junctional permselectivity (junctional dye permeance / conductance; k_{dye} / g_j) values for Cx43 gap junctions varies across several orders of magnitude. These data suggest that Cx43 channels can adopt states with considerably different selectivity properties.

The aims of the present study were to measure the charge and size selectivity of Cx43 junctions and to determine the extent to which the reported heterogeneity in junctional k_{dye} / g_j for Cx43 is due to heterogeneity in these selectivities. To do this, it was necessary to use an approach that could provide specific information about the charge or size selectivity of individual gap junctions. The approach used in this study was to simultaneously compare the permeance of individual Cx43 gap junctions to two dyes differing by either size or charge. This approach allowed for comparison of the permeance of the same Cx43 channels to molecules differing primarily by only one parameter (size or charge) and, as such, was ideal for determining the extent to which charge and size selectivity vary among different populations of Cx43 channels. We show that Cx43 junctions, as formed in several cell types, demonstrate a constant dye selectivity profile that is based solely on the size of the dye permeant. Thus the previously observed interjunctional variation in permselectivity cannot be due to a similar interjunctional variation in the selectivity of the comprising Cx43 channels. Furthermore, the relative dye permeance sequence and unitary conductance data are consistent with

hindered diffusion through a reasonably uniform aqueous pore with an approximate radius of 10Å.

METHODS

Cells:

Four rat Cx43 (rCx43) expressing cell lines were used: rat insulinoma cells stably transfected with rCx43 (Rin43) (from Dr. Paolo Meda) (19), HeLa cells stably transfected with rCx43 (HeLa43) (from Dr. Ross Johnson), normal rat kidney epithelial cells (NRKe, from Dr. Paul Lampe) that endogenously express rCx43, and fetal rat cardiac ventricular myocytes (from Dr. Joe Bahl) prepared as described (20) that also endogenously express rCx43. Generation of the rat Cx40 (rCx40) expressing cell line (Rin40) was described previously (21). Rin43 and Rin40 cells were grown in RPMI (Sigma) with 10% FBS and 300 μg/ml G418. HeLa43 cells were grown in DMEM (Sigma) with 10% FBS and 500 μg/ml G418. NRKe cells were grown in DMEM (Sigma) with 10% FBS. Cardiac myocytes were grown and maintained as previously described (20). All cells were maintained at 37°C in a 5% CO_2, humidified incubator.

Electrophysiological Measurements:

Solutions (composition in mM): *KCl Internal Solution*: KCl 133.5, HEPES 8.6, EGTA 8.6, $CaCl_2$ 0.5, glucose 4.5, TEACl 8.6, Na_2ATP 4.8, $MgCl_2$ 2.9; *KGlutamate Internal Solution:* KGlutamate 128.5, HEPES 7.8, EGTA 7.8, $CaCl_2$ 0.4, glucose 4.1, TEACl 7.8, Na_2ATP 4.3, $MgCl_2$ 2.6; *TEACl Internal Solution:* TEACl 138.0, HEPES 8.4, EGTA 8.4, $CaCl_2$ 0.5, glucose 4.4, TEACl 8.4, Na_2ATP 4.7, $MgCl_2$ 2.8; *External solution*: NaCl 142.5, KCl 4, $MgCl_2$ 1, glucose 5, sodium pyruvate 2, HEPES 10, CsCl 15, TEACl 10, $BaCl_2$ 1 , $CaCl_2$ 1. The pH of all solutions was adjusted to 7.2 by addition of KOH and the osmolarity was adjusted to 315-320 mOsm/L by addition of H_2O (Wescor 5520 osmometer; Logan, Utah). Conductivities (mS/cm) of the internal solutions were: 15.95 (KCl), 11.17 (Kglutamate), 11.24 (TEACl) (VWR model 2052 conductivity meter).

Data Collection: Cells were trypsinized (0.25% trypsin in Ca^{2+} and Mg^{2+} free solution) and plated at low density on glass coverslips 4-24 hours prior to experimental use. Coverslips were mounted in a chamber and bathed in external solution. Dual whole cell voltage clamp experiments were performed on Rin43 cells as described previously (22). Briefly electrodes were pulled from 1.2-mm filament glass (A-M Systems; Everett, WA) to resistances of 5-10 MΩ using a Sutter Instruments puller (Novato, CA) and filled with one of the internal solutions listed above. Gigaohms seals were established on both cells of a pair and direct access to the cytosol was obtained by light suction and ringing (capacitance overcompensation) of the electrode. Cell pairs were electrically uncoupled by suffusion of halothane to allow measurement of single channel events. Single channel recordings were made at a transjunctional voltage of 40 mV with one cell held at 0 mV

and the other at +40 mV or -40 mV (Axopatch 1C amplifiers; Axon Instruments; Burlingame, CA). Current signals were low pass filtered at 100 Hz (Model LPF-202; Warner Instruments; Hamden, CT) and current and voltage signals were digitized (Digidata 1322A; Axon Instruments; Burlingame, CA) and stored electronically using Clampex software (pClamp8; Axon Instruments; Burlingame, CA) for subsequent analysis.

Data Analysis: Current traces were notch filtered at 60 Hz (Clampfit; Axon Instruments; Burlingame, CA) to further reduce noise. Gap junction channel events were recognized as equal amplitude but opposite polarity events in the two current traces; for events of 50 msec or longer duration, transition amplitude was measured in the cell held at 0 mV using Clampfit and the data exported to Excel (Microsoft, Redmond, WA) for analysis. Conductance of these channel events was calculated according to Ohm's law:

$$\gamma_j = \Delta I_{junction} / \Delta V_{junction} \qquad \text{Eq.1}$$

Where:
γ_j = channel event conductance
$\Delta I_{junction}$ = quantal change in junctional current amplitude
$\Delta V_{junction} = V_{cell\ 1} - V_{cell\ 2}$

The resulting conductance values were binned into 5 pS bins and event frequency histograms were generated and fit with Gaussian peaks using Origin software (Rockware Inc, Golden, CO) to yield the final γ_j values.

Dye Selectivity Measurement

Filters and Dyes: The junctionally permeable anionic dyes used (all from Molecular Probes; Invitrogen, Carlsbad, CA) were Lucifer Yellow CH Lithium Salt (MW 457), Alexa 350 Hydrazide Sodium Salt (MW 349), Alexa 488 Hydrazide Sodium Salt (MW 570), and Alexa 594 Hydrazide Sodium Salt (MW 759;). The junctionally permeable cationic dye used was NBD-M-TMA {N,N,N-trimethyl-2-[methyl-(7-nitro-2,1,3-benzoxadiol-4-yl)amino]ethanaminium} (23). The junctionally impermeable dextran dyes used (Molecular Probes) were Alexa Fluor 488 Dextran (MW 3000) or Tetramethlyrhodamine Dextran (MW 3000). Physical properties of these dyes are summarized in Table 1. Dye spectra and the filter sets used to visualize each dye can be found in the supplemental information.

Calculation of Dye Aqueous Diffusion Constant and Stokes-Einstein radii: Diffusion constants for each of the dyes were calculated according to the Wilke-Chang Correlation (Eq.2) (24) and then used to calculate Stokes-Einstein radii for each dye (Eq. 3) (25,26).

$$D_{dye} = \left(7.4 \times 10^{-8}\right) \times \frac{\left(2.6M\right)^{0.5} T}{\eta V^{0.6}} \qquad \text{Eq. 2}$$

Where:
D_{dye} = dye diffusion constant (cm^2/s)
M = molecular weight of solvent (g/mole)
T = temperature (°Kelvin) (298)
η = solvent viscosity (centipoise)(0.89 for H_2O @ 298°K)
V = molar volume of dye (cm^3/mol)*

*Calculated using Schroder increments (cm^3/mol) of (+7 per C, H, O, N and double bond, +21 per S, and -7 per ring) for prediction of molar volumes (27).

$$R_{dye} = \frac{KT}{D_{dye} 6\pi\eta} \times 10^{17} \qquad \text{Eq. 3}$$

Where:
R_{dye} = Stokes-Einstein radius of dye (Å)
D_{dye} = dye diffusion constant (cm^2/s)
η = solvent viscosity (centipoise)(0.89 for H_2O @ 298°K)
K = Boltzman's constant (1.38×10^{-23} joule/°K)
T = temperature (°Kelvin) (298)

Data Collection: Cells were trypsinized and replated on glass coverslips 4 to 48 hours prior to study. The coverslips were mounted in a chamber that was placed on and secured to the stage of a fluorescent microscope (Olympus IX71). Injection electrodes (pulled from thin-walled 1.0mm glass to 15-30 MΩ resistance when back-filled with 3M KCl) were filled via capillary action with a dye mixture that included: 2.5mM Alexa 350, 1mg/ml labeled dextran (Alexa 488 or rhodamine), and either 2.5mM NBD-M-TMA, 2.5mM Alexa 488 or 1mM Alexa 594 in internal electrophysiology solution (KCl; see above) and backfilled with 3M KCl. The dye mixture was injected into one cell of a pair by "ringing" the electrode, which deposited a single bolus of dye, followed by immediate removal of the electrode. Sets of fluorescent images with the appropriate filter sets (see supplemental data) were then taken at regular intervals with a CCD camera (CoolSnap ES from Photometrics driven by V++ software); each image set contained images for each dye that were taken at five second intervals (with intervening switch of the filter sets necessary for the dye-specific image). Timing of images and exposure durations were controlled by a program written in V++, which controlled both the camera and light source shutter, allowing for cells to be exposed to excitation light only during image capture. This reduced the impact of photobleaching (exposure times < 500 ms) and allowed for excellent reproducibility in the timing of images. These images were labeled and stored to the computer for future analysis.

Data Processing: Fluorescence intensity was measured using ImageJ software (public domain; http://rsb.info.nih.gov/ij/download.html). The images acquired for each pair were stacked in chronological order. An analysis area was then selected that encompassed the entire donor or recipient cell and the total intensity of the pixels in this

selected area was measured for each frame. A selection area outside but near the cell pair was similarly analyzed for background fluorescence. This was repeated for all images in the stack for each dye and the values were exported to a spreadsheet (Excel) for analysis.

Data Analysis: Analysis of the diffusion of dyes between the two cells was performed based on Fick's equation for diffusion between two compartments as previously described (28,29) with modification as follows.

$$C_{(t)} = C_{eq} - (C_{eq} - C_{(0)}) \times e^{-Bt} \qquad \text{Eq. 4}$$

Since concentration (C) is proportional to fluorescence intensity (F) then:

$$F_{(t)} = F_{eq} - (F_{eq} - F_{(0)}) \times e^{-Bt} \qquad \text{Eq. 5}$$

Where:
$F_{(t)}$ = total fluorescence in the cell at time t
F_{eq} = total fluorescence in the cell at equilibrium
$F_{(0)}$ = total fluorescence in the cell at the time of the first image
B = rate constant describing permeance of the junction

To best fit the data from the current study two modifications to the above equation were made. To determine permeance for junctions where F_{eq} for one or both dyes was not observed, F_{eq} for the donor and recipient cells was defined as follows (**Modification 1)**:

$$F_{eq(donor)} = \left(V_{donor}/V_{total}\right) \times F_{total(t0)} \quad \text{or} \quad F_{eq(recipient)} = \left(V_{recipient}/V_{total}\right) \times F_{total(t0)} \qquad \text{Eq. 6}$$

where V represents volume, $V_{total} = V_{donor} + V_{recipient}$, $F_{total(to)} = F_{donor(to)} + F_{recipient(to)}$, and t_0 is the time of the first image of the sequence of images taken during the experiment. V_{donor}/V_{total} and $V_{recipient}/V_{total}$ were defined by a single parameter $V_{ratio} = V_{donor}/V_{recipient}$ as follows: $V_{donor}/V_{total} = V_{ratio}/(V_{ratio} + 1)$ and $V_{recipient}/V_{total} = 1/(V_{ratio} + 1)$. V_{ratio} was best fit when intercellular diffusion approached equilibrium. In cases where the more slowly diffusing dye did not approach equilibrium, the volume ratio from the more quickly diffusing dye was used for both dyes; if neither dye approached equilibrium, V_{ratio} was set to 1.

To account for dye loss due to photobleaching or leakage, a factor describing the decrease in total intensity of dye in the two cell system over time was incorporated (**Modification 2**). This was done by combining the total intensity from the donor and recipient cells at each time point yielding the total intensity ($F_{total(t)}$) and then defining $F_{total(t/t0)} = F_{total(t)} / F_{total(t0)}$ for each time point. With these modifications, the final form of Eq. 5 becomes:

$$F_{(t)} = ((F_{eq} - (F_{eq} - F_{(0)}) \times e^{-Bt}) \times F_{total(t/t0)} \qquad \text{Eq. 7}$$

Fluorescence as a function of time data for both the donor and recipient cells were fit simultaneously using the above formula and the solver feature in Excel set to minimize rms deviation between observed and predicted values as parameters B and V_{ratio} were varied.

Eq. 7 can be rearranged to the following form:

$$B = \frac{-\ln\left(\left(F_{eq} - F_{(t)} / F_{total(t/to)}\right) / \left(F_{eq} - F_{(0)}\right)\right)}{T} \qquad \text{Eq. 8}$$

where the permeance rate constant B is defined as the slope of a linear relationship between the two parameters $-\ln((F_{eq} - F_{(t)} / F_{total(t/t0)})/(F_{eq} - F_{(0)}))$ and time (T). If the data were not fit by a line of constant slope, then the rate constant and therefore the permeance was not constant throughout the experiment; such data (<10 % of junctions) were discarded. Cell pairs where the decrease in intensity in the donor cell was noticeably faster than the increase in intensity in the recipient cell or where the exponential rate constant (B_{loss}) describing the rate of loss in total intensity (donor + recipient) over time was greater than 0.1 min^{-1} likely indicated damage to the cell by injection; these data were also not included. This occurred in ≈10-20% of junctions. In order to accurately fit higher permeance pairs to a single rate constant, it was necessary to have at least two images following the first image of a sequence where the intensity in the recipient was detectably increasing. This eliminated some (<5% of all junctions) of the highest permeance cell pairs. For the lower permeance junctions, only those junctions where the intensity of the recipient detectably increased between all images of the time of measurement were included. This eliminated some (<5% of all junctions) of the lowest permeance cell pairs.

Rationale for and suitability of Modification 1

Since channel number, open state and even selectivity could be acutely regulated, determining the selective properties (size and charge) of specific Cx43 junctions requires simultaneous measurement of two dyes differing in either their size or charge characteristics. For dyes with substantially different intercellular diffusion rates, for example Alexa 594 vs. Alexa 350, the need for simultaneous measurement required deriving permeance values from non-equilibrium data for the slowly diffusing dye. This was accomplished by using the cell volume ratio value derived from the quickly diffusing dye for fitting of the slowly diffusing dye. The appropriateness of these strategies is evaluated here.

To determine whether rate constants differed when derived from the entire vs. early portion of a long time course of intercellular diffusion, two comparisons were made using data from a junctional selectivity experiment where intercellular diffusion was monitored to equilibrium for both Alexa 350 and Alexa 594 (≈1.5 and 60 min, respectively; Figure 4). First, the rate constant for Alexa 594 determined by fitting all time points (0.073 min^{-}

^{1}) was not obviously different from that determined by fitting only those points occurring prior to equilibrium of Alexa 350 (0.069 min^{-1}). Second, using the plot of $-\ln((F_{eq} - F_{(t)} / F_{total(t/t0)})/(F_{eq} - F_{(0)}))$ vs. time, the rate constants derived by regression analysis of all time points (0.072 min^{-1}) vs. only early time points (0.071 min^{-1}) were not obviously different. These comparisons demonstrate that fitting the early time points of a longer time course of intercellular dye diffusion adequately describes the dye permeance of a junction.

To verify that the volume ratio values determined for dyes with rapid vs. slow intercellular diffusion rates were comparable, we derived these values from dual dye experiments where dye diffusion approached equilibrium for both Alexa 350 and Alexa 594, the two dyes showing the largest difference in intercellular diffusion rates. For the experiment illustrated in Figure 3, the volume ratios for Alexa 350 and Alexa 594 were 1.09 and 1.02, respectively. In addition, the average volume ratios obtained for each dye from four cell pairs that were connected by cytoplasmic bridges, where both dyes were followed to equilibrium, were 1.03 and 1.07 for Alexa 350 and 594, respectively. All of these cell pairs consisted of two cells that appeared visually similar in volume. These data indicate no significant tendency for either Alexa 350 or Alexa 594 to remain bound in the donor cell; thus the use of the volume ratio obtained during fitting of Alexa 350 intercellular diffusion can be used to fit Alexa 594 data.

Dual dye technique applied to cytoplasmic bridges and Cx40 comprised junctions.

Prior to complete cytokinesis, a cytoplasmic bridge connects apparently distinct cells. These bridges are readily permeated by molecules in excess of 3000 Da as well as small, charged molecules such as the dyes used in this study (16). Cytoplasmic bridges should be revealed as non-charge selective by the dual dye injections and analysis technique proposed for use in our studies. To verify this, cell pairs were injected with a mixture of Alexa 350, NBD-M-TMA and rhodamine-dextran; when the rhodamine dextran diffused rapidly from the injected donor to the recipient cell the presence of a cytoplasmic bridge was concluded. The rate constants for intercellular diffusion of the NBD-M-TMA and Alexa 350 were determined as described above, and their relative permeance calculated. As expected, the results (figure 3) were consistent with a non-charge selective pathway for diffusion of molecules between the cells with all points falling near the line of unity (mean $B_{NBD\text{-}M\text{-}TMA} / B_{Alexa\ 350} = 0.99 \pm 0.06$, n = 7); the two permeabilities were significantly well correlated ($r = 0.93$; $p < 0.05$).

Several studies (10,30,31) have shown that Cx40 comprised junctions display cation selectivity. To demonstrate that the dual dye technique can detect such charge selectivity, we injected pairs of Rin40 cells with NBD-M-TMA, Alexa 350, and rhodamine dextran for detection of bridges. The average $B_{NBD\text{-}M\text{-}TMA} / B_{Alexa\ 350}$ for Cx40 junctions revealed by 6 such experiments was 15.1 ± 3.35 (figure 2B) with all of the points falling above the line of unity (figure 2A).

Relationship of rate constant to permeance.

Channel permeability to a molecule is the product of the effective diffusion constant (length^{2}/time) within the channel and a dimensionless partition coefficient divided by the

length of the channel (32). The product of permeability (length/time) and concentration difference (molecules/length^3) across the channel then predicts a rate per unit of area (molecules/time/length^2) for flux of molecules through the channel for a given difference in concentration across the channel. In the case of junctional permeability, the contribution of all permeable channels per unit area of junctional membrane are considered together. Without an accurate knowledge of the cross sectional area of a channel or junction, the parameter that is often described is the product of channel or junctional area and permeability, which is termed permeance (volume/time) (18,33,34). Permeance (P_{dye}) of a junction predicts a rate of dye flux across the junction at a given concentration gradient. This flux rate is determined by measuring the rate of change in fluorescence and thus concentration in the recipient cell, which is proportional to the flux rate divided by the recipient cell volume. In the absence of a cell volume measurement, the resultant parameter is a rate constant (time^{-1}). Eq. 7 and Eq. 8 above were used to fit the data to an exponential rate constant (B_{dye}) (time^{-1}) that is proportional to the permeance according to cell volume (see below). Comparison of individual rate constants as a measure of relative permeance is thus rigorously valid only for cells with identical volumes. Such relative comparisons in the current study were done only across the same junction, thus the actual volume of the cells need not be determined. The rate constant B_{dye} can be related specifically to P_{dye} by arrangement of the derivative of Eq. 4 with respect to time:

$$B_{dye} = \frac{dC/dt}{C_{eq} - C_{(t)}} \ , \qquad \text{Eq. 9}$$

which is similar to that for permeance

$$P_{dye} = \frac{dC/dt}{C_{don(t)} - C_{rec(t)}} \times Volume_{cell} \ . \qquad \text{Eq. 10}$$

If the two cells are equal in volume and all dye is available to transfer then

$$(C_{don(t)} - C_{rec(t)}) = 2 \times \left| C_{eq} - C_{(t)} \right| \qquad \text{Eq. 11}$$

and

$$P_{dye} = B_{dye} \times 1/2 Volume_{cell} \qquad \text{Eq. 12}$$

Cytoplasmic resistance was not significant relative to junctional resistance.

Some studies that have measured intercellular dye diffusion via gap junctions between *Xenopus* ooctyes have characterized the resistance to diffusion of the cytoplasm so that its contribution to intercellular permeance measurements could be accounted for

(7,34). This was necessitated in those studies, in large part, by the relatively large (≈1 microliter) volume of these cells (34). The smaller (≈1 picoliter) volume of the mammalian cells used in the current study were treated as two well stirred compartments for analysis. For this to be the case, diffusion through the gap junction must be substantially rate limiting relative to diffusion in the cytosol. Evidence for this from the current study was that, even in the largest cells, there was no apparent redistribution of dye within individual cells even between the first and second images (10-15 sec interval). This indicated that each cell was behaving as a well stirred compartment, thus the permeance values obtained for dye diffusion between cells could be taken as indicative of the permeance of the connecting gap junction.

RESULTS

Cx43 junctions are not charge selective.

The charge selectivity of Cx43 comprised junctions has previously been tested using current carrying ions (KCl, TEACl, KGlutamate, TEA-Asp) and electrophysiological approaches. In most cases (12,35,36), the fully open channel was revealed as non-selective, but in at least one case cation selectivity was reported (11). The latter study explored Cx43 channel behavior in a different cell type from the former studies, raising the possibility that selectivity could differ in a cell-specific manner. Consequently, we determined the channel conductance of Cx43 channels in Rin43 cells, one of the cell types used herein for the dye selectivity studies that was not used in the above mentioned studies, using KCl, TEACl, and KGlutamate as the prominent current carrying ions. Frequency histograms of channel event conductances for each salt solution (figure 1A) were well fit with single Gaussian peaks revealing conductances of 104.6 ± 0.3 pS (KCl), 69.7 ± 0.3 pS (TEACl), and 67.5 ± 0.4 pS (KGlutamate). Comparison of these conductances to the conductivity of each of the salt solutions (figure 1B) showed that the values for both TEACl and KGlutamate were very near the values predicted by the solution conductivities relative to KCl. These data indicate that Cx43 forms a conductive pathway that is non-selective with regard to charge. The measured values for both TEACl and KGlutamate fell slightly below the predicted conductance values indicating a very modest size selectivity of Cx43 channels for molecules in this size range.

It has been suggested (17,18) that the heterogeneity in permselective properties of Cx43 channels could reflect enhanced or reduced dye flux relative to ionic current due to regulated changes in charge selectivity of these channels. To test the possibility that charge selectivity differences might sometimes occur for larger dye molecules that may not be easily resolved by comparing conductances of smaller ions, we determined the relative permeances of individual Cx43 comprised gap junctions to dyes of similar size but opposite charge, NBD-M-TMA (1^+, 4.3Å) and Alexa 350 (1^-, 4.4Å). These dyes can be visualized independently using appropriate filter sets (see supplemental data), thus their passage across the same junction can be monitored essentially simultaneously. After injection of one cell of a pair, the movement of dye from the injected cell to the neighboring recipient cell was monitored over time (Figure 2A). Fluorescence intensity

values from the resulting images for the donor and recipient cells were fit with an exponential rate constant for each dye (B_{dye}) (see methods Eq. 7, 8)(Figure 2B and C). These rate constants were then compared to give a relative permeance or selectivity of the junction. Data from multiple Cx43-expressing cell pairs revealed average $B_{NBD\text{-}M\text{-}TMA}/B_{Alexa350}$ was 1.00 ± 0.03, n = 42 (Figure 3B). A plot (Figure 3A) of these data points showed they were well approximated by the slope of unity (non-selective) and were significantly well correlated ($r = 0.98$, $p < 0.05$). Thus, although the dual dye technique could detect charge selective junctions when present (see Cx40 data, Figure 3), the results of the Cx43 dual dye charge selectivity experiments indicated a constant lack of charge selectivity for Cx43 comprised gap junctions across a wide range of permeance rate constants (≈250 fold in 42 cell pairs) in four different cell types.

Cx43 size selectivity sequence is constant and well predicted by dye molecule size.

The data presented above indicate that the observed heterogeneity in Cx43 junctional permselectivity (k_{dye}/g_j) does not result from similar heterogeneity in junctional charge selectivity. Heterogeneous junctional permselectivity could also result from channel configurations that variably restrict the passage of large vs. small molecules. To test for possible heterogeneity in junctional size selectivity, the permeance of individual Cx43-comprised junctions to dyes of similar charge but different size were compared (figure 4). The dyes used for these experiments were Alexa 350, Lucifer Yellow, Alexa 488, and Alexa 594 (characterized in Table 1). Results of experiments for Alexa 350 vs. either Lucifer Yellow, Alexa 488, or Alexa 594 (figure 5) showed significant correlation between the permeances of the dyes ($r = 0.99$, 0.99, and 0.93, respectively; all three $p < 0.05$). This excellent correlation between permeance of dyes of different sizes indicates a consistent size selectivity between the dye molecules for Cx43 junctions with a broad range of permeance rate constants (≈100 fold in 67 cell pairs; 12 Lucifer Yellow, 28 Alexa 488 and 27 Alexa 594). Thus, heterogeneous permselectivity of Cx43 junctions (17,18) is not explained by an equivalent heterogeneity in the size selectivity of dye permeable Cx43 channels. Additionally, the trend of relative permeances ($B_{Lucifer\ Yellow}/B_{Alexa350}$ 0.35 ± 0.02; $B_{Alexa488}/B_{Alexa350}$ 0.27 ± 0.01; $B_{Alexa594}/B_{Alexa350}$ 0.029 ± 0.002) is consistent with what is expected from diffusion through a simple channel pore for which the diameter of Alexa 594 approaches the limiting diameter of the pore.

Size selectivities are not simply due to differences in cytoplasmic diffusion.

To test whether the observed size selectivity was simply a result of the relative abilities of the dyes to diffuse freely in the cytoplasmic environment, the permeances relative to Alexa 350 for Lucifer Yellow, Alexa 488, and Alexa 594 were determined for cytoplasmic bridges (incompletely divided cells) using the dual dye technique. Cytoplasmic bridges were detected by their ability to pass 3000 Dalton dextran dyes, which are too large to pass through gap junctions. The relative permeances ($B_{Lucifer\ Yellow}/B_{Alexa350}$ 0.57 ± 0.03; $B_{Alexa488}/B_{Alexa350}$ 0.50 ± 0.02; $B_{Alexa594}/B_{Alexa350}$ 0.27 ± 0.02) (figure 5) presumably represent the relative diffusion constants for the dyes in the cytoplasmic

environment, which would be expected to be inversely proportional to the size of the molecule as seen here. Table 1 shows calculated aqueous diffusion constants (see methods Eq. 2) for each of the dyes used in the current study. The relationship between these calculated aqueous diffusion constants for the dyes used to measure size selectivity ($D_{Lucifer\ Yellow}$ / $D_{Alexa350}$ 0.89; $D_{Alexa488}$ / $D_{Alexa350}$ 0.75; $D_{Alexa594}$ / $D_{Alexa350}$ 0.59) was somewhat different from the cytoplasmic bridge relative permeances above. These differences are likely due to increased hindrance for diffusion of larger molecules in the cytoplasm (37). Despite these increased size selectivities in the cytoplasm over those predicted by aqueous diffusion constants, the size selectivities across Cx43 junctions were significantly different from cytoplasmic bridges for Lucifer Yellow ($B_{Alexa350}$ / $B_{Lucifer\ Yellow}$ 3.0 ± 0.1 (junctions) versus 1.8 ± 0.1 (bridges)), Alexa 488 ($B_{Alexa350}$ / $B_{Alexa488}$ 3.7 ± 0.2 (junctions) versus 2.0 ± 0.1 (bridges)), and Alexa 594 ($B_{Alexa350}$ / $B_{Alexa594}$ 37 ± 2 (junctions) versus 3.8 ± 0.4 (bridges)) (figure 4). This indicates that the extent of size selectivity observed across Cx43 junctions was not due simply to differences in cytoplasmic diffusion of each of the dyes but rather was also due to greater restriction of diffusion of larger dyes by the Cx43 channels themselves. Additionally, no redistribution of dye in each individual cell was observed over time (figure 4). This indicates that the cells behaved as well stirred compartments and that permeance measurements were indeed indicative of the permeance of the gap junction and not diffusion in the cytoplasm.

Diffusion of multiple dyes through Cx43 channels is independent.

The permeance sequence (Alexa 350 > Lucifer Yellow > Alexa 488 >> Alexa 594) found in the current study is what is expected based on the relative sizes of the dye molecules and the proposed size of the Cx43 channel (11,38), but it is different from that derived from comparison of the permselectivity values for each of the dyes measured separately (7,39). In these latter studies, the intermediately sized Alexa 488 displayed a higher permselectivity than either Alexa 350, or Alexa 594. It was also suggested (7) that Alexa 488 was more permeable than Lucifer Yellow. To determine whether differences in the permeance sequence stemmed from interactions between the dyes in the dual dye experiments, the permeance of Cx43 junctions was determined for each of these dyes individually by injecting only the dye to be tested along with a labeled dextran for detection of cytoplasmic bridges. No significant difference in average permeance rate constant was detected for any of these dyes when measured alone or in concert with another dye (figure 6). These data indicate the absence of any interaction between the dyes that significantly affects their permeances through Cx43 channels.

DISCUSSION

Recently published data show that junctional permselectivity (the quotient of a junction's dye permeance to its conductance) varies over several orders of magnitude for Cx43 comprised junctions (17,18). This heterogeneous junctional permselectivity suggests the presence of multiple selectivity states for Cx43 channels. Discrimination between permeants based on permeant size or charge are the two most obvious criteria for specifying channel selectivity. Thus, one goal of the present study was to determine if

variability in charge or size selectivity of Cx43 channels could explain the observed heterogeneity in junctional permselectivity. Several approaches to test this were considered. While comparison of permselectivity values for individual dyes is sufficient to demonstrate differences in permselective properties between junctions, it is insufficient to determine the extent to which charge or size is important for this variability, as there are possible differences in both size and charge of the dye permeants and the current carrying ions used for the measurement. Conversely, comparison of the average junctional permeances to individual dyes can demonstrate the average size or charge selectivity of junctions, but the extent to which these selectivities could vary cannot be distinguished from variability in channel number between junctions. The simultaneous measurement of the permeance of a single gap junction to multiple dyes of differing size or charge done in the current study allowed for direct determination of the relative permeance or selectivity of the same population of channels to the dyes being tested. If different junctions displayed different selectivities for the parameter (size or charge) being measured, it would be readily apparent from the comparison of permeance rate constants for the two dyes across each junction. Simultaneous measurement of multiple dyes was thus ideally suited both to determine selectivity of individual gap junctions and to detect any differences in the selectivity properties of junctions from one cell pair to the next. Additionally, since the comparison of rate constants was done across the same junction, the measurement of cell volumes needed to make a valid comparison of permeance rate constants between different cell pairs is obviated.

Comparison of Charge Selectivity to Previously Published Work.

The results of the charge selectivity experiments in this study are consistent with previously published data. Using technical approaches somewhat different from those used here, others have compared the permeance of Cx43 junctions to dyes of differing charge and found no consistent trend for discrimination between the dyes based on charge (5,12,40). Additionally, the comparison of single channel conductances using different salt solutions in the current study also indicated a lack of charge selectivity among current carrying ions. This is also consistent with other studies using the same approach (35,36) or a reversal potential strategy (12). These combined results point to a consistent lack of charge selectivity for Cx43 gap junctions and channels that are not forced into a residual subconductance state by large (≥60 mV) transjunctional voltages. Additionally the results of the Cx40 dual dye, charge selectivity experiments (≈15:1 cationic selectivity) were similar to published selectivities found by comparing the permeance of the same dyes used in the current study but measured separately (40) or using electrophysiological measurements (10,31).

Comparison of size selectivity data to previously published work.

Studies done by Weber et al (7) and Dong et a; (39) are the only studies in which the permeance of Cx43 channels to each of the Alexa dyes (350, 488, 594) used herein was determined in a manner suitable for comparison to current values. In these studies the permselectivity of Cx43 junctions was determined separately for each of these dyes. The

permselectivity sequences relative to Alexa 350 of ≈ 1 : 2 : 0.5 (Weber) and ≈ 1 : 3 : 1 (Dong) for Alexa 350, 488, and 594, respectively, are not entirely consistent with the relative permeance sequence of ≈ 1 : 0.25 : 0.025 found in the current study. The reasons for the disparate results are not clear but could reflect several factors. Differences in technical approach would not (necessarily) be expected to lead to the disparate results. Some degree of error could result from measurement of the conductance of junctions with the high levels of electrical coupling found in both the Dong and Weber studies. Both studies, however, addressed the impact of such error in an apparently appropriate fashion. Errors in measuring junctional dye permeances could also arise from the impact of photobleaching and leakage of dye across the non-junctional membrane. A comparison of $F_{total(t)}/F_{total(t0)}$ (see methods) values at equivalent time points in the current study showed that loss in intensity over time was approximately ten times faster for Alexa 350 and Lucifer Yellow than for either Alexa 488 or 594 (Figure 4B inset). The rate of dye intensity loss of Alexa 350 and Lucifer Yellow ($B_{loss} \approx 0.02$ min^{-1}) relative to the rate of intercellular diffusion was not sufficiently large to have a significant impact on measured permeances in the current study for which intercellular dye diffusion was typically complete in <10 min. However, the slow rates of transfer ($B_{dye} \approx 0.2$ min^{-1}) found in HeLa43 cells by Dong and the long duration (>5 hours) of experiments in oocytes by Weber could increase the significance of the loss in intensity of Alexa 350 in measuring junctional dye permeance. The impact of this loss in intensity, however, would not necessarily be expected to explain the extent of the difference in the relative permeance sequences. Alternatively, Cx43 channels could display an additional selectivity state not present in the current study that could explain the disparate results. To address possible cell specific regulation of Cx43 selectivity we measured the dye selective properties of Cx43 junctions formed by four different cell types: Rin43, NRK, HeLa43, and fetal rat cardiac ventricular myocytes. The junctional size and charge selectivities were similar for all of the cell types**.**

***Comparison of permeance values to previously published work*.**

The most appropriate measure for the specific description of ease of diffusion through a gap junction is permeance (permeability × total cross sectional area of the junction) (18,33,34). The rate constant (B_{dye}) from the current study can be converted to junctional permeance (volume rate) by multiplying B_{dye} by half the cell volume (see methods Eqs 8-11). If all cells are assumed to have a volume of 1 picoliter the resulting average junctional permeance values were (in mm^3/sec) ≈ 2.0 x 10^{-8} (NBD-M-TMA and Alexa 350), ≈ 6.0 x 10^{-9} (Lucifer Yellow), ≈ 5.0 x 10^{-9} (Alexa 488), and ≈ 5.0 x 10^{-10} (Alexa 594). Specific comparisons with permeance values from other studies are limited by the fact that junctional permeances are dependent on open channel number, which is not directly available from the current study. The average junctional permeance for NBD-M-TMA in the current study was similar, however, to that found by Ek-Vitorin (17) (≈ 2.0 x 10^{-8} mm^3/sec) in the same cell types (Rin43 and NRK) using a somewhat different approach.

Channel pore radius estimated from relative dye permeances and channel conductances.

If the Cx43 channel behaves as a simple mechanical filter discriminating solely on the basis of permeant size, the relative permeability sequence (Table 2) of the molecules of different sizes used for the size selectivity experiments (figure 5) can be used to estimate the Cx43 channel pore radius according to the following formula (11,41):

$$\frac{P(x)}{P(\text{Alexa 350})} = \frac{C \times (1-\alpha)^2 \times (1 - 2.105\alpha + 2.0865\alpha^3 - 1.7068\alpha^5 + 0.72603\alpha^6)}{1 - 0.75857\alpha^5} \qquad \text{Eq.13}$$

Where:
P = permeance
α = permeant radius/pore radius
C = scaling factor

Based on the ratio of permeant to pore radii (α), this formula predicts the extent to which the effective diffusion constant of a molecule is decreased in a simple aqueous pore relative to bulk aqueous solution. This decrease in effective diffusion constant is due primarily to two effects. The $(1 - \alpha)^2$ term describes the impact of the entire cross section of the channel not being available to each ion. The remaining term describes the effect of solvent drag on a sphere moving through an aqueous cylinder. The combined effect of solvent drag and available cross sectional area reduces the permeance (diffusion constant × partition coefficient × channel area / channel length) for each dye. As such, Eq. 13 can be used to generate a predicted relative permeability sequence for a given channel pore radius (41). A plot of the permeance relative to Alexa 350 versus hydrodynamic radius for each of the dyes (Figure 7) was best fit with a channel radius of ≈10 Å. Lucifer Yellow was fit with a somewhat smaller (≈7.5 Å) radius indicating that, despite moving more quickly than the larger dyes, it did not move as well through the pore relative to its size as the other dyes moved. This could represent a modest selectivity among these molecules beyond that predicted by their size. However, a similar relative permeance profile was observed across cytoplasmic bridges (figure 7 inset). This indicates that, instead of being due to channel selectivity, the apparent slowing of Lucifer Yellow relative to its size was a result of the calculated hydrodynamic radius for Lucifer Yellow (Table 1) not accurately predicting its ability to diffuse in solution relative to the other dyes. Indeed, if the hydrodynamic radius of Lucifer Yellow is estimated according to its permeance across cytoplasmic bridges relative to that of the Alexa dyes (figure 7 inset; gray triangle), the relative permeance of Lucifer Yellow is also consistent with an aqueous channel pore of ≈10 Å (figure 7; gray triangle).

The assumptions involved in applying such a continuum hydrodynamic model (Eq. 13) to gap junction channels and the appropriateness of these assumptions are well described by Nitsche et al (34). Briefly, the assumptions are that 1) concentrations of permeant molecules (modeled as hard spheres) are assumed to be low enough that permeant molecule movements are independent (42), 2) permeant molecules are treated

as being localized to the center of the pore (radially) during transit (43), and 3) the aqueous environment in the channel is assumed to represent a continuum relative to the permeant where the only effect of the channel wall on mobility is through the boundary condition that the velocity of water at the wall is zero (42). Continuum hydrodynamic theory can be applied only approximately to pores as small as gap junction channels (particularly as α approaches 1) (42,44), thus the pore size estimated from Eq. 13 should only be considered as approximate. The fit of the relative dye permeance data to a single pore size, however, does suggest that dye selectivities of Cx43 channels can be well described based solely on the sizes of the dye permeants.

Cx43 channel radius has also been estimated from channel conductance values (6). Conductance of channels modeled as simple cylindrical pores can be calculated from the following equation (32):

$$\gamma_j = \pi r^2 c / (l + \pi r/2) \qquad \text{Eq. 14}$$

where:
γ_j = channel conductance
l = channel length
r = channel radius
c = conductivity of salt solution

If the length of the channel is assumed to be 160Å (6,34), the channel conductances from the current study (figure 1A) were best fit by a channel with an average radius of ≈6 Å using Eq. 14. This is clearly different from the ≈10 Å radius estimated from the relative dye permeances (figure 7). It is worth noting, however, that a channel radius of 6 Å would in fact be too small to accommodate passage of Alexa 594 (7.4 Å) and would also essentially eliminate passage of Alexa 488 (5.8 Å). It is clear from the current study and others, however, that these dyes permeate (at least some configurations of) Cx43 channels.

The discrepancy between pore radii estimated by relative dye permeance and by channel conductance could be due to assumptions that are inherent to the estimation of channel radius from channel conductance using Eq. 14. The first assumption is that the diffusion constant for the ions in the channel is equal to that in bulk solution. For a channel as long as a gap junction channel, this is likely not a valid assumption (41,45). In fact, the estimates of pore size in figure 7 using Eq. 13 are based on the extent to which the effective diffusion constant is expected to decrease in the channel compared to bulk solution as a function of the ratio of permeant to pore radii. The resultant correction factor from Eq. 12 can be applied to the solution conductivity in Eq. 13 to incorporate the predicted decrease in effective diffusion constant in the channel into the conductance estimate, since ion conductivity is directly dependent on the diffusion constant of the ion (Stokes-Einstein relation) (25,26,32). When the expected change in diffusion constant was taken into account, single channel conductances from the current study were best fit by a radius of ≈9 Å, which is similar to the ≈10 Å radius predicted from the relative dye permeances. Another assumption inherent to Eq. 14 is that ion movement through the

channel is independent. If movement of ions is not entirely independent, as could be the case for a channel as long as a gap junction channel, the estimated channel radius based on channel conductance could increase further still to reach the radius estimated by relative dye permeances. Thus, channel conductance and dye permeance data are consistent with a channel pore radius of ≈10 Å.

The channel conductance and dye permeance data are also consistent with a channel pore of reasonably uniform diameter along its length. In a non-charge selective channel, single channel conductance to small inorganic ions is dominated by average cross sectional area of the pore, while relative permeances of larger dye molecules could be dominated by a brief constriction along the length of the pore (46). A significant constriction along an otherwise wider pore would then be expected to yield a pore size estimate from relative dye permeances that would be smaller than that estimated from channel conductance to smaller ions. The fact that channel conductance and relative dye permeance yield a similar pore size estimate indicates the lack of a significant constriction along the length of dye permeable Cx43 channels. If such a constriction were present as a selectivity filter in other connexin channels yet absent in Cx43 channels, it could help explain how Cx43 channels have higher permeabilities to larger molecules than other, more selective connexins with higher unitary conductances (6,7). The combined Cx43 dye selectivity and single channel conductance data are well described by simple hindered diffusion through an aqueous channel pore with a radius of ≈10 Å that is devoid of significant electrostatic influences and reasonably uniform in geometry along its length. In such a pore, the selectivity of the channel would be primarily determined by permeant size, as was seen here.

While the Cx43 dye selectivity and unitary conductance data reported herein are well described by hindered diffusion through an aqueous pore (≈10 Å radius and 160 Å length), other investigators (7,17,18) have reported Cx43 single channel dye permeances much higher than those predicted using unitary conductance as an estimator of pore size. These higher permeances would require pore radii of ≥20 Å, which are inconsistent with structural data (47,48). Consequently, these high permeances have been ascribed to favorable permeant pore interactions that result in increased permeant concentration in the pore and therefore enhanced flux rates. Determining absolute per channel flux rates or single channel permeances for each dye was not the focus of the current study; however, the junctional permeance values found in the current study are similar to those reported by Ek-Vitorin et al (17) for the same cell types. If we assume that channel numbers per junction in the two studies are similar, it is likely that the absolute dye permeances of the channels comprising the junctions studied herein are also higher than predicted by hindered diffusion through a 10 Å radius aqueous pore. If favorable permeant pore interactions occur, our selectivity data suggest that 1) mobility of larger permeants must still be hindered by all or a portion of the channel pore that has a radius of ≈10 Å and 2) permeant pore interactions must be independent of permeant charge polarity and (to the extent that the dyes NBD-M-TMA, Lucifer Yellow, Alexa 350, Alexa 488, and Alexa 594 represent variability in permeant structure and composition; see data supplement) independent of permeant structure and composition as well. Such interactions would

generally be consistent with the van der Waals type interactions that were initially proposed for this affinity (7,34).

Variable permselectivity cannot be explained by variable charge or size dye selectivity.

Recently published data show a very poor correlation between dye permeance and electrical conductance across Cx43 junctions (17,18). One aim of the present study was to determine whether heterogeneity in the selectivity of Cx43 junctions to dye charge or size could explain heterogeneity in permselectivity of Cx43 junctions. The dual dye technique used here is ideal for addressing this issue. The strong correlations ($r \geq 0.93$) between permeance of Cx43 junctions to dyes of either similar size and opposing charge (figure 3) or of similar charge and differing size (figure 5) from many junctions for each dye combination indicated that charge and size selectivity are fixed parameters for dye-permeable Cx43 channels. The ≈2-3 fold range in junctional charge and size selectivity measured herein was similar to that found for cytoplasmic bridges and presumably represents the variability in the dual dye measurement approach. These data suggest that the greater than 2 orders of magnitude variability seen for permselectivity of Cx43 junctions cannot be explained by variable charge or size dye selectivity of the comprising channels.

A dye-impermeable open state could lead to independence of conductance and dye permeance.

The data from the current study showing that the size and charge dye selectivities of Cx43 junctions were essentially fixed parameters seem at odds with the recently published data that show a large range in junctional permselectivities (17,18). These seemingly disparate results can be reconciled by the variable presence of a conductive yet dye impermeable open state of Cx43 channels (Figure 8). In this model Cx43 channels are proposed to exist in one of two open state configurations, dye-permeable or dye-impermeable, with both states being conductive to smaller ions. Junctional dye permeance would then be mediated by a single channel state with constant selectivity properties, leading to constant junctional dye selectivities. If the proportion of dye-permeable and dye-impermeable channels contributing to junctional conductance varied between junctions, this would produce the reported variable relationship between junctional dye permeance and junctional conductance (permselectivity) despite a constant relationship between relative dye permeances (dye selectivity). Figure 8 shows how variable contribution of these two conductive states to a junction would provide a mechanism by which cells independently regulate electrical and chemical communication via Cx43 gap junctions. It is noteworthy that some studies of Cx43 permselectivity have found a consistent relationship between dye permeance and electrical conductance (7,8,39,49). A lack of variable permselectivity could also be consistent with the model proposed above if, in some cell types or under certain conditions, the proportion of channels occupying dye-permeable vs. dye-impermeable open states was consistent.

While it is clear that permeance of channels must change between permselective states, it is worth noting that conductance of channels need not change in parallel with

changes in dye permeance or significantly change at all. In fact, channel conductance has been shown to be a poor predictor of permeability for a number of connexins (6,7,50). An excellent example is recent work (39) showing that substitution of the N-terminus of chick Cx45.6 with that of Cx43 confers permeability to Alexa 594 (the largest of the Alexa dyes in these studies) through Cx45.6 channels that is absent in wtCx45.6 channels, while decreasing channel conductance from ≈200 pS to ≈100 pS. The apparent disconnection between conductance and dye permeance could be due in large part to the relative sizes of the dye molecules, the current carrying ions, and the Cx channel pores. For smaller molecules (K^+ or Cl^-) passage through gap junction channels is likely dominated by the average cross section of the channel, while larger molecules (dyes) may be more affected by interactions with the channel wall or brief points of constriction along the length of the channel. By this mechanism, the approximate shape of the dye-impermeable open state in figure 8 could represent a configuration change resulting in an alteration of dye permeance without a significant accompanying change in channel conductance.

Cx43 can gate to a conductive but dye-impermeable open state.

Partial closure of Cx43 channels to the voltage-induced 'residual' conductance state significantly increases size selectivity of the channel. Indeed, whereas the conductance decreases by ≈65% (from ≈100 to ≈35 pS) permeability to larger molecules such as fluorescent tracers and cAMP decreases to undetectable levels (36,46). The absence of an applied transjunctional voltage in our dual dye experiments makes the presence of a voltage-induced residual state unlikely; thus, our results suggest the existence of a gating mechanism that alters the size selectivity of Cx43 comprised junctions to a state that becomes dye impermeable but remains conductive. It is possible that a similar mechanism could be induced by events other than large trans-junctional voltages, such as phosphorylation of the channel's subunits, which has indeed been shown to alter communicative properties of both Cx43 single channels and junctions (17,51). In fact, recently published data demonstrate that phosphorylation of Cx43 results in a significant increase in size selectivity of Cx43 hemichannels (52). In the latter study, reconstituted Cx43 hemichannels were permeated by both ethylene glycol and sucrose (hydrodynamic radii ≈2.2 Å and 4.6 Å, respectively) when not phosphorylated at S368 but were permeated only by ethylene glycol, not sucrose, when phosphorylated at S368. A similar mechanism could be involved in regulation of Cx43 junctional channels as well, resulting in a channel that is permeated by small inorganic ions such as K^+ and Cl^- (hydrodynamic radii ≈1.3 Å) but not by the dyes used in the current study or in the permselectivity studies (hydrodynamic radii ≥4.3 Å). These channel configurations could represent the dye-permeable and dye-impermeable open states proposed here.

Significance

Based on the rate at which Lucifer Yellow traverses Cx43 channels calculated by Valiunas et al (8), the effective ability of intercellular diffusion across Cx43 junctions of short-lived signaling molecules such as cyclic nucleotides, calcium and inositol tris

phosphate (IP_3), which are generally present at very low (micromolar) concentrations, was challenged. In fact, Valiunas calculated that the per channel flux rate for the dye Lucifer Yellow was ≈ 90 molecules per second at a 120 μM gradient. Recent data (7,17,18) and the data from the current study, however, indicate that the flux rates for diffusion of larger solutes across junctions can vary by several orders of magnitude and display flux rates orders of magnitude higher than those initially described (8). Indeed, the average single channel permeance determined by Weber et al (7) for Alexa 488 (similar in size and charge to Lucifer Yellow) yields a per channel flux rate of 35,000 molecules per second at a 120 μM gradient. Given the likely possibility for effective communication of even short-lived signals via gap junction mediated intercellular diffusion, the ability to regulate the effective permeability to diffusion of chemical signals largely independently from effects on electrical communication could be of physiological benefit in a number of situations. This independence of regulation of chemical and electrical communication could be of particular benefit for tissues that require constant electrical communication for proper functioning, such as the heart, but may also require variable control of permeability to chemicals and second messengers. Unique properties of regulation of these communication types could provide insight into connexin-specific roles in physiological and pathophysiological situations. Further study is required to ascertain the regulatory mechanisms involved in conversion of channels between permeance states and to further characterize the specific permeance, selectivity, and conductive properties of Cx43 channels in each of these states.

ACKNOWLEDGEMENTS

We thank Drs. Jose Ek-Vitorin, David Kurjiaka and Tim Secomb for helpful discussions and Tasha Nelson for excellent technical assistance. This work was supported by grants from the National Institutes of Health (to J.M.B): HL58732 and HL007249, the latter providing pre-doctoral support to N.S.H.

REFERENCES

1. Sohl,G. and K.Willecke. 2004. Gap junctions and the connexin protein family. *Cardiovasc. Res.* 62:228-232.
2. Evans,W.H. and P.E.Martin. 2002. Gap junctions: structure and function (Review). *Mol. Membr. Biol.* 19:121-136.
3. Delorme,B., E.Dahl, T.Jarry-Guichard, J.P.Briand, K.Willecke, D.Gros, and M.Theveniau-Ruissy. 1997. Expression pattern of connexin gene products at the early developmental stages of the mouse cardiovascular system. *Circ. Res.* 81:423-437.
4. Haefliger,J.A., E.Castillo, G.Waeber, G.E.Bergonzelli, J.F.Aubert, E.Sutter, P.Nicod, B.Waeber, and P.Meda. 1997. Hypertension increases connexin43 in a tissue-specific manner. *Circ.* 95:1007-1014.
5. Elfgang,C., R.Eckert, H.Lichtenberg-Frate, A.Butterweck, O.Traub, R.A.Klein, D.Hulser, and K.Willecke. 1995. Specific permeability and selective formation of gap junction channels in connexin-transfected HeLa cells. *J. Cell Biol.* 129:805-817.

6. Veenstra,R.D., H.Z.Wang, D.A.Beblo, M.G.Chilton, A.L.Harris, E.C.Beyer, and P.R.Brink. 1995. Selectivity of connexin-specific gap junctions does not correlate with channel conductance. *Circ. Res.* 77:1156-1165.
7. Weber,P.A., H.C.Chang, K.E.Spaeth, J.M.Nitsche, and B.J.Nicholson. 2004. The permeability of gap junction channels to probes of different size is dependent on connexin composition and permeant-pore affinities. *Biophys. J.* 87:958-973.
8. Valiunas,V., E.C.Beyer, and P.R.Brink. 2002. Cardiac gap junction channels show quantitative differences in selectivity. *Circ. Res.* 91:104-111.
9. Nicholson,B.J., P.A.Weber, F.Cao, H.Chang, P.Lampe, and G.S.Goldberg. 2000. The molecular basis of selective permeability of connexins is complex and includes both size and charge. *Braz. J. Med. Biol. Res.* 33:369-378.
10. Beblo,D.A. and R.D.Veenstra. 1997. Monovalent cation permeation through the connexin40 gap junction channel Cs, Rb, K, Na, Li, TEA, TMA, TBA, and effects of anions Br, Cl, F, acetate, aspartate, glutamate, and NO_3. *J. Gen. Physiol.* 109:509-522.
11. Wang,H.-Z. and R.D.Veenstra. 1997. Monovalent ion selectivity sequences of the rat connexin43 gap junction channel. *J. Gen. Physiol.* 109:491-507.
12. Trexler,E.B., F.F.Bukauskas, J.Kronengold, T.A.Bargiello, and V.K.Verselis. 2000. The first extracellular loop domain is a major determinant of charge selectivity in connexin46 channels. *Biophys. J.* 79:3036-3051.
13. Goldberg,G.S., V.Valiunas, and P.R.Brink. 2004. Selective permeability of gap junction channels. *Biochim. Biophys. Acta* 1662:96-101.
14. Goldberg,G.S., P.D.Lampe, and B.J.Nicholson. 1999. Selective transfer of endogenous metabolites through gap junctions composed of different connexins. *Nat. Cell Biol.* 1:457-459.
15. Harris,A.L. 2007. Connexin channel permeability to cytoplasmic molecules. *Prog. Biophys. Mol. Biol.* 94:120-143.
16. Ek-Vitorin,J.F. and J.M.Burt. 2005. Quantification of gap junction selectivity. *Am. J. Physiol Cell Physiol* 289:C1535-C1546.
17. Ek-Vitorin,J.F., T.J.King, N.S.Heyman, P.D.Lampe, and J.M.Burt. 2006. Selectivity of connexin 43 channels is regulated through protein kinase C-dependent phosphorylation. *Circ. Res.* 98:1498-1505.
18. Eckert,R. 2006. Gap-junctional single-channel permeability for fluorescent tracers in mammalian cell cultures. *Biophys. J.* 91:565-579.
19. Vozzi,C., S.Ullrich, A.Charollais, J.Philippe, L.Orci, and P.Meda. 1995. Adequate connexin-mediated coupling is required for proper insulin production. *J. Cell Biol.* 131:1561-1572.
20. Gustafson,T.A., J.J.Bahl, B.E.Markham, W.R.Roeske, and E.Morkin. 1987. Hormonal regulation of myosin heavy chain and alpha-actin gene expression in cultured fetal rat heart myocytes. *J. Biol. Chem.* 262:13316-13322.
21. Cottrell,G.T. and J.M.Burt. 2001. Heterotypic gap junction channel formation between heteromeric and homomeric Cx40 and Cx43 connexons. *Am. J. Physiol Cell Physiol* 281:C1559-C1567.

22. Kurjiaka,D.T., T.D.Steele, M.V.Olsen, and J.M.Burt. 1998. Gap junction permeability is diminished in proliferating vascular smooth muscle cells. *Am. J. Physiol.* 275:C1674-C1682.
23. Bhasker,R., M.Ahad, Mash E.A., D.Bednarczyk, and S.H.Wright. 2006. Synthesis and fluorescence of N,N,N-trimethyl-2-[methyl(7-nitrobenzo[*c*][1,2,5]oxadiazol-4-yl)amino]ethaminium iodide, a pH-insensitive reporter of organic cation transport. *Synthetic Communications*701-705.
24. Wilke,C.R. and P.Chang. 1955. Correlation of diffusion coefficients in dilute solutions. *A. I. Ch. E. Journal* 1:264-270.
25. Miller C.C. 1924. The Stokes-Einstein law for diffusion in solution. *Proc. R. Soc. Lond.* 106:724-749.
26. Einstein,A. 1905. Uber die von der molekularkinetischen Theorie der Warme geforderte Bewegung von in ruhenden Flussigkeiten suspendiertin Teilchen. *Annalen der Physik* 322:549-560.
27. Reid,R.C., J.M.Prausnitz, and T.K.Sherwood. 1977. The Properties of Gases and Liquids. McGraw-Hill, New York.
28. Dakin,K., Y.Zhao, and W.H.Li. 2005. LAMP, a new imaging assay of gap junctional communication unveils that Ca^{2+} influx inhibits cell coupling. *Nat. Methods* 2:55-62.
29. Wade,M.H., J.E.Trosko, and M.Schindler. 1986. A fluorescence photobleaching assay of gap junction-mediated communication between human cells. *Science* 232:525-528.
30. Cottrell,G.T., Y.Wu, and J.M.Burt. 2002. Cx40 and Cx43 expression ratio influences heteromeric/heterotypic gap junction channel properties. *Am. J. Physiol.* 282:C1469-C1482.
31. Lin,X., E.Fenn, and R.D.Veenstra. 2006. An amino-terminal lysine residue of rat connexin40 that is required for spermine block. *J. Physiol.* 570:251-269.
32. Hille,B. 1992. Ionic Channels of Excitable Membranes. Sinauer Associates Inc., Sunderland, MA.
33. Biegon,R.P., M.M.Atkinson, T.F.Liu, E.Y.Kam, and J.D.Sheridan. 1987. Permeance of Novikoff hepatoma gap junctions: quantitative video analysis of dye transfer. *J. Membr. Biol.* 96:225-233.
34. Nitsche,J.M., H.C.Chang, P.A.Weber, and B.J.Nicholson. 2004. A transient diffusion model yields unitary gap junctional permeabilities from images of cell-to-cell fluorescent dye transfer between Xenopus oocytes. *Biophys. J.* 86:2058-2077.
35. Valiunas,V., F.Bukauskas, and R.Weingart. 1997. Conductances and selective permeability of connexin43 gap junction channels examined in neonatal rat heart cells. *Circ. Res.* 80:708-719.
36. Bukauskas,F.F., A.Bukauskiene, and V.K.Verselis. 2002. Conductance and permeability of the residual state of connexin43 gap junction channels. *J. Gen. Physiol* 119:171-186.
37. Mastro,A.M. and A.D.Keith. 1984. Diffusion in the aqueous compartment. *J. Cell Biol.* 99:180s-187s.

38. Unger,V.M., N.M.Kumar, N.B.Gilula, and M.Yeager. 1997. Projection structure of a gap junction membrane channel at 7 Å resolution. *Nature Structural Biology* 4:39-43.
39. Dong,L., X.Liu, H.Li, B.M.Vertel, and L.Ebihara. 2006. Role of the N-terminus in permeability of chicken connexin45.6 gap junctional channels. *J. Physiol.* 576:787-799.
40. Cottrell,G.T., Y.Wu, and J.M.Burt. 2001. Functional characteristics of heteromeric Cx40-Cx43 gap junction channel formation. *Cell Commun. Adhes.* 8:193-197.
41. Dwyer,T.M., D.J.Adams, and B.Hille. 1980. The permeability of the endplate channel to organic cations in frog muscle. *J. Gen. Physiol.* 75:469-492.
42. Levitt,D.G. 1975. General continuum analysis of transport through pores. I. Proof of Onsager's reciprocity postulate for uniform pore. *Biophys. J.* 15:533-551.
43. Deen,W.M. 1987. Hindered transport of large molecules in liquid filled pores. *AIChE Jl* 33:1409-1425.
44. Adams,D.J., T.M.Dwyer, and B.Hille. 1980. The permeability of endplate channels to monovalent and divalent metal cations. *J. Gen. Physiol.* 75:493-510.
45. Levitt,D.G. 1991. General continuum theory for multiion channel. II. Application to acetylcholine channel. *Biophys. J.* 59:278-288.
46. Qu,Y. and G.Dahl. 2002. Function of the voltage gate of gap junction channels: selective exclusion of molecules. *Proc. Natl. Acad. Sci. U. S. A.* 99:697-702.
47. Yeager,M., V.M.Unger, and M.M.Falk. 1998. Synthesis, assembly and structure of gap junction intercellular channels. *Curr. Opin. Struct. Biol.* 8:517-524.
48. Unger,V.M., N.M.Kumar, N.B.Gilula, and M.Yeager. 1999. Three-dimensional structure of a recombinant gap junction membrane channel. *Science.* 283:1176-80.
49. Ma,M. and G.Dahl. 2006. Cosegregation of permeability and single-channel conductance in chimeric connexins. *Biophys. J.* 90:151-163.
50. Gong,X.Q. and B.J.Nicholson. 2001. Size selectivity between gap junction channels composed of different connexins. *Cell Commun. Adhes.* 8:187-192.
51. Burt,J.M. and T.D.Steele. 2003. Selective effect of PDGF on connexin43 versus connexin40 comprised gap junction channels gap junction channels. *Cell Commun. Adhes.* 10:287-291.
52. Bao,X., S.C.Lee, L.Reuss, and G.A.Altenberg. 2007. Change in permeant size selectivity by phosphorylation of connexin 43 gap-junctional hemichannels by PKC. *Proc. Natl. Acad. Sci. U. S. A.* 104:4919-4924.

Table 1: Physical Properties of Permeants

	MW (no counter ion)	D_{Aqeous} (25°C) (10^{-6} cm^2/sec)	Stokes-Einstein radius (Å)	λ_{ex} / λ_{em} (nM)	Net charge
NBD-M-TMA	280	5.8*	4.3	458/580	1^+
Alexa 350	326	5.6*	4.4	345/445	1^-
Lucifer Yellow	443	5.0*	4.9	428/536	2^-
Alexa 488	546	4.2*	5.8	493/517	2^-
Alexa 594	734	3.3*	7.4	588/613	2^-
K	39	19.6†	1.3	-	1^+
Cl	35	20.3†	1.2	-	1^-
TEA	130	9.7†	2.9	-	1^-
Glutamate	164	9.7‡	2.9	-	1^+

**Calculated using Wilke-Chang correlation (see methods) †Calculated from mobility(32) ‡Assumed equal to TEA due to similar solution conductivities.*

Table 2: Permeances Relative to Alexa 350

	NBD-M-TMA	Lucifer Yellow	Alexa 488	Alexa 594
Cx43wt	1.00 ± 0.03 (n=41)	0.35 ± 0.02 (n=12)	0.27 ± 0.01 (n=28)	0.029 ± 0.002 (n=27)
Bridges	0.96 ± 0.03 (n=8)	0.56 ± 0.03 (n=3)	0.52 ± 0.03 (n=4)	0.28 ± 0.01 (n=4)
Cx40 wt	15 ± 3.3 (n=6)	-	-	-

FIGURE LEGENDS:

Figure 1: Cx43 conductance measurements show a lack of charge selectivity among ions. (A) Channel event conductances (40 mV transjunctional voltage) determined from fitting channel event frequency histograms with single Gaussian peaks for KCl (324 events, 2 preparations), TEACl **(**148 events, 1 preparation), and KGlutamate (138 events, 1 preparation). **(B)** Plot of channel event conductance vs. solution conductivity for Cx43wt junctions measured using KCl (○), TEACl (△), and KGlutamate (■) as primary current carrying ions. The dotted line represents conductances relative to KCl predicted by solution conductivities.

Figure 2: Dual dye charge selectivity measurement method. (A) An image sequence from a typical experiment comparing NBD-M-TMA (left column) to Alexa 350 (right column)(false color)(NRK cells). Yellow bar represents 10 microns. **(B)** Experimental data from panel A plotted as a function of time either as fluorescence normalized to total intensity (donor + recipient) at t_0 (top panel) or as the $-\ln((F_{eq} - F_{(t)} / F_{total(t/t0)})/(F_{eq} - F_{(0)}))$ (Eq. 8) (bottom panel). Data from both dyes are well fit to a single rate constant (1.0 min^{-1}) by Eq. 7 (top panel) or by linear regression of data points converted using Eq. 8 (bottom panel) as evidenced by the fit lines through the data points.

Figure 3: Cx43 junctions are not charge selective for diffusion of dyes. (A) Rate constants for NBD-M-TMA ($B_{NBD\text{-}M\text{-}TMA}$) vs. Alexa 350 ($B_{Alexa\ 350}$) for multiple Cx43 junctions (●) (n = 4, HeLa43; n = 12, Rin43; n = 25, NRK; n = 1, cardiac ventricular myocytes), cytoplasmic bridges (△) (n = 8), and Cx40 junctions (□) (n = 6, Rin40). The dotted line represents relative calculated aqueous diffusion constants for NBD-M-TMA / Alexa 350 (Table 1). **(B)** Average $B_{NBD\text{-}M\text{-}TMA} / B_{Alexa350}$ (charge selectivity) for junctions shown in panel A. The dotted line represents relative calculated aqueous diffusion constants for NBD-M-TMA/ Alexa 350. *Cx40 junctions were significantly different ($p < 0.05$) from both Cx43 junctions and cytoplasmic bridges. Selectivity of Cx43 junctions was not significantly different from bridges.

Figure 4: Dual dye size selectivity measurement method. (A) Results from a typical dye experiment showing intercellular dye diffusion over time for Alexa 350 (left) and Alexa 594 (right). Yellow bar represents 10 microns. (**B)** Total cell fluorescence intensity values for donor (upper curves) and recipient (lower curves) cells normalized to the total (donor + recipient) intensity of the first image. Curves represent the fits of the data by Eq. 7 to determine the rate constants (B_{dye}) of diffusion ($B_{Alexa350}$ = 2.8 min^{-1}; $B_{Alexa594}$ = 0.08 min^{-1}). The **inset** shows the loss in total fluorescence intensity (donor + recipient) over

time. The lines are fits to an exponential decay function with rate constants of 0.02 min^{-1} (Alexa 350) and 0.002 min^{-1} (Alexa 594). (**C)** Plot of same intensities from panel B converted using Eq. 8 (methods). Lines represent linear regressions, the slopes of which equal the diffusion rate constants ($B_{Alexa350}$ = 2.7 min^{-1}; $B_{Alexa594}$ = 0.08 min^{-1}). (**D)** Results from a typical dye experiment showing dye transfer over time for the same cell pair for Alexa 350 (left) and Alexa 488 (right). Yellow bar represents 10 microns. (**E)** The resulting total cell fluorescence intensity values for donor (upper curves) and recipient (lower curves) cells normalized to the total (donor + recipient) intensity of the first image. Curves represent fits of the data by Eq. 7 ($B_{Alexa350}$ = 2.96 min^{-1}; $B_{Alexa488}$ = 0.77 min^{-1}). (**F)** Plot of same intensities from panel E converted using Eq. 8. Lines are linear regressions, the slopes of which represent the diffusion rate constants ($B_{Alexa\ 350}$ = 2.81 min^{-1}; $B_{Alexa\ 594}$ = 0.76 min^{-1}).

Figure 5: Cx43 junctions show constant size selectivity. (A) Plot of permeance rate constants (B_{dye}) for Lucifer Yellow (●) (Rin43, n = 6; NRKe, n = 3; HeLa43, n = 3), Alexa 488 (△) (NRKe, n = 14; Rin43, n = 9; HeLa43, n = 5), and Alexa 594 (□) (NRKe, n = 11; Rin43, n = 10; HeLa43, n = 2; cardiac ventricular myocytes, n = 2) vs. Alexa 350 ($B_{Alexa\ 350}$) from individual cell pairs for Cx43wt junctions. Lines are linear regressions for each dye combination. All combinations were significantly correlated ($p < 0.05$). (**Inset)** The same plot as in panel A for cytoplasmic bridges where the dotted lines represent the regression fits from junctions. **(B)** Average $B_{Alexa\ dye}$ / $B_{Alexa\ 350}$ of experiments shown in panel A. *All dye combinations are significantly different ($p < 0.05$) from cytoplasmic bridges for the same dye combination.

Figure 6: Dye diffusion is independent in dual dye measurements. Plot of average rate constants for Alexa 350, Lucifer Yellow, Alexa 488, and Alexa 594 from the dual dye size selectivity experiments (dual dye) from NRK and Rin43 cells (Alexa 350, n = 53; Lucifer Yellow, n = 9; Alexa 488, n = 23; Alexa 594, n = 21) compared to the average rate constant for each dye when injected alone (single dye) using the same cell types (Alexa 350, n = 23; Lucifer Yellow, n = 7; Alexa 488, n = 10; Alexa 594, n = 9). None of the dyes showed significantly different rate constants when measured alone as compared to when measured in concert with another dye.

Figure 7: Permeance measurements yield a 10Å pore radius estimate. (A) Logarithmic scale plot of relative junctional permeances (B_{dye} / $B_{Alexa\ 350}$) vs. calculated Stokes-Einstein radii (see methods) for each of the dyes used in the size selectivity measurements: Alexa 350 (●), Lucifer Yellow (□ ▼), Alexa 488 (■), and Alexa 594(◆). Also shown (□ ▼) is the relative permeance of Lucifer Yellow plotted against its radius corrected for its diffusion across cytoplasmic bridges. Dotted lines represent predicted relative permeances for simple aqueous pores of the given channel radii according to Eq. 13. (**Inset)** Logarithmic scale plot of relative permeance (B_{dye} / $B_{Alexa\ 350}$) across cytoplasmic bridges vs. calculated Stokes-Einstein radii for each of the dyes used in the size selectivity measurements (symbols as in main figure). Also plotted here is the radius

of Lucifer Yellow predicted by its relative permeance to Alexa 350 (□ ▼). Dotted line is a simple line graph connecting the Alexa series.

Figure 8: Model for independent regulation of conductance (A) and permeance (B) for Cx43 gap junctions. (A) A model for regulation of conductance independent of permeance by changing the number of dye-impermeable conductive channels without changing the number of dye-permeable conductive channels. **(B)** A model for regulation of permeance independent of conductance by conversion of channels between dye-permeable and dye-impermeable conductive states. In both panels the lower diagrams indicate the resulting changes in each parameter of junctional function that would occur as a result of the gradual shift in channel populations shown above.

Figure 1

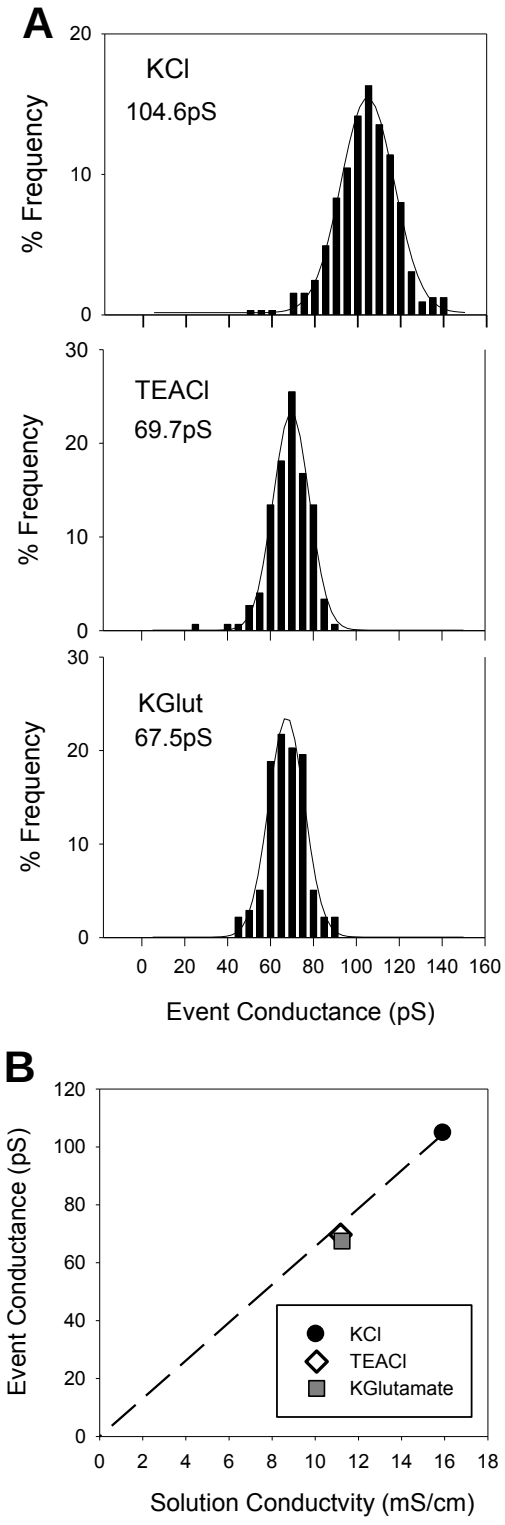
A
KCl
104.6pS
TEACl
69.7pS
KGlut
67.5pS
% Frequency
Event Conductance (pS)
B
Event Conductance (pS)
Solution Conductvity (mS/cm)
KCl
TEACl
KGlutamate

Figure 2

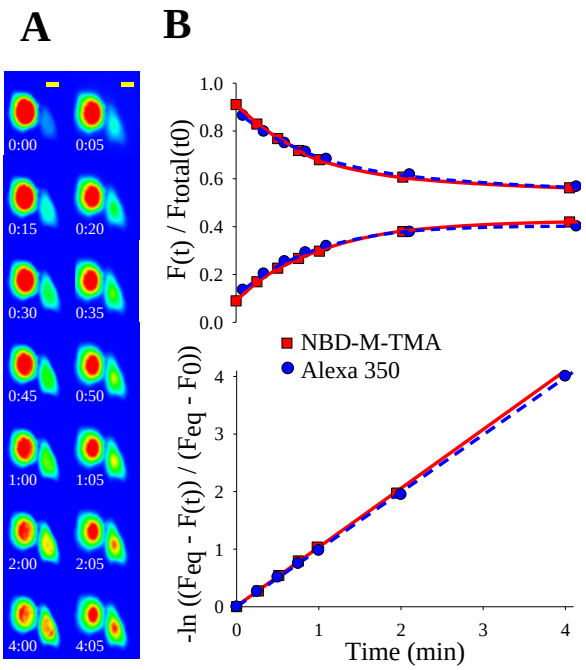
A
B
0:00
0:05
0:15
0:20
0:30
0:35
0:45
0:50
1:00
1:05
2:00
2:05
4:00
4:05
F(t) / Ftotal(t0)
NBD-M-TMA
Alexa 350
-ln ((Feq - F(t)) / (Feq - F0))
Time (min)

Figure 3

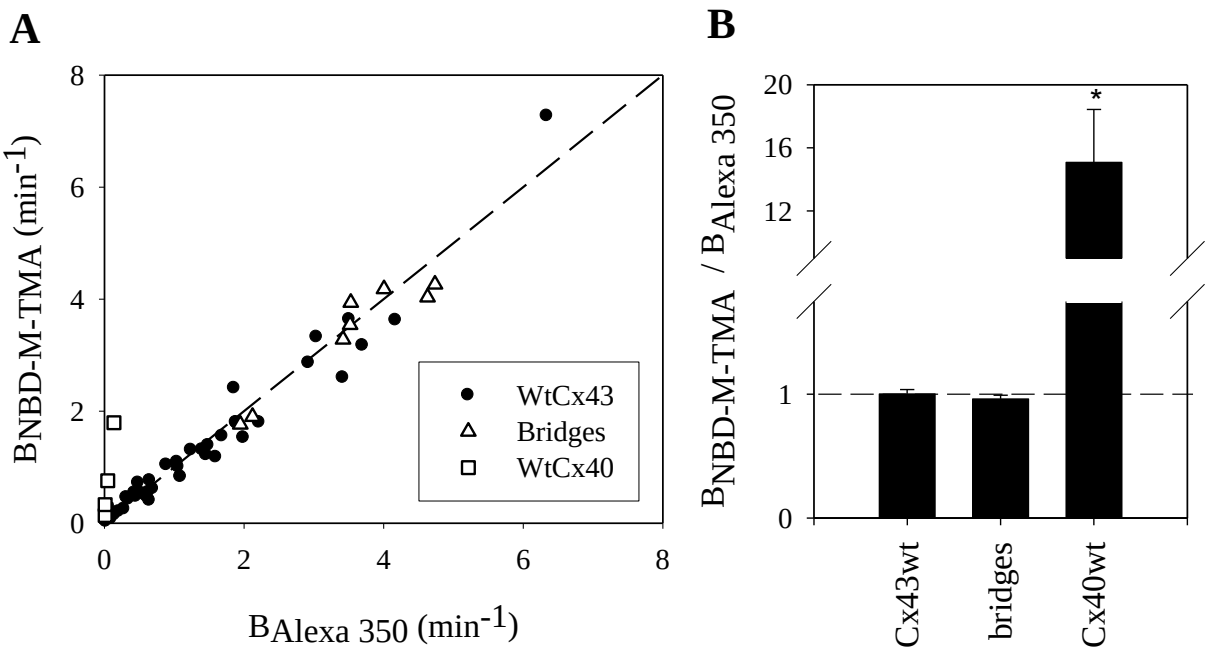
A
B
8
6
4
2
0
0
2
4
6
8
BNBD-M-TMA (min-1)
BAlexa 350 (min-1)
WtCx43
Bridges
WtCx40
20
16
12
1
0
*
BNBD-M-TMA / BAlexa 350
Cx43wt
bridges
Cx40wt

Figure 4

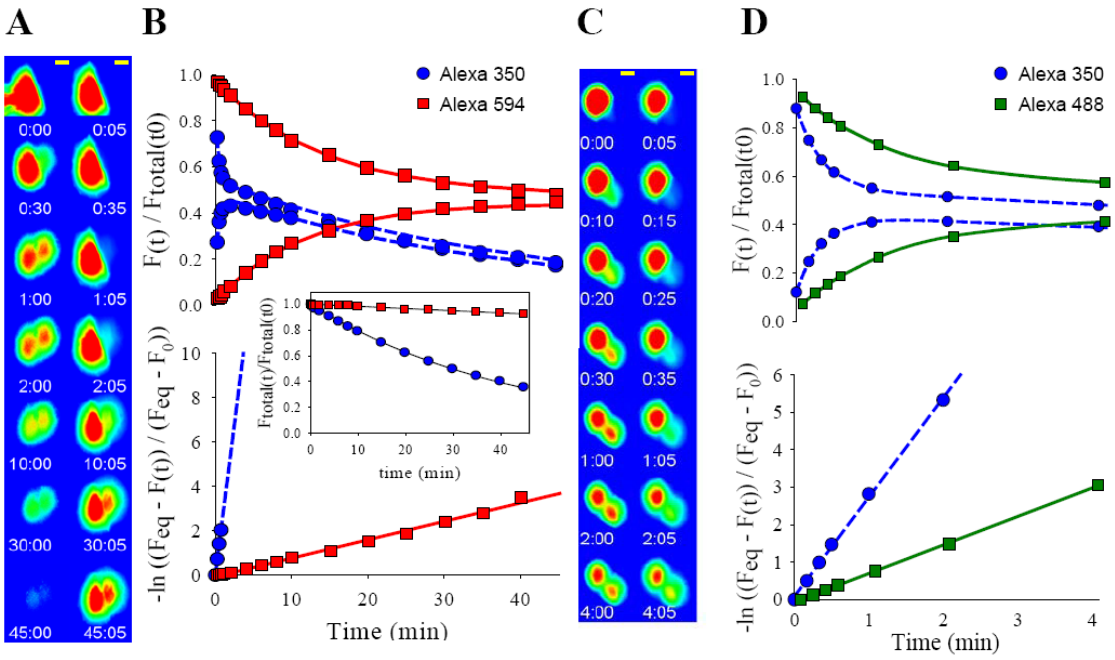
A
B
C
D
0:00
0:05
0:30
0:35
1:00
1:05
2:00
2:05
10:00
10:05
30:00
30:05
45:00
45:05
Alexa 350
Alexa 594
F(t) / Ftotal(t0)
-ln ((Feq - F(t)) / (Feq - F0))
Ftotal(t)/Ftotal(t0)
time (min)
Time (min)
0:10
0:15
0:20
0:25
4:00
4:05
Alexa 488

Figure 5

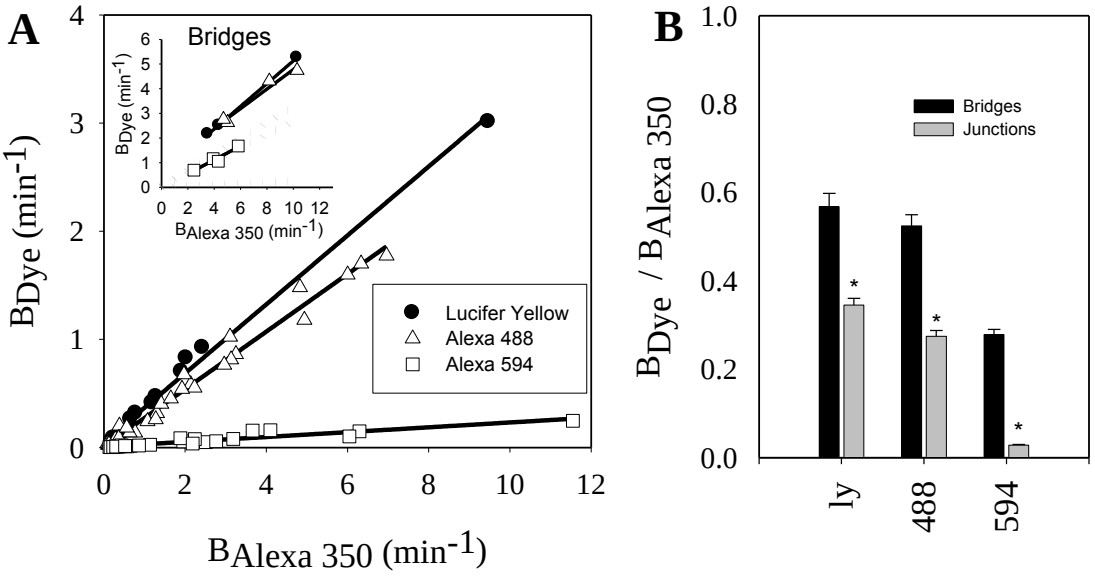
A
Bridges
B_{Dye} (min^{-1})
$B_{Alexa\ 350}$ (min^{-1})
Lucifer Yellow
Alexa 488
Alexa 594
B
B_{Dye} / $B_{Alexa\ 350}$
Bridges
Junctions
ly
488
594

Figure 6

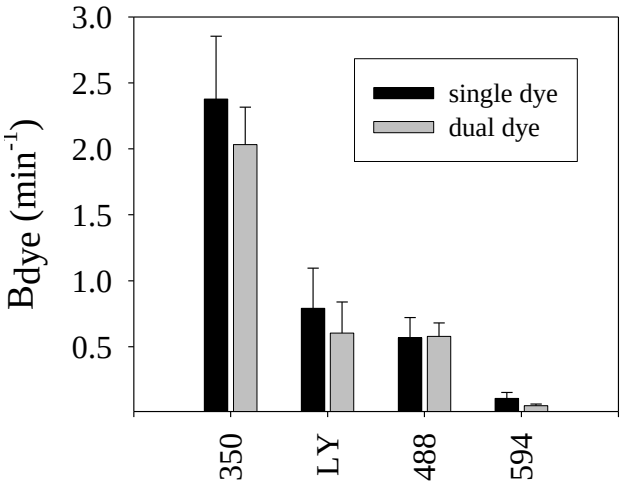

Figure 7

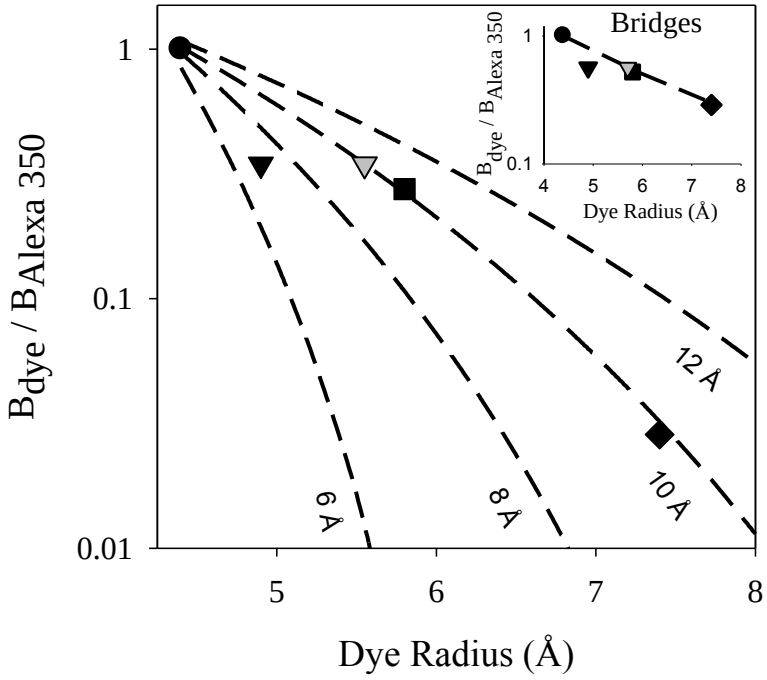
Bridges
B_{dye} / $B_{Alexa\ 350}$
1
0.1
0.01
5
6
7
8
Dye Radius (Å)
6 Å
8 Å
10 Å
12 Å
4
5
6
7
8
Dye Radius (Å)

FIGURE 8

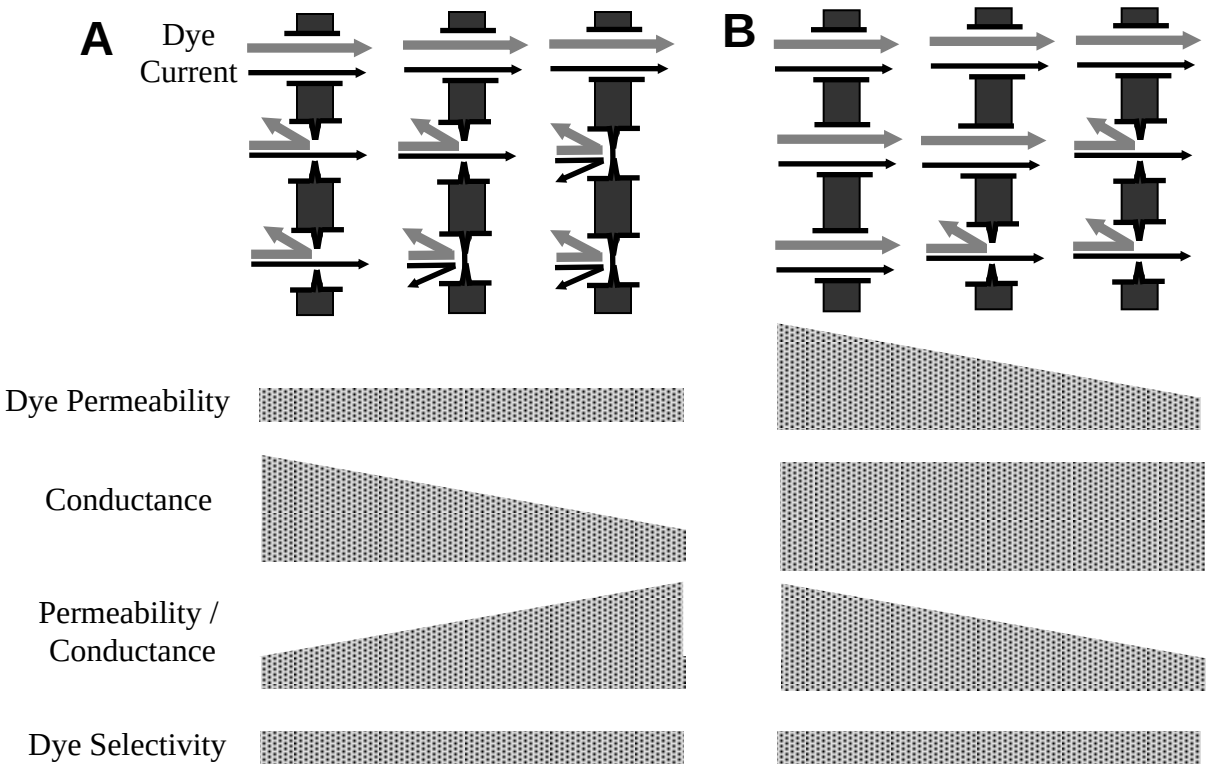
A
Dye
Current
B
Dye Permeability
Conductance
Permeability /
Conductance
Dye Selectivity

APPENDIX D

DATA SUPPLEMENT TO APPENDIX C

Alexa 350 **

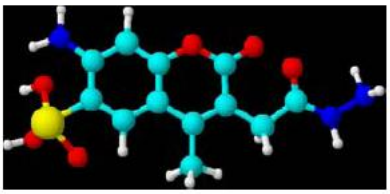

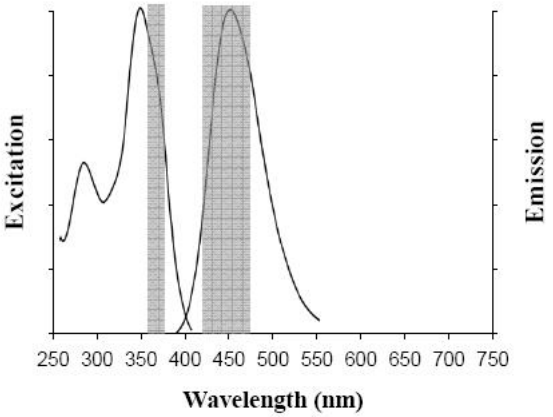

NBD-M-TMA *

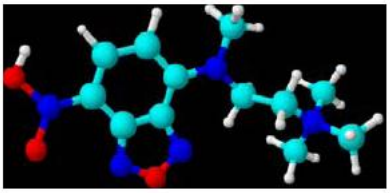

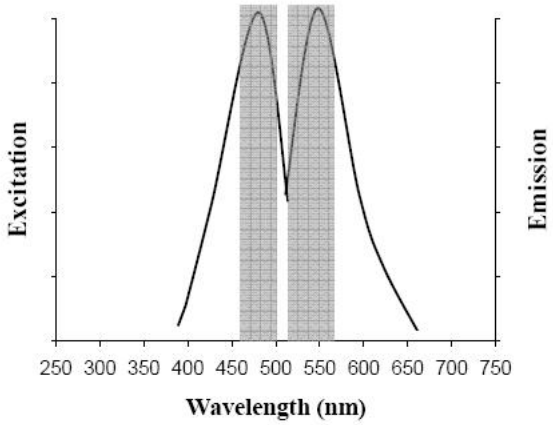

Lucifer Yellow **

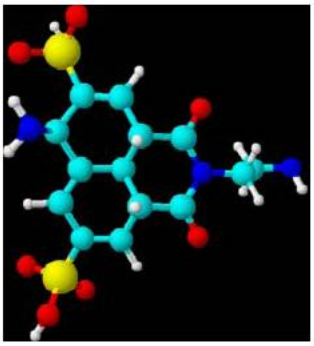

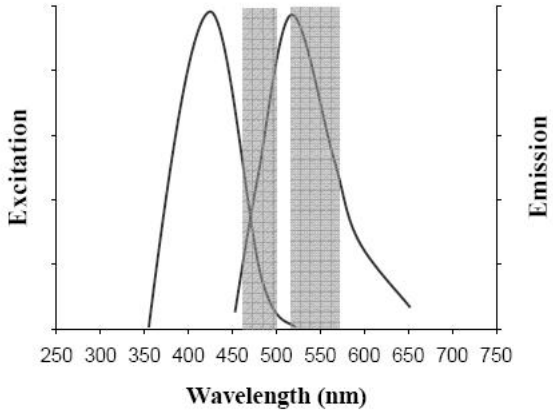

Alexa 488 **

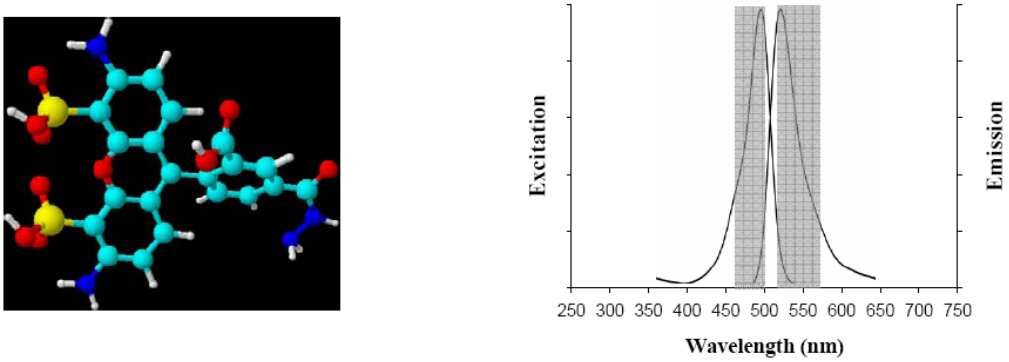

Alexa 594 **

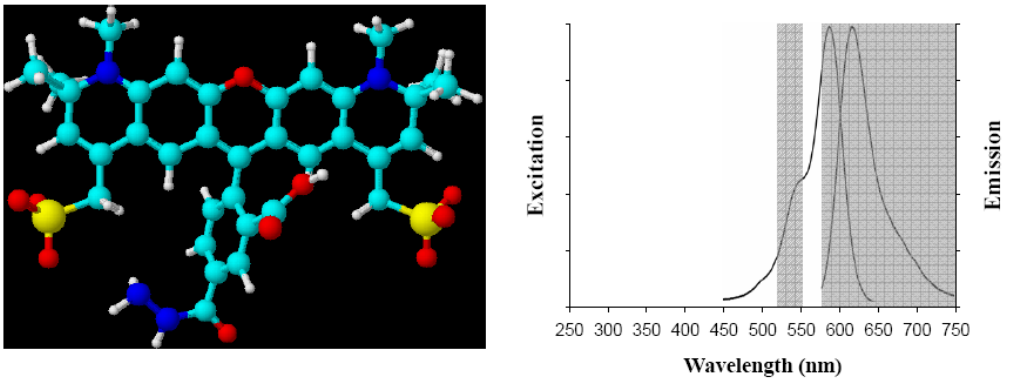

Supplemental Figure: Dye structures, spectra, and filter sets. Shown here are the structures (drawn in Chemsketch) and fluorescence emission and excitation spectra for the dyes used in the study. Gray bars indicate excitation and emission wavelengths of the filter set used to visualize each dye. The filters that were used were 41001HQ (Chroma) (NBD-M-TMA, Lucifer Yellow, and Alexa 488), UMNUA2 (Olympus) (Alexa 350), and WIG2 (Olympus) (Alexa 594). *NBD-M-TMA spectra modified from Bhasker et al (23). **Lucifer Yellow, Alexa 350, Alexa 488, and Alexa 594 spectra modified from the Molecular Probes website (http://probes.invitrogen.com/). All dual dye experiments involved visualization of Alexa 350 and one of the remaining dyes.

APPENDIX E

CO-EXPRESSION OF CX40 AND CX43 ALLOWS FOR REGULATION OF JUNCTIONAL CHARGE SELECTIVITY

Nathanael S. Heyman, David T Kurjiaka, Janis M. Burt

ABSTRACT

Previous reports have shown that Cx43 displays a consistent lack of charge selectivity whereas Cx40 shows preference for the passage of cations over anions. In the present study we analyzed the junctional charge selectivity of individual cell pairs expressing either Cx43, Cx40, or both connexins by simultaneous comparison of junctional permeance rate constant (B_{dye}) to dyes of similar size but opposing charge, NBD-M-TMA (4.3Å radius, 1^+ charge) and Alexa 350 (4.4 Å radius, 1^- charge), to assess the extent to which junctions composed of single or multiple Cx isoforms display variable selectivities. Cx43wt and Cx40wt junctions showed charge selectivities ($B_{NBD\text{-}M\text{-}TMA}$ / $B_{Alexa\ 350}$) of 0.97 ± 0.06 and 10.7 ± 0.5, respectively. Both Cx43 and Cx40 junctions showed significant correlation between $B_{NBD\text{-}M\text{-}TMA}$ and $B_{Alexa\ 350}$ (r = 0.97 and 0.98, respectively) and limited (<2 fold) variability of selectivity that was similar to the variability seen for cytoplasmic bridges. Variable phosphorylation of the Cx43 C-terminus induced either by treatment with TPA, mutation of Serine368 to alanine, or truncation of the C-terminus at amino acid 257 did not lead to significantly altered charge or size selectivity of Cx43 junctions. Cell lines that co-express Cx40 and Cx43 at ratios of 3:1 and 10:1 showed increasing mean cationic selectivities ($B_{NBD\text{-}M\text{-}TMA}$ / $B_{Alexa\ 350}$ = 4.5 ± 0.6 and 10.1 ± 0.9 respectively) as expected from the individual selectivities of Cx43 and Cx40. The 3:1 expressing cells also displayed a range of selectivies extending from the non-selectivity of Cx43 to the ≈11:1 cation selectivity of Cx40 and were pushed toward the higher selectivity of Cx40 following treatment with TPA, which essentially

eliminated dye permeability through Cx43 junctions but had no significant effect on the permeability or selectivity of Cx40 junctions. These combined data suggest that, while dye selectivities of both Cx43 and Cx40 junctions appear to be fixed parameters, the selectivities of junctions expressing both connexin isoforms can vary considerably, are bounded only by the selectivities of the comprising connexin isoforms, and can be altered by the relative expression or phosphorylation state of the comprising connexins. This could represent a mechanism by which cells regulate the selectivity of intercellular passage of molecules over a broad range of selectivities in both a short and long term manner.

INTRODUCTION

Gap junctions are aggregates of intercellular channels forming low resistance pathways for direct communication of electrical and chemical signals between neighboring cells. Gap junction channels are composed of protein subunits termed connexins (Cx), for which there are twenty-one and twenty genes in the human and mouse genomes, respectively (1). The importance of gap junctions in development and proper function of cells, tissues, organs, and organ systems is increasingly supported by connexin-linked hereditary diseases and the results of targeted gene deletion and replacement studies (2). The large number of connexin types and the controlled expression and co-expression of different connexin types at different locations, times, and both physiological and pathophysiological states (3,4) suggest connexin-specific functional roles.

An important functional role for connexin proteins is their ability to form intercellular channels capable of allowing for exchange of molecules up to ≈1000 daltons in size between cells (5). A possible reason for the large number of connexin proteins is the potential ability of channels formed of each connexin to differentially discriminate amongst available permeant molecules (ie. display different selectivities) as well as differences in the ability to regulate these selectivities. In fact, different connexin isoforms have been shown to form channels and junctions with differing selectivity and conductance properties (5). Channels formed of the same connexin type have also been shown to display variable permeabilities to the same permeants (6,7) suggesting the possible regulation of permeability properties of channels formed of even single connexin isoforms. The different selectivities between connexin isoforms and the variability in permeability of connexin isoforms could represent a means by which cells control intercellular exchange of small substances such as signaling molecules and metabolites, which have been shown to permeate gap junction channels (5,8).

The aims of the present study were to determine the extent to which junctional selectivities could be varied by two mechanisms: 1. alteration of the selectivity properties of junctions and therefore channels formed of a single connexin isoform (Cx43 or Cx40) 2. alteration of junctional connexin composition (Cx43 and Cx40). To test this, the selectivity of individual junctions was measured by simultaneous comparison of junctional permeance to dyes differing by either size or charge using a previously published technique (9). This approach allows for both the specific measure of junctional selectivity for individual gap junctions as well as for valid comparison of selectivity

between different gap junctions. As a result, both the average selectivity properties of a large number of junctions as well as the extent to which these selectivity properties vary from one junction to the next can be assessed. We show that dye selectivities of junctions formed of either Cx43 or Cx40 are essentially fixed parameters and that selectivity of junctions expressing both Cx43 and Cx40 show average selectivities intermediate to those of Cx43 and Cx40 junctions in an expression ratio dependent manner. We also show that, while average selectivity in cells that co-express Cx40 and Cx43 is intermediate to the selectivity of Cx43 and Cx40, the selectivity of individual junctions can vary from that of Cx43 to that of Cx40 and that TPA treatment of co-expressing cells shifts junctional charge selectivity towards the cationic charge selectivity of Cx40 junctions by decreasing permeability through non-selective Cx43 channels. Finally, we show that the C-terminus of Cx43 and any phosphorylation present therein in the cells tested here do not contribute significantly to the charge or size selectivity of dye permeable Cx43 channels.

METHODS

Cells:

Rat insulinoma (Rin) cells stably transfected with rat Cx43 (Rin43) (from Dr. Paolo Meda) (10) or rat Cx40 (Rin40) (11) were used for the wild type (wt) single connexin isoform experiments. Rin43 and Rin40 cells were grown in RPMI (Sigma) with 10%FBS and 300 μg/ml G418. Normal rat kidney epithelial (NRK) cells transfected for inducible expression of the carboxyl terminus (CT) of Cx43 were used for the Cx43 +CT

experiments (12). NRK+CT cells were grown in DMEM (Sigma D-1152 with 4.5 mg/mL glucose) with 500 μg/mL G418 and hygromycin; CT expression was induced in the NRK-CT cells with 1 μg/mL doxycycline for 24-48 hours (6,12). Rin cells transiently transfected (using Nucleofector II, Amaxa Biosystems) with rat Cx43 truncated at amino acid 257 (Cx43tr) were used for the Cx43tr experiments. These cells were maintained in RPMI with 10% FBS and were used 12-48 hours after transfection. Cx43-S368A cells were generated previously as described (13) by stable transfection of $Cx43^{-/-}$ cells stably transfected with rCx43-S368A and were maintained in Low Glusose-DMEM with 275 μg/mL hygromycin and 75 μg/mL ECGS. A7R5 cells, an embryonic rat aortic smooth muscle cell naturally co-expressing Cx40 and Cx43 (American Type Culture Collection, Manassas, VA) (ATCC), were grown in DMEM with 10%FBS. A7R5C3 cells, engineered to express higher levels of Cx40 than the A7r5 parental cells (14), were grown in DMEM (Sigma D-1152) with 10%FBS and 300 μg/ml G418.

TPA Treatment: Cells on cover slips were incubated in culture media containing 100 ng/ml Phorbol 12-myristate 13-acetate (TPA)(Alexis Biochemicals) for 15 minutes at 37^{o}C prior to dye selectivity experiments. Dye injection experiments were then carried out at room temperature in external solution citation and composition need to be indicated also containing 100 ng/ml TPA.

Dye Selectivity Measurement

The approach used to assess charge and size selectivity was previously described in detail (9) and thus is only briefly described here.

Filters and Dyes: The junctionally permeable anionic dyes used (all from Molecular Probes; Invitrogen, Carlsbad, CA) were Alexa 350 hydrazide sodium salt, and Alexa 594 hydrazide sodium salt. The junctionally permeable cationic dye used was NBD-M-TMA {N,N,N-trimethyl-2-[methyl-(7-nitro-2,1,3-benzoxadiol-4-yl)amino]ethanaminium}(15). The junctionally impermeable dextran dyes used (Molecular Probes) were Alexa Fluor 488 dextran (MW 3000) or Tetramethlyrhodamine dextran (MW 3000). Physical properties of these dyes are summarized in table 1. Dye spectra and the filter sets used to visualize each dye can be found in Appendix D.

Calculation of Dye Aqueous Diffusion Constant and Stokes-Einstein radii: Diffusion constants for each of the dyes were calculated according to the Wilke-Chang Correlation (16) using molar volumes estimated from Schroeder increments (17) and then used to calculate Stokes-Einstein radii for each dye (18,19).

Data Collection: Cells were trypsinized and replated on glass coverslips 4 to 48 hours prior to study. The coverslips were then placed in a chamber containing external solution and cell-pairs visualized using an Olympus IX71 fluorescence microscope. One cell of a pair was then injected (using a 1.0 mm thin walled microelectrode) with a mixture of 2 junctionally permeable dyes as well as a junctionally impermeable dye (used to

distinguish cytoplasmic bridges from true gap junctions). After overcompensating electrode capacitance to facilitate dye injection and removal of the electrode, images were then taken (with CoolSnap ES from Photometrics driven by V++ software and dye-specific filter sets) to document transjunctional diffusion of each dye as a function of time. These digital images were stored for future analysis.

Data Processing: Fluorescence intensity for selection areas encompassing the donor and then recipient cells were measured using ImageJ software (public domain; http://rsb.info.nih.gov/ij/download.html). A selection area outside but near the cell pair was similarly analyzed for background fluorescence. This was repeated for all images in the sequence for each dye and the values were exported to a spreadsheet (Excel) for analysis.

Data Analysis: Analysis of the transjunctional diffusion of dyes between the two cells was performed based on Fick's equation for diffusion between two compartments with modification for differences in cell volume and loss in total dye intensity over time as previously described (9). This analysis strategy yields an exponential rate constant (B_{dye}) (min^{-1}) that is proportional to the permeance (permeability × junctional area) of the junction being measured for each of the dyes being assessed.

RESULTS

Cx43wt shows no charge selectivity

Using an approach that has been published previously (9), the charge selectivity of Cx43wt junctions was investigated by simultaneous comparison of the junctional permeances of individual Rin43 cell pairs to dyes of similar size but differing charge (table 1). This was done by injecting one cell of a pair with a mixture of NBD-M-TMA (4.3Å radius, 1^+ charge) and Alexa 350 (4.4 Å radius, 1^- charge) and taking images of transjunctional dye diffusion over time. The resulting image sequences were analyzed to obtain fluorescence intensity over time for both donor (injected) and recipient cells (Figure 1). These fluorescence intensity data were then fit with an exponential decay model (9) yielding a rate constant that is proportional to the permeance (permeability × cross sectional area) of each junction to each of the dyes measured. The selectivity is then defined as the ratio of the rate constant (B_{dye}) of each dye for the junction being tested. The results of these experiments are shown in Figure 2. The high correlation coefficient and the small (< 2 fold) range in charge selectivity ($B_{NBD\text{-}M\text{-}TMA}$ / $B_{Alexa\ 350}$), which is similar to that seen between undivided cells and likely represents variability in the dual dye measurement, suggest that charge selectivity is an essentially fixed property of Cx43 junctions and thus channels as has been published previously (9).

Reduction or elimination of phosphorylation at serine 368 does not significantly affect Cx43 charge or size dye selectivity.

Eckert (7) suggested that phosphorylation of the CT might change the electrostatic environment at the mouth of the channel thereby altering the channel's charge selectivity. Ek Vitorin et al (6) suggested that phosphorylation of the CT of Cx43

(at S368) might stabilize the CT such that its permselectivity (permeability relative to conductance) could increase. Expression of the Cx43 CT as a separate entity in cells expressing Cx43wt reduces phosphorylation of Cx43wt protein and permselectivity (dye permeability / electrical conductance) of Cx43wt junctions (6). We therefore tested the charge (NBD-M-TMA, 1^+, 4.3 Å vs. Alexa 350, 1^-, 4.4 Å) and size (Alexa 350; 1^-, 4.4 Å vs. Alexa 594; 2^-, 7.4 Å) selectivity of junctions formed by Cx43wt functioning in the presence of excess Cx43-CT. The results (Figure 3) show that charge and size dye-selectivity of Cx43wt junctions are unaffected by excess CT expression. Because excess CT expression does not completely eliminate phosphorylation of Cx43wt, we next determined whether mutation of S368 to alanine, to prevent all phosphorylation at this site, might alter the selectivity of Cx43 comprised junctions. The results (Figure 3) reveal no differences in dye charge or size selectivity of Cx43-S368A vs. Cx43wt comprised junctions. Taken together, these data suggest that phosphorylation at S368 either does not influence channel selectivity or that dye-permeable Cx43wt channels are not phosphorylated at this site (such that Cx43wt and Cx43-S368A junctions are indistinguishable).

Truncation of the cytoplasmic C-terminus of Cx43 does not affect selectivity of junction relative to dye charge or size.

To determine whether the selectivity Cx43wt junctions to dye charge and size might be determined independently of the CT domain, we measured the (dye) charge and size selectivity of junctions formed by only the pore-forming domain of Cx43, i.e.

Cx43tr. Figure 3 shows that junctions composed of Cx43tr (the pore-forming domain) displayed charge and size selectivity not significantly different from the full length wild type protein. These data (Cx43tr, Cx43-S368A, Cx43+CT) suggest that the cytoplasmic C-terminus of Cx43 does not contribute significantly to the selectivity of dye-permeable Cx43 channels.

TPA treatment eliminates dye permeability of Cx43 but not Cx40 comprised junctions.

To determine whether increased phosphorylation of Cx43 (and S368) leads to an increase in junctional charge selectivity and cationic dye permeability as suggested by Reiner (7), the charge selectivity of the junctions formed by cells expressing Cx43wt and treated with TPA was determined. TPA treatment has been shown to increase phosphorylation of Cx43 at S368 in several cell types (13). Rin43 cells were pretreated for 15 minutes at 37^{o}C with 100ng/ml TPA and junctional selectivity determined during continued exposure to TPA in the bathing solution. No detectable junctional dye transfer (excluding cytoplasmic bridges that were identified by their ability to pass 3000 dalton dextran dyes which are too large to transit gap junctions) was seen in a total of 18 successfully injected cell pairs from 3 different treatment groups. In contrast, untreated Rin43 cells showed dye coupling in 73 ± 8% of cells injected per coverslip from 6 coverslips (26 out of 37 total injections). The extent to which this loss of dye coupling in TPA treated Rin43 cells is due to full or partial channel closure or removal of channels from the membrane, all of which have been reported previously for Cx43 (13,20,21), can

not be resolved from the current data. The data do suggest, however, that increased phosphorylation does not lead to cation selective junctions with higher permeability to positively charged dyes.

Since it appears that charge selectivity of Cx43 junctions is a relatively fixed and therefore likely unregulated parameter, we wanted to see if this fixed nature of junctional charge selectivity might also apply to junctions composed of a connexin isoform that forms channels and junctions that demonstrate selectivity amongst molecules based on permeant charge. Cx40 junctions are cation selective (9,14,22). To test whether Cx40wt charge selectivity is a variable parameter under control or TPA treatment conditions, the charge selectivity of Rin40 cell pairs was measured using the dual dye approach under both conditions (see Figure 1). The $B_{NBD\text{-}M\text{-}TMA}$ / $B_{Alexa\ 350}$ ratio for 15 Rin40 pairs was 10.7 ± 0.5 (Figure 2) indicating an approximate 11:1 preference for permeation by cations over anions. NBD-M-TMA versus Alexa 350 permeances were significantly correlated ($r = 0.98$) and well described by linear regression with a slope of 11.2 ($r^2 = 0.97$). Additionally, the small (< 2 fold) range in selectivities was similar to that seen across Cx43 junctions and cytoplasmic bridges and thus likely represents variability in the measurement technique. These data suggest that the charge selectivity of Cx40 junctions, like Cx43 junctions, is an essentially fixed parameter. Rin40 cells treated with TPA in a manner comparable to the treatment of Rin43 cells described above showed no significant difference in frequency of dye coupled pairs as a consequence of TPA treatment (TPA: 71 ± 3% per coverslip, 13 out of 18 total; Control: 75 ± 8% per coverslip, 24 out of 31 total) or change in the NBD-M-TMA/Alexa 350 selectivity ratio

(Figure 4). These results indicate that the loss of dye coupling observed in TPA treated Rin43 cells was not due to a non-specific effect of TPA treatment on Rin cells and that the incidence of functional junctions and the overall dye selectivity of Cx40 junctions is unaffected by TPA treatment.

Alteration of junctional connexin composition alters junctional charge selectivity in a predictable manner.

Since the selectivity of both Cx43 and Cx40 junctions was essentially fixed, with Cx43 being non-selective and Cx40 being cation selective, we next characterized the selectivity of junctions formed by cells that co-express Cx40 and Cx43. This was done by measuring junctional charge selectivity using the dual dye technique with cells that co-express Cx40 and Cx43 at ratios (Cx40:Cx43) of ≈3:1(A7r5) and ≈10:1(A7r5C3) (23). The results (Figure 5) show that average charge selectivity increases as the ratio of the selective (Cx40) to non-selective (Cx43) connexin isoform increases. Additionally, the results of the A7r5 experiments displayed a significant but poorly correlated relationship ($r = 0.34$) between the permeance to NBD-M-TMA and Alexa 350. While all other cell types and cytoplasmic bridges showed a less than 2-fold range in their charge selectivities, A7r5 cells demonstrated a greater than 10-fold range in charge selectivities; selectivities ranged from that observed for Cx43 wt junctions, non-selective, to the ≈11:1 cationic selectivity stereotypic of Cx40wt junctions. This variability is much more than is expected from inherent variability in the measurement using the dual dye approach, especially given that recently published data using the same approach shows only 2 fold

variability in charge selectivity and excellent correlation (r = 0.98) comparing permeance of NBD-M-TMA and Alexa 350 for 42 Cx43wt expressing cell pairs (9). These data thus indicate that the selectivity of individual junctions from cells that co-express Cx40 and Cx43 can vary in their charge selectivity from that of pure Cx40 to that of pure Cx43.

TPA treatment increases cationic selectivity of junctions formed by Cx43 and Cx40 co-expressing cells.

Since the function of Cx40 junctions is unaffected by TPA treatment whereas function of Cx43 junctions is significantly compromised, we next tested whether the function and selectivity of mixed Cx40 and Cx43 junctions was regulated by TPA activated mechanisms. TPA treatment was the same as used for the Rin43 and Rin40 experiments. TPA treatment of A7R5 cells significantly increased average charge selectivity of these junctions compared to untreated A7R5 cells ($B_{NBD\text{-}M}$-TMA = 9.8 ± 1.7 TPA treated vs. 4.5 ± 0.6 untreated, $p < 0.05$). These data indicate that co-expression of a connexin subject to regulation with one that is not, provides cells with an acute (as little as 15 minutes) mechanism (PKC-dependent) for regulation of junctional charge selectivity. The action of PKC in this setting is likely due to a decrease in dye permeability through Cx43 (containing) channels in favor of the more charge selective Cx40 channels.

DISCUSSION

In the current study we have investigated the level of (charge and size) selectivity displayed by Cx43, Cx40, and mixed Cx40 and Cx43 junctions and the extent to which these selectivities could be variable and thus potentially regulated. The technical approach used in this study is ideally suited for determining both the level of selectivity and the extent of variability in this selectivity. By providing a specific and quantitative measure of selectivity across the same junction and therefore the same number and population of channels, comparison of selectivity measures from different cells with different numbers of channels and potentially different channel populations can be rigorously made. This allows for valid assessment of the extent to which junctional selectivities might change from one cell pair to the next, an evaluation that can not be done using traditional measures where dye permeability for different dyes are measured in separate experiments across separate junctions. In addition, the approach used here affords the ability to generate highly quantitative selectivity measures from a large number of junctions for accurate assessment of average junctional selectivity properties that are independent of variations in channel number, which can be expected to occur between different cell pairs, cell types, and connexin isoforms.

C-terminus of Cx43 does not detectably regulate dye selectivity of Cx43 junctions.

The C-terminus of Cx43 is reported to be involved in pH- (24), voltage- (25), and phosphorylation-dependent gating (13,20,26) as well as in targeting and removal of the protein/channel to and from the membrane (21,27). Phosphorylation of the C-terminus of

Cx43 may also be involved in regulation of channel permeability (6) and charge selectivity (7). In the present study we show that removal of the cytoplasmic C-terminus did not significantly affect the charge or size selectivity of dye-permeable Cx43 channels. We also show that strategies known to reduce (excess CT) or prevent (S368A mutation) phosphorylation of the CT do not change the charge or size selectivity of Cx43 junctions. Finally, TPA treatment reduced the incidence of dye coupling but provided no evidence of phosphorylation-mediated changes in Cx43 junctional charge selectivity. These results suggest that the C-terminus does not contribute significantly to the electrostatic environment or limiting diameter of dye-permeable Cx43 channels, although the proportion of dye-permeable to impermeable channels may be altered. When taken in conjunction with previously published data showing that removal of the C-terminus does not significantly alter the unitary conductance (≈100 pS) of Cx43 channels (25), the data suggest that for 'fully open', dye-permeable Cx43 channels the cytoplasmic C-terminus does not contribute significantly to the channel properties of length, limiting diameter, average diameter, or electrostatic environment. This is consistent with the results from other studies involving different connexins showing that the primary determinants of conductance, permeability, and selectivity do not reside in the residues of the C-terminus but elsewhere in the connexin molecule (28-30). It is noteworthy that, while data from the current study suggest a lack of involvement of the Cx43 CT in determining channel properties of 'fully open', dye-permeable channels, the data do not preclude the involvement of the C-terminus and phosphorylation therein in the generation of channel

substates that might not be permeable to molecules the size of the dyes used herein (26,31).

Cx43 and Cx40 charge selectivities are not variable parameters.

It has been suggested that charge selectivity of Cx43 channels, which can be variably phosphorylated on the cytoplasmic C-terminus, could be altered by the extent of resident negative charge resulting from C-terminal phosphorylation (7). This could result in the ability of gap junctions composed of single connexin isoforms to display a broad range of charge selectivities in a manner that could be regulated by altering the phosphorylation state of the cytoplasmic CT of the connexin subunits. The approach used in the current study is ideally suited to determine the extent to which junctional charge selectivities and therefore the combined selectivities of the comprising channels vary from one junction to the next. The excellent correlation between permeance to NBD-M-TMA and Alexa 350 across junctions formed of either Cx40 or Cx43 channels (Figure 2A) and the fact that the < 2 fold range in variability in these selectivities is similar to that found across cytoplasmic bridges (Figure 5B) suggest that the charge selectivity of junctions and therefore channels formed of either of these two connexins do not vary significantly from one cell pair to the next and thus appear to be relatively fixed properties of the channel pore.

Cx43 and Cx40 co-expression allows for acute regulation of junctional charge selectivity.

Given that Cx43 and Cx40 junctions and channels display different selectivities that appear to be essentially fixed parameters, one would predict that junctions that contain both connexins would result in selectivities intermediate to Cx43 and Cx40 junctions. Indeed, this is what was seen in the current study; mixed composition junctions displayed average charge selectivities intermediate to those of Cx40 and Cx43 homomeric/homotypic junctions and selectivity increased as the relative amount of the more selective connexin (Cx40) increased (Figure 5). This is consistent with previous results obtained using a somewhat different approach (14) and indicates that co-expression of these connexins (Cx40 and Cx43) does not lead to novel dye selectivity properties. Selectivity of the junctions formed by co-expressing cells would then be expected to depend on the relative contribution to junctional permeability and the inherent selectivity properties of each connexin isoform present. Our data also suggest that relative average whole cell connexin protein levels are at least moderately predictive of average relative junctional connexin composition.

If the relative junctional composition of Cx40:Cx43 was not constant from one cell pair to the next, one would predict that the junctional charge selectivity would vary directly with this ratio (Cx40:Cx43) with cells expressing higher levels of Cx40 showing higher levels of cationic charge selectivity and cells with higher levels of Cx43 showing lower levels of charge selectivity. This was observed in the current study in two ways. First, A7r5C3 cells (10:1 Cx40:Cx43) showed significantly higher average charge selectivities than A7r5 cells (3:1 Cx40:Cx43) (Figure 5C). Second, the range of selectivities measured in A7r5 cells varied across the entire range of selectivities from the

non-selectivity of Cx43 to the ≈11:1 cationic charge selectivity of Cx40 (Figure 5B). This indicates that the contribution of each connexin isoform to dye-permeable junctional channels varied across the spectrum from entirely Cx40 to entirely Cx43 and suggests that, while the average Cx40:Cx43 protein expression ratio in these cells may be predictive of average junctional connexin composition, it is not necessarily predictive of the junctional composition of individual cell pairs. Supporting this observation is previously published work showing that average Cx40:Cx43 expression ratio can vary from 1.5:1 to 4.5:1 (32) and electrical and dye coupling characteristics differ (33) when A7r5 cells are maintained in different growth states by incubating in media containing 1% or 10% growth serum. It is possible that, despite being grown under similar conditions, A7r5 cells in the current study were captured in differing growth states resulting in at least some of the variability in charge selectivity that was seen. Data from the current study do not allow for determination of the specific mechanism for this variable contribution of Cx40 and Cx43 to junctional dye permeabilities. The extent to which variable protein expression, membrane localization, degradation, or gating between dye-permeable and impermeable states contributed to the observed variability in selectivity of these junctions is not yet known and requires further investigation. The data do however suggest that A7r5 cells, even when grown under the same conditions, can display variability in their selectivity and presumably junctional composition ranging from essentially purely Cx43 to purely Cx40.

Increased phosphorylation of Cx43, particularly by PKC, has been shown to reduce dye permeability of Cx43wt junctions (21,34) and the permeability of Cx43wt

hemichannels to molecules similar in size to the dyes used in the current study (26). Increased phosphorylation of Cx43, through PDGF or TPA treatment, has also been shown to reduce both macroscopic and unitary conductance of Cx43 junctions and channels (13,20,35), while having no effect on the electrical communication properties of Cx40 junctions (35). The data from the current study showing a reduction in dye permeability of Cx43 upon TPA treatment and no change in Cx40 permeability or selectivity are consistent with these electrical communication data. Additionally, PDGF application has been shown to lead to a reduction in macroscopic conductance and a shift in single channel conductance towards that of Cx40 in the same Cx40:Cx43 co-expressing cell lines used here and to do this, at least in part, through PKC-mediated phosphorylation of Cx43 (35). While there were trends toward decreased dye permeability ($B_{NBD\text{-}M\text{-}TMA}$ = 0.66 ± 0.12 vs. 0.27 ± 0.05 for untreated and TPA treated, respectively) and frequency of coupled cells (71 ± 9% untreated vs. 42 ± 12% TPA treated) for A7r5 cells following TPA treatment, neither reached significance at $p < 0.05$. These trends in combination with the significant increase in charge selectivity toward that of pure Cx40 channels are consistent with elimination or reduction of permeability through channels that were predominantly Cx43 in composition and are consistent with the electrical communication data. The extent to which channel removal, closure, or gating to a dye-impermeable conductance state are involved in the decrease in Cx43 dye permeability cannot be evaluated. However, the data do suggest that PKC activation preferentially reduces permeability through Cx43 containing channels and results in

increased cationic charge selectivity of junctions formed by Cx40 and Cx43 co-expressing cells.

Significance

While selectivity properties for permeants of the size of the dyes tested in the current study (≈4-7Å radii) do not appear to be variable parameters for junctions composed of the individual connexin isoforms Cx43 or Cx40, data from the current study suggest that co-expression of these connexin isoforms provides a means for both long and short term control of junctional selectivity in a manner that is predictable from the selectivity and permeability properties of the comprising connexins. This could represent a general mechanism by which the selectivity of diffusion of signaling molecules or metabolites through gap junctions could be controlled in an acute or long term manner at different times, locations, or physiological and pathophysiological conditions where the ability to differentially discriminate between possible junctional permeants could be of great importance. Understanding of the selectivity and permeability properties of junctions and channels formed of each connexin isoform and the potential ability to modulate these parameters could then lead to reasonable predictions of the selective properties of permeation through junctions formed of mixed connexin composition under different conditions. The ability of different connexin isoforms to respond differentially to similar stimuli and to then alter the selectivity and permeability properties of gap junctions of mixed connexin composition could prove to be a key concept in connexin-specific functional roles and to be an important reason for the large number of connexin

isoforms found. Further work is needed to characterize the selectivity and permeability properties for each connexin isoform as well as the potential ability to regulate these parameters.

Table 1: Physical Properties of Permeants

	MW (no counter ion)	D_{Aqeous} (25°C) (10^{-6} cm^2/sec)	Stokes-Einstein radius (Å)	λ_{ex} / λ_{em} (nM)	Net charge
NBD-M-TMA	280	5.8*	4.3	458/580	1^+
Alexa 350	326	5.6*	4.4	345/445	1^-
Alexa 594	734	3.3*	7.4	588/613	2^-

**Calculated using Wilke-Chang correlation (see methods).*

FIGURE LEGENDS

Figure 1. Representative results and calculated fits from Cx43wt and Cx40wt dye charge selectivity experiments. Shown here are the results of the analysis of two dye charge selectivity experiments. **A.** Total fluorescence intensity for NBD-M-TMA (upper panel) or Alexa 350 (lower panel) for both donor (injected) and recipient cells as a function of time for a Rin43 cell pair. Dashed lines are fits to an exponential decay model (9) yielding junctional permeance rate constants (B_{dye}) of 2.1 min^{-1} and 2.3 min^{-1} for NBD-M-TMA and Alexa 350, respectively, for a charge selectivity ($B_{NBD\text{-}M\text{-}TMA}$ / $B_{Alexa350}$) of 0.91, which indicates a general lack of charge selectivity. **B**. Total fluorescence intensity for NBD-M-TMA (upper panel) or Alexa 350 (lower panel) for both donor and recipient cells as a function of time for a Rin40 cell pair. Dashed lines are fits to an exponential decay model (9) yielding junctional permeance rate constants (B_{dye}) of 3.5 min^{-1} and 0.31 min^{-1} for NBD-M-TMA and Alexa 350, respectively, for a charge selectivity ($B_{NBD\text{-}M\text{-}TMA}$ / $B_{Alexa350}$) of 11.3 indicating an ≈11:1 cationic charge selectivity.

Figure 2. Cx43 non-selectivity and Cx40 cationic selectivity are invariant. Shown here are the results of dye charge selectivity results on cytoplasmic bridges (incompletely divided cells) from Rin43 and Rin40 cells, Cx43wt junctions (Rin43 cells), and Cx40wt junctions (Rin40 cells). **A.** A plot of permeance rate constants of NBD-M-TMA vs. Alexa 350 for cytoplasmic bridges (▲), Cx43wt junctions (●), and Cx40wt junctions (□). These parameters were significantly correlated for all 3 groups ($p < 0.05$) with correlation coefficients of 0.97 (n = 5) for bridges, 0.97 (n = 7) for Cx43wt junctions, and 0.98 (n = 15) for Cx40wt junctions. **B.** Average charge selectivities ($B_{NBD\text{-}M\text{-}TMA}$ / $B_{Alexa350}$) for the experiments plotted in panel **A** of 0.91 ± 0.06 (n = 5) (bridges), 0.97 ± 0.06 (n = 7) (Rin43), and 10.7 ± 0.5 (n = 15) (Rin40). *Cx40wt junctions showed significantly higher

cationic selectivity than both Cx43wt junctions and cytoplasmic bridges ($p < 0.05$). Cx43 selectivity was not significantly different from that of cytoplasmic bridges.

Figure 3. Cx43 dye selectivity is not affected by the cytoplasmic C-terminus. A. Plot showing the average charge selectivity ($B_{NBD\text{-}M\text{-}TMA}$ / $B_{Alexa\ 350}$) for cells expressing Cx43wt alone (Cx43wt) (0.97 ± 0.06; n = 7), Cx43wt with excess CT expressed as a separate entity (Cx43+CT) (1.03 ± 0.08; n = 6), Cx43 truncated at amino acid 257 (Cx43tr) (0.98 ± 0.07; n = 5), or Cx43 with serine 368 mutated to alanine (Cx43 S368A) (0.84 ± 0.4; n = 8). There were no significant differences between groups by single factor ANOVA. **B.** A plot showing the average size selectivity ($B_{Alexa\ 350}$ / $B_{Alexa\ 594}$) for the cells expressing Cx43wt alone (Cx43wt) (35.8 ± 3.8; n = 4), Cx43wt with excess CT expressed as an independent entity (Cx43+CT) (39.4 ± 4.7; n = 5), Cx43 truncated at amino acid 257 (Cx43tr) (39.3 ± 6.6; n = 4), or Cx43 with Serine 368 mutated to alanine (Cx43 S368A) (35.6 ± 3.4; n = 7). There were no significant differences between groups by single factor ANOVA.

Figure 4. TPA treatment eliminates Cx43 dye coupling but does not affect Cx40 dye coupling. A. A plot of the average number of cell pairs showing intercellular dye diffusion relative to the total number of cells successfully injected (% dye coupling) per coverslip (excluding cytoplasmic bridges) for untreated (black bars) vs. TPA treated (gray bars) Rin43 and Rin40 cells. *Note the complete absence of dye coupling observed for TPA treated Rin43 cells (18 injections). There was no significant difference in coupling frequency for untreated vs. TPA treated Rin40 cells. **B.** A plot of average permeance rate constant (B_{dye}) for NBD-M-TMA and Alexa 350 for Rin40 cells that were untreated (black bars) or TPA treated (gray bars). There was no significant change in rate constant for either dye in untreated vs. TPA treated Rin40 cells.

Figure 5. Cx43 and Cx40 co-expression yields intermediate junctional charge selectivities that are increased by TPA treatment. A. Plot of $B_{NBD\text{-}M\text{-}TMA}$ vs. $B_{Alexa\ 350}$ for A7r5C3 (■), A7r5 (●), and A7r5 with TPA treatment (▽). Dotted lines are linear regression fits to Cx40wt and Cx43wt junctions from the data in Figure 2A. **B.** Charge selectivity ($B_{NBD\text{-}M\text{-}TMA}$ / $B_{Alexa\ 350}$) from all experiments in panel **A** and the experiments from Figure 2A plotted on logarithmic scale to emphasize the ~11 fold range in junctional selectivity. **C.** Plot of average charge selectivity ($B_{NBD\text{-}M\text{-}TMA}$ / $B_{Alexa\ 350}$) from all experiments in panel **B**. *Untreated A7r5 cells showed significantly different selectivity ($p < 0.05$) from all other groups. **Cytoplasmic bridges and Cx43wt junctions showed significantly different selectivity from all other cell types and treatments ($p < 0.05$) but were not significantly different from each other. The remaining groups (Cx40, Cx40 +TPA, A7r5C3, and A7r5 +TPA) were not significantly different from each other.

Figure 1

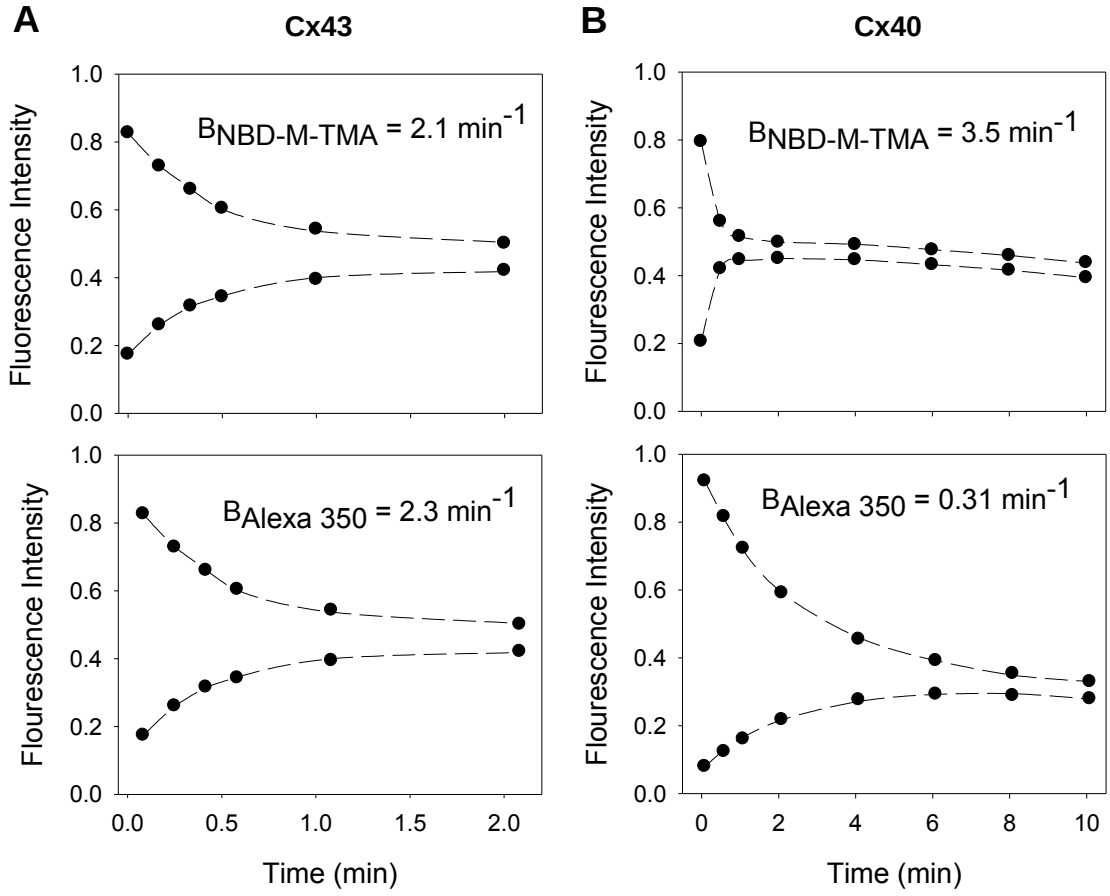
A
Cx43
B
Cx40
Fluorescence Intensity
Flourescence Intensity
$B_{NBD\text{-}M\text{-}TMA}$ = 2.1 min^{-1}
$B_{NBD\text{-}M\text{-}TMA}$ = 3.5 min^{-1}
$B_{Alexa\ 350}$ = 2.3 min^{-1}
$B_{Alexa\ 350}$ = 0.31 min^{-1}
0.0
0.2
0.4
0.6
0.8
1.0
0.5
1.5
2.0
2
4
6
8
10
Time (min)

Figure 2

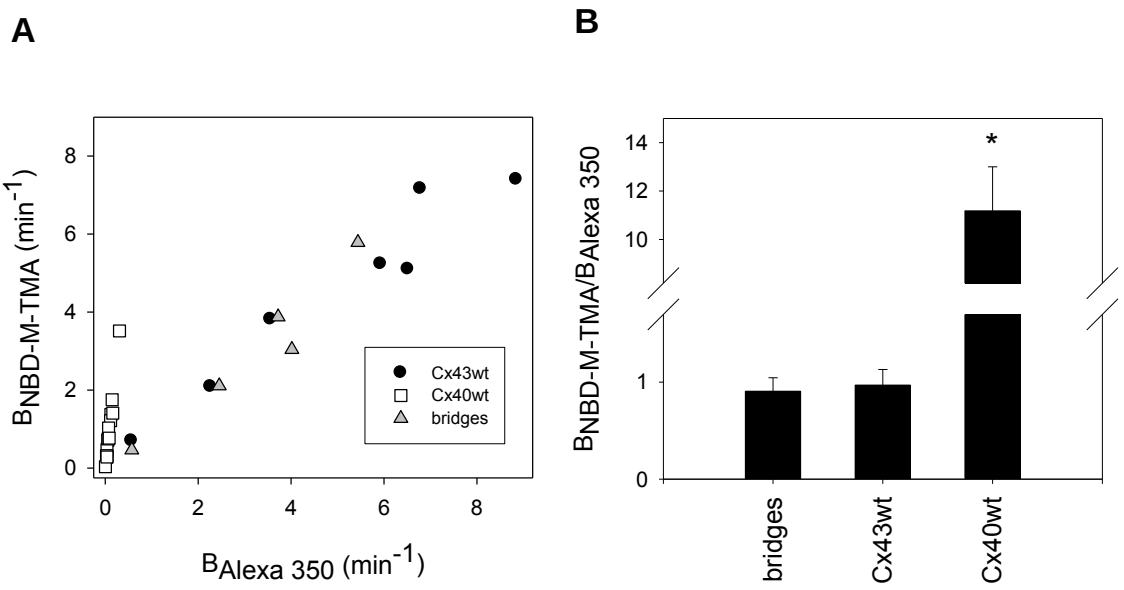
A
B
$B_{NBD\text{-}M\text{-}TMA}$ (min^{-1})
$B_{Alexa\ 350}$ (min^{-1})
Cx43wt
Cx40wt
bridges
$B_{NBD\text{-}M\text{-}TMA}/B_{Alexa\ 350}$
*
bridges
Cx43wt
Cx40wt

Figure 3

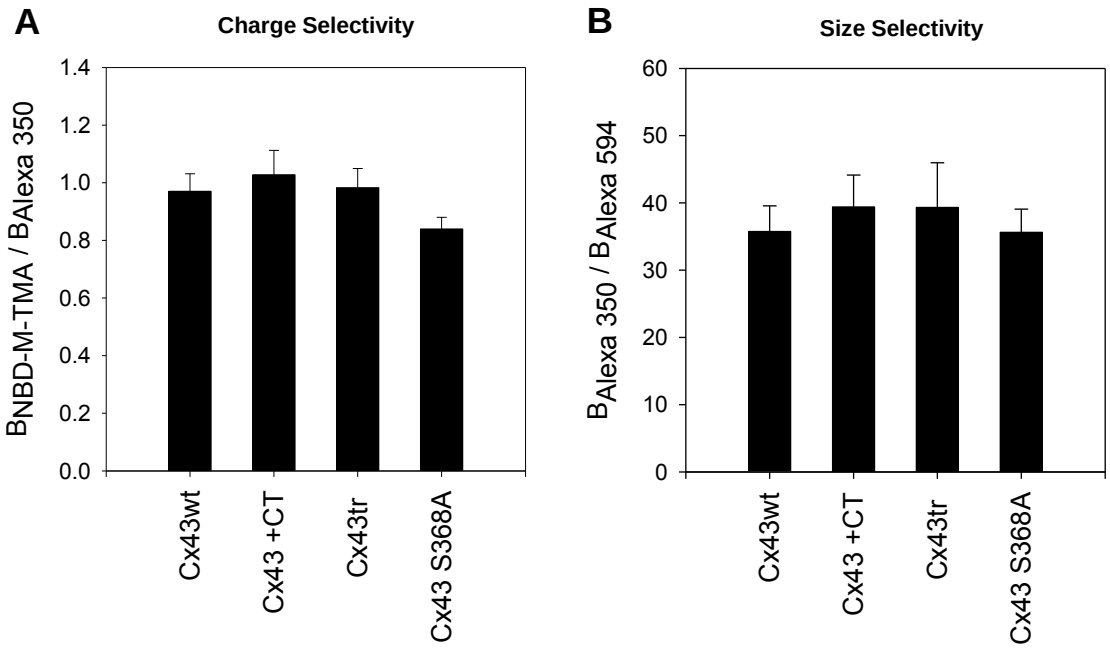
A
Charge Selectivity
$B_{NBD\text{-}M\text{-}TMA}$ / $B_{Alexa\ 350}$
1.4
1.2
1.0
0.8
0.6
0.4
0.2
0.0
Cx43wt
Cx43 +CT
Cx43tr
Cx43 S368A
B
Size Selectivity
$B_{Alexa\ 350}$ / $B_{Alexa\ 594}$
60
50
40
30
20
10
0
Cx43wt
Cx43 +CT
Cx43tr
Cx43 S368A

Figure 4

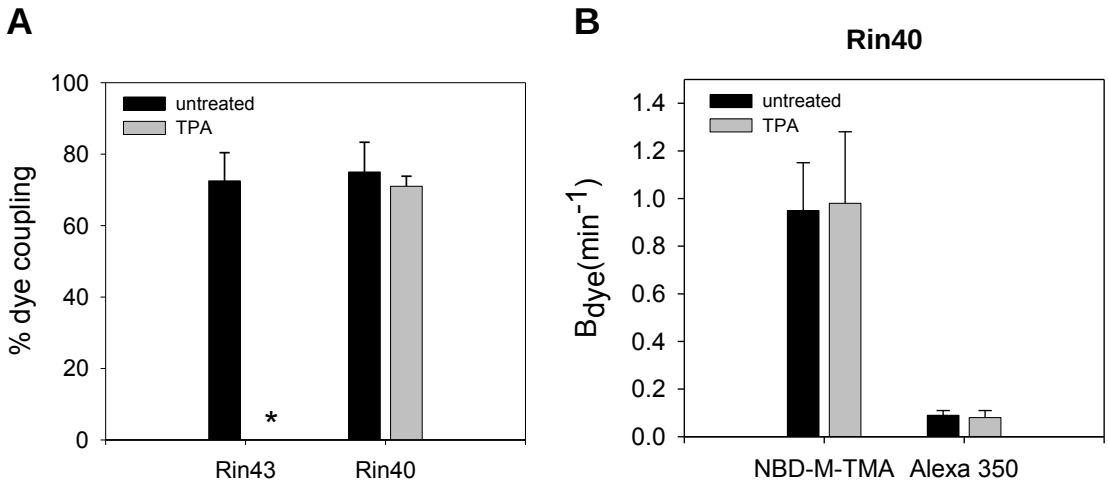
A
% dye coupling
100
80
60
40
20
0
untreated
TPA
*
Rin43
Rin40
B
Rin40
$B_{dye}(min^{-1})$
1.4
1.2
1.0
0.8
0.6
0.4
0.2
0.0
untreated
TPA
NBD-M-TMA
Alexa 350

Figure 5

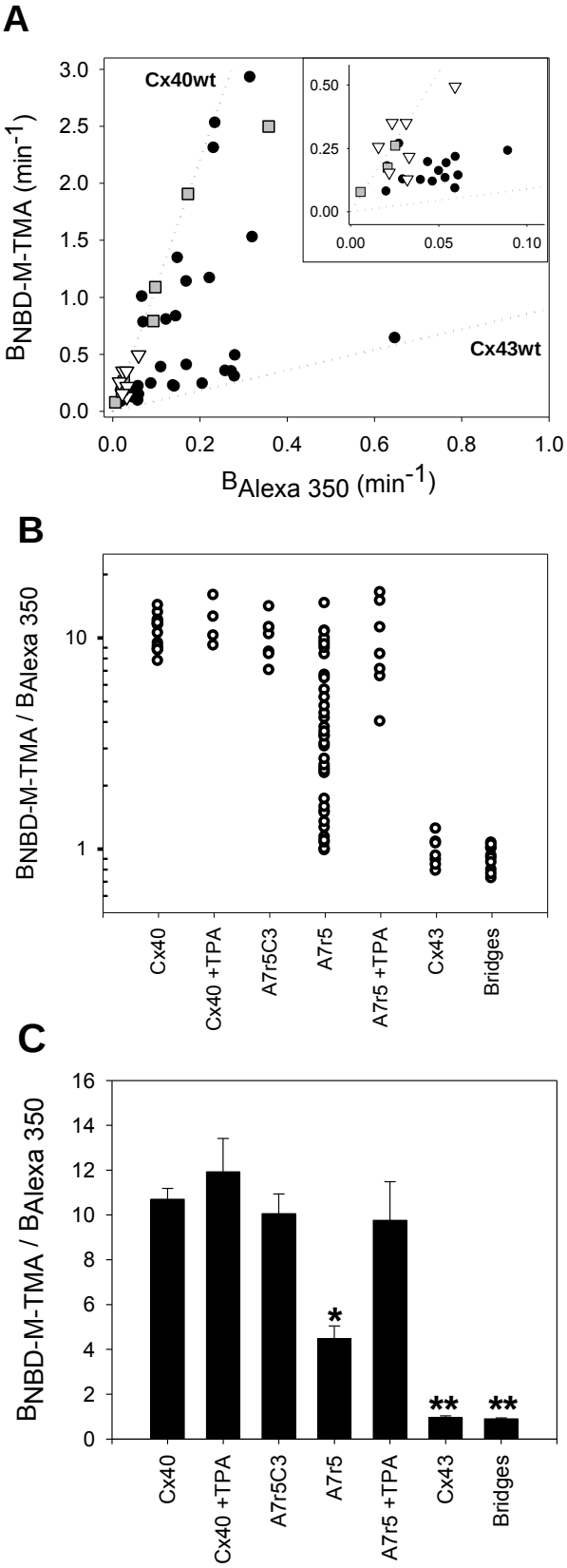
A
Cx40wt
Cx43wt
$B_{NBD\text{-}M\text{-}TMA}$ (min^{-1})
$B_{Alexa\ 350}$ (min^{-1})
B
$B_{NBD\text{-}M\text{-}TMA}$ / $B_{Alexa\ 350}$
Cx40
Cx40 +TPA
A7r5C3
A7r5
A7r5 +TPA
Cx43
Bridges
C
$B_{NBD\text{-}M\text{-}TMA}$ / $B_{Alexa\ 350}$
Cx40
Cx40 +TPA
A7r5C3
A7r5
A7r5 +TPA
Cx43
Bridges

Reference List

1. Sohl,G. and K.Willecke. 2004. Gap junctions and the connexin protein family. *Cardiovasc. Res.* 62:228-232.

2. Evans,W.H. and P.E.Martin. 2002. Gap junctions: structure and function (Review). *Mol. Membr. Biol.* 19:121-136.

3. Delorme,B., E.Dahl, T.Jarry-Guichard, J.P.Briand, K.Willecke, D.Gros, and M.Theveniau-Ruissy. 1997. Expression pattern of connexin gene products at the early developmental stages of the mouse cardiovascular system. *Circ. Res.* 81:423-437.

4. Haefliger,J.A., E.Castillo, G.Waeber, G.E.Bergonzelli, J.F.Aubert, E.Sutter, P.Nicod, B.Waeber, and P.Meda. 1997. Hypertension increases connexin43 in a tissue-specific manner. *Circ.* 95:1007-1014.

5. Harris,A.L. 2007. Connexin channel permeability to cytoplasmic molecules. *Prog. Biophys. Mol. Biol.* 94:120-143.

6. Ek-Vitorin,J.F., T.J.King, N.S.Heyman, P.D.Lampe, and J.M.Burt. 2006. Selectivity of connexin 43 channels is regulated through protein kinase C-dependent phosphorylation. *Circ. Res.* 98:1498-1505.

7. Eckert,R. 2006. Gap-junctional single-channel permeability for fluorescent tracers in Mammalian cell cultures. *Biophys. J.* 91:565-579.

8. Goldberg,G.S., V.Valiunas, and P.R.Brink. 2004. Selective permeability of gap junction channels. *Biochim. Biophys. Acta* 1662:96-101.

9. Heyman,N.S. and J.M.Burt. 2007 in press. Hindered diffusion through an aqueous pore describes invariant dye selectivity of Cx43 junctions. *Biophys. J.*

10. Vozzi,C., S.Ullrich, A.Charollais, J.Philippe, L.Orci, and P.Meda. 1995. Adequate connexin-mediated coupling is required for proper insulin production. *J. Cell Biol.* 131:1561-1572.

11. Cottrell,G.T. and J.M.Burt. 2001. Heterotypic gap junction channel formation between heteromeric and homomeric Cx40 and Cx43 connexons. *Am. J. Physiol Cell Physiol* 281:C1559-C1567.

12. Shin,J.L., J.L.Solan, and P.D.Lampe. 2001. The regulatory role of the C-terminal domain of connexin43. *Cell Commun. Adhes.* 8:271-275.

13. Lampe,P.D., E.M.Tenbroek, J.M.Burt, W.E.Kurata, R.G.Johnson, and A.F.Lau. 2000. Phosphorylation of connexin43 on serine368 by protein kinase C regulates gap junctional communication. *J. Cell Biol.* 149:1503-1512.

14. Cottrell,G.T., Y.Wu, and J.M.Burt. 2002. Cx40 and Cx43 expression ratio influences heteromeric/heterotypic gap junction channel properties. *Am. J. Physiol.* 282:C1469-C1482.

15. Bhasker,R., M.Ahad, Mash E.A., D.Bednarczyk, and S.H.Wright. 2006. Synthesis and Fluorescence of N,N,N-Trimethyl-2-[methyl(7-nitrobenzo[*c*][1,2,5]oxadiazol-4-yl)amino]ethaminium Iodide, a pH-Insensitive Reporter of Organic Cation Transport. *Synthetic Communications*701-705.

16. Wilke,C.R. and P.Chang. 1955. Correlation of Diffusion Coefficients in Dilute Solutions. *A. I. Ch. E. Journal* 1:264-270.

17. Reid,R.C., J.M.Prausnitz, and T.K.Sherwood. 1977. The Properties of Gases and Liquids. McGraw-Hill, New York.

18. Einstein,A. 1905. Uber die von der molekularkinetischen Theorie der Warme geforderte Bewegung von in ruhenden Flussigkeiten suspendiertin Teilchen. *Annalen der Physik* 322:549-560.

19. Miller C.C. 1924. The Stokes-Einstein Law for Diffusion in Solution. *Proc. R. Soc. Lond.* 106:724-749.

20. Moreno,A.P., G.I.Fishman, and D.C.Spray. 1992. Phosphorylation shifts unitary conductance and modifies voltage dependent kinetics of human connexin43 gap junction channels. *Biophys. J.* 62:51-53.

21. Rivedal,E. and E.Leithe. 2005. Connexin43 synthesis, phosphorylation, and degradation in regulation of transient inhibition of gap junction intercellular communication by the phorbol ester TPA in rat liver epithelial cells. *Exp. Cell Res.* 302:143-152.

22. Beblo,D.A. and R.D.Veenstra. 1997. Monovalent cation permeation through the connexin40 gap junction channel Cs, Rb, K, Na, Li, TEA, TMA, TBA, and effects of anions Br, Cl, F, acetate, aspartate, glutamate, and NO_3. *J. Gen. Physiol.* 109:509-522.

23. Burt,J.M., A.M.Fletcher, T.D.Steele, Y.Wu, G.T.Cottrell, and D.T.Kurjiaka. 2001. Alteration of Cx43:Cx40 expression ratio in A7r5 cells. *Am. J. Respir. Cell Mol. Biol.* 280:C500-C508.

24. Delmar,M., W.Coombs, P.Sorgen, H.S.Duffy, and S.M.Taffet. 2004. Structural bases for the chemical regulation of Connexin43 channels. *Cardiovasc. Res.* 62:268-275.

25. Moreno,A.P., M.Chanson, S.Elenes, J.Anumonwo, I.Scerri, H.Gu, S.M.Taffet, and M.Delmar. 2002. Role of the carboxyl terminal of connexin43 in transjunctional fast voltage gating. *Circ. Res.* 90:450-457.

26. Bao,X., S.C.Lee, L.Reuss, and G.A.Altenberg. 2007. Change in permeant size selectivity by phosphorylation of connexin 43 gap-junctional hemichannels by PKC. *Proc. Natl. Acad. Sci. U. S. A.* 104:4919-4924.

27. Leithe,E. and E.Rivedal. 2004. Ubiquitination and down-regulation of gap junction protein connexin-43 in response to 12-O-tetradecanoylphorbol 13-acetate treatment. *J. Biol. Chem.* 279:50089-50096.

28. Dong,L., X.Liu, H.Li, B.M.Vertel, and L.Ebihara. 2006. Role of the N-terminus in permeability of chicken connexin45.6 gap junctional channels. *J. Physiol.* 576:787-799.

29. Trexler,E.B., F.F.Bukauskas, J.Kronengold, T.A.Bargiello, and V.K.Verselis. 2000. The first extracellular loop domain is a major determinant of charge selectivity in connexin46 channels. *Biophys. J.* 79:3036-3051.

30. Ma,M. and G.Dahl. 2006. Cosegregation of permeability and single-channel conductance in chimeric connexins. *Biophys. J.* 90:151-163.

31. Bukauskas,F.F., A.Bukauskiene, and V.K.Verselis. 2002. Conductance and permeability of the residual state of connexin43 gap junction channels. *J. Gen. Physiol* 119:171-186.

32. Cottrell,G.T., Y.Wu, and J.M.Burt. 2001. Functional characteristics of heteromeric Cx40-Cx43 gap junction channel formation. *Cell Commun. Adhes.* 8:193-197.

33. Kurjiaka,D.T., T.D.Steele, M.V.Olsen, and J.M.Burt. 1998. Gap junction permeability is diminished in proliferating vascular smooth muscle cells. *Am. J. Physiol.* 275:C1674-C1682.

34. Kwak,B.R. and H.J.Jongsma. 1996. Regulation of cardiac gap junction channel permeability and conductance by several phosphorylating conditions. *Molecular and Cellular Biochemistry* 157:93-99.

35. Burt,J.M. and T.D.Steele. 2003. Selective effect of PDGF on connexin43 versus connexin40 comprised gap junction channels
gap junction channels. *Cell Commun. Adhes.* 10:287-291.

APPENDIX F

FUTURE DIRECTIONS

FUTURE DIRECTIONS

Test the impact of C-terminal truncation on Cx43 permselectivity. It is proposed in the current study that interjunctional variability in Cx43 junctional permselectivity (dye permeability / electrical conductance) is due to variable phosphorylation of the C-terminus of Cx43. Measuring the permselectivity of junctions formed only of Cx43 with the C-terminus truncated should test the role of C-terminal phosphorylation in altering the proportion of channels occupying different permselectivity states. If occupation of each permselectivity state is either random or dependent upon the phosphorylation status of the Cx43 C-terminus, conductance and dye permeability would be expected to show strong correlation without significant interjunctional variability among junctions formed of Cx43 with the C-terminus removed.

Investigate the role of the C-terminus in determining charge selectivity of junctions composed of connexins that form charge selective channels. Previously, it has been suggested that the physical presence of negative charge resulting from C-terminal phosphorylation could sufficiently affect the electrostatic environment of the Cx43 channel mouth to alter charge selectivity for transit through the channel. In the current study, variable phosphorylation or even the removal of the C-terminus of Cx43 did not detectably affect the selectivity of dye-permeable Cx43 channels. These data suggest that the C-terminus of Cx43 is not necessary for the selectivity of dye-permeable Cx43 channels. Determining the impact of C-terminal truncation on the selectivity of charge-

selective gap junctions, such as those formed by Cx40 and Cx37, would help to determine whether the C-terminus and any phosphorylation present therein is necessary for charge selectivity in transit through gap junctions formed of these channels.

Examine whether the proposed dye-impermeable but electrically conductive Cx43 channel open state is produced by PKC activation. Data from the current study suggest that activation of PKC by TPA eliminates dye permeability for Cx43 junctions and thus channels. It remains to be determined whether electrical coupling in such pairs is also eliminated. If electrical coupling remains while dye coupling is lost, this would support the existence of a dye-impermeable but electrically conductive open state for Cx43 channels proposed in the current study and provide at least one mechanism for shifting Cx43 channels into this state. If electrical coupling is also eliminated or significantly reduced by the TPA treatment, the effect of TPA treatment on the amount and location of Cx43 protein could be analyzed by western blot (including both membrane fraction and whole cell protein) and immunocytochemistry. This would help to determine the extent to which elimination of dye permeability upon TPA treatment is due to Cx43 protein removal, degradation, relocalization, or channel closure.

Determine the extent to which phosphorylation of Cx43 by PKC or MAPK are responsible for the loss in dye permeability. The extent to which PKC or MAPK mediated phosphorylation of Cx43 (both of which have been shown to result from TPA treatment) are responsible for the loss in dye permeability of Cx43 channels upon TPA

treatment could be investigated by exploring the effects of TPA treatment on dye coupling through junctions formed with Serine to Alanine mutations of the appropriate PKC and MAPK phosphorylation sites. If the loss in dye permeability upon TPA treatment is eliminated or reduced by mutation of Serine to Alanine, this would suggest that phosphorylation at the mutated site or sites is involved in the reduction in dye permeability.